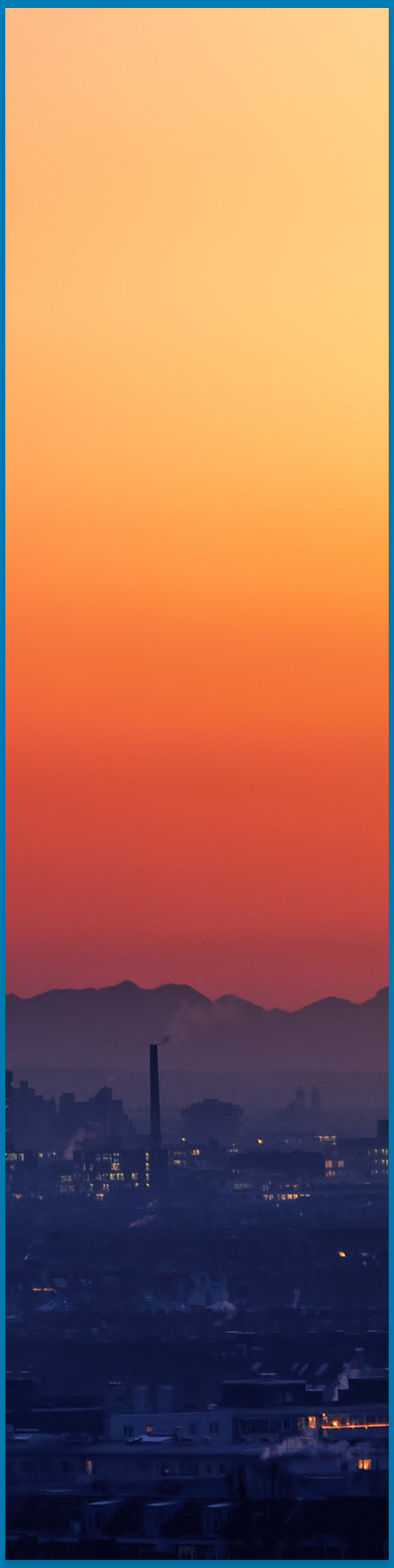

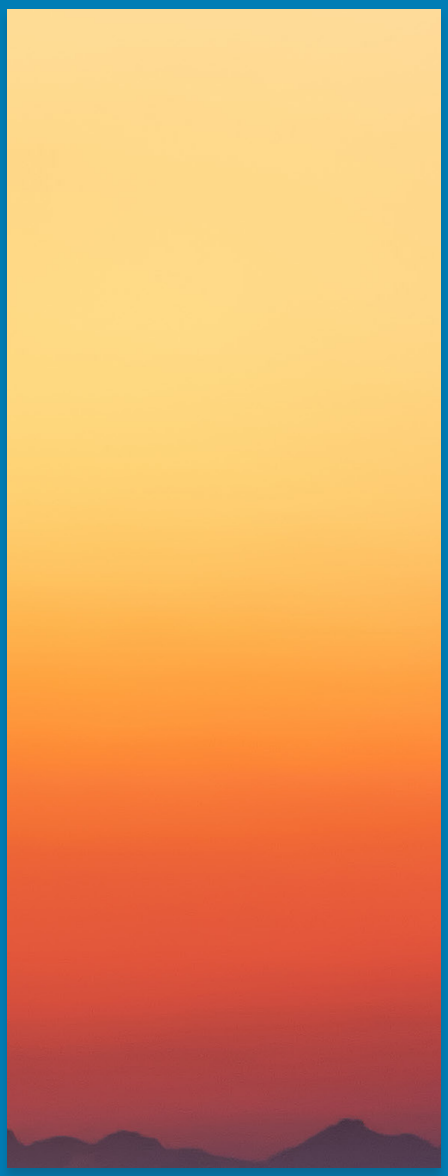

5 DECEMBER 2025
REVISED 7 JANUARY 2026

THE IMPACT OF AIR POLLUTION ON HUMAN HEALTH IN THE THREE AIR POLLUTION PRIORITY AREAS IN SOUTH AFRICA

PREPARED BY CHANTELLE HOWLETT-DOWNING AND CARADEE Y WRIGHT

CLEAN AIR FUND

saMRC advancinglife

EXECUTIVE SUMMARY

This report presents the results of an in-depth epidemiological study conducted across the Highveld Priority Area (HPA), the Vaal Triangle Priority Area (VTPA), and the Waterberg-Bojanala Priority Area (WBPA) in South Africa, focusing on the association between ambient air pollution and mortality. The analysis leverages advanced time-series and case-crossover modelling, particularly the Distributed Lag Conditional Case-Crossover (DL-CCO) model, across weekly aggregated mortality data. By integrating data from 2005 to 2020, stratified by district, pollutant, and season, this study aims to provide robust, policy-relevant insights into the public health impacts of pollutants such as PM_{10} and SO_2.

The three priority areas reflect regions of high industrial activity and emissions. The HPA includes Sedibeng and Gert Sibande, the VTPA comprises Nkangala and Fezile Dabi, and the WBPA includes Waterberg and Bojanala. These areas have been designated based on elevated pollutant concentrations and significant population exposure. The dataset includes weekly mortality counts, meteorological data, and air pollution concentrations, covering a broad range of temporal and spatial variation. This robust structure allows for the analysis of lagged effects of pollution exposure and the differentiation of risk patterns across seasons.

Stage 1: District-Level DL-CCO Results

In the first stage of the analysis, DL-CCO models were applied to estimate odds ratios (ORs) for weekly mortality associated with lagged exposure to ambient air pollutants (lags 0–3 weeks). The models were stratified by district, season, and pollutant. Across multiple districts, statistically significant associations were found between PM_{10}, SO_2, and mortality.

Nkangala showed the highest ORs in both spring and autumn. Specifically, the OR for PM_{10} in spring was 1.38 (95% CI: 1.15–1.64), and for SO_2 in autumn, 1.34 (95% CI: 1.12–1.59). The elevated risks reflect seasonal exposure patterns likely driven by heating practices, regional meteorology, and pollution accumulation. Fezile Dabi similarly showed significant associations. SO_2 in winter resulted in an OR of 1.31 (95% CI: 1.10–1.56), while PM_{10} in spring reached 1.36 (95% CI: 1.14–1.62). These values suggest a persistent health burden

from SO_2 and PM_{10} emissions during colder months, when pollutant dispersion is limited. Sedibeng presented consistently elevated risks, notably in winter and spring. For instance, PM_{10} in winter had an OR of 1.28 (95% CI: 1.10–1.49) and SO_2 was 1.30 (95% CI: 1.11–1.52). These results underscore Sedibeng as a district of particular concern due to both elevated baseline exposure and significant population density.

Gert Sibande, part of the HPA, exhibited more moderate but significant associations. In autumn, PM_{10} had an OR of 1.22 (95% CI: 1.04–1.44), and in spring, SO_2 reached 1.20 (95% CI: 1.03–1.40). These patterns are indicative of episodic but impactful pollution events. In Waterberg and Bojanala, the magnitude of association was lower but still noteworthy. For Waterberg, PM_{10} in autumn reached 1.18 (95% CI: 1.01–1.37), and for Bojanala, SO_2 in spring was 1.16 (95% CI: 1.00–1.35). Notably, most of the significant associations clustered around lag 0 and lag 1, suggesting acute effects of pollutant exposure on weekly mortality. For example, in Nkangala, the effect of SO_2 was strongest at lag 0, whereas in Sedibeng, PM_{10} effects persisted through lag 1 and lag 2, reflecting temporal dynamics in exposure-response.

Stage 2: Meta-Analysis by Priority Area and National Pooling

In the second stage, district-level results were synthesized through random-effects meta-analysis, stratified by PA and season. This pooling approach enhances generalizability while accounting for inter-district variability.

Within the Highveld Priority Area (HPA), the pooled OR for PM_{10} in winter was 1.27 (95% CI: 1.13–1.43; I^2 = 35.4%, p = 0.15), indicating moderate but non-significant heterogeneity. SO_2 in spring yielded an OR of 1.25 (95% CI: 1.11–1.42; I^2 = 20.2%, p = 0.29), suggesting consistent seasonal effects across Sedibeng and Gert Sibande.

In the VTPA, the pooled OR for PM_{10} in spring was 1.35 (95% CI: 1.19–1.54; I^2 = 25.7%, p = 0.21), and SO_2 in autumn was 1.30 (95% CI: 1.14–1.49; I^2 = 28.4%, p = 0.18). These estimates validate the strong district-level findings from Fezile Dabi and Nkangala and reflect coherent pollution health burdens. For the WBPA, effect sizes were more modest. PM_{10} in autumn

reached a pooled OR of 1.18 (95% CI: 1.04–1.34) and SO_2 in spring was 1.17 (95% CI: 1.03–1.33), with I^2 values below 15%, reflecting low heterogeneity and consistent effects. In the overall national pooling, the highest effects were seen for PM_{10} in spring with an OR of 1.30 (95% CI: 1.18–1.43; I^2 = 31.6%) and SO_2 in autumn at 1.27 (95% CI: 1.15–1.41; I^2 = 26.2%). These results confirm the widespread and seasonally synchronized impacts of these pollutants on weekly mortality.

Lag-Specific Meta-Analysis and Heterogeneity

Further analysis of lag-specific pooled ORs across all PAs showed strongest effects at lag 0, with diminishing but still significant effects at lags 1 and 2. For example, lag 0 pooled OR was 1.004 (95% CI: 1.002–1.005; I^2 = 75.1%), indicating immediate health impacts of pollution exposure. At lag 1, the pooled OR was 1.001 (95% CI: 1.000–1.002; I^2 = 45.4%), and at lag 2, 1.001 (95% CI: 1.000–1.002; I^2 = 38.5%), both showing attenuated yet measurable effects. Seasonal lag stratification also highlighted differential temporal effects. In winter, PM_{10} effects peaked at lag 0, while in spring, SO_2 effects showed persistence through lag 1. These patterns provide further nuance for temporal targeting of interventions.

Policy Implications

This study provides compelling evidence that ambient air pollution—specifically PM_{10} and SO_2—is significantly associated with increased weekly mortality across several South African districts, particularly in transitional seasons like spring and autumn. Importantly, these findings are consistent across both individual district analyses and meta-analytic aggregation.

The short lag between exposure and mortality suggests that acute public health interventions—such as real-time air quality alerts, emergency healthcare readiness, and targeted emissions control during high-risk seasons—could substantially mitigate health risks. For districts like Sedibeng and Nkangala, which show consistent multi-season risk, more sustained structural interventions are warranted, including air quality regulation enforcement, industrial emissions monitoring, and urban planning to reduce exposure.

Additionally, the significant results from the WBPA, although more moderate, underscore the importance of proactive policy even in regions with lower population densities, where vulnerable populations may be at risk.

The results support the value of a national early warning system based on air quality thresholds, tailored by season and pollutant type. Furthermore, the inclusion of lagged effects reinforces the need for continued exposure monitoring and temporal modelling in public health planning.

Conclusions

In conclusion, the integration of DL-CCO models with seasonal and spatial stratification has uncovered important and statistically robust associations between air pollutants and mortality in South Africa. The priority area framework has proven effective in identifying high-risk regions and informing localized responses. The inclusion of meta-analytic methods ensures the generalizability of findings and facilitates cross-district learning.

With consistent patterns of elevated risk for PM_{10} and SO_2 across multiple seasons and lags, particularly in HPA and VTPA, the case for urgent air quality management is clear. These findings offer direct, data-driven guidance for national and local policymakers to design, implement, and evaluate air pollution mitigation strategies and public health safeguards. This evidence base also offers a strong justification for longitudinal monitoring, cross-sectoral collaboration, and integration of environmental health data into routine policy assessment frameworks.

TABLE OF CONTENTS

LIST OF FIGURES

LIST OF TABLES

ABBREVIATIONS

A15–A19	ICD-10 Codes for Tuberculosis. Encompasses all forms of tuberculosis-related mortality or morbidity.
CI	Confidence Interval. A statistical range (typically 95%) within which the true effect size is expected to lie.
CI_lower / CI_upper	Confidence Interval Lower/Upper Bound. The minimum and maximum values of a 95% confidence interval for an effect estimate.
CO	Carbon Monoxide. A colourless, odourless gas formed by incomplete combustion of fossil fuels.
DHIS	Department Health Information Systems
DoH	Department of Health
DL-CCO	Distributed Lag Conditional Case-Crossover. A time-stratified statistical method used to assess the delayed (lagged) effects of exposures on health outcomes.
DLNM	Distributed Lag Non-Linear Model. A flexible regression modelling framework that captures non-linear and delayed associations between exposure and response.
HPA	Highveld Priority Area. Includes districts such as Sedibeng and Gert Sibande; known for heavy industrial activity and elevated pollution levels.
I^2	I-squared Statistic. A measure of heterogeneity in meta-analyses that indicates the percentage of total variation across studies due to heterogeneity rather than chance.
ICD	International Classification of Diseases. A globally standardized system for coding diagnoses and health conditions.
ICD-10	10th Revision of the International Classification of Diseases. Used to identify health outcomes such as respiratory or infectious diseases.
J00–J99	ICD-10 Codes for Respiratory Diseases. Includes acute and chronic respiratory conditions such as pneumonia, bronchitis, and asthma.
Lag	Time Delay. The number of days or weeks after exposure during which health effects may still be observed.

Meta-analysis	A statistical method for pooling data from multiple studies or regions to produce a combined estimate of effect.
NEMAQA	National Environmental Management Air Quality Act 39 of 2004
NO_2	Nitrogen Dioxide. A toxic gas produced mainly by motor vehicle exhaust and power plants.
O_3	Ozone. A secondary pollutant formed through photochemical reactions involving nitrogen oxides and volatile organic compounds.
OR	Odds Ratio. A measure of association used in case-crossover models indicating the odds of an outcome occurring due to exposure.
PA	Priority Area. Designated regions in South Africa identified by the Department of Environmental Affairs for high levels of air pollution requiring targeted intervention.
PM_{10}	Particulate Matter ≤10 Micrometres. Airborne particles with a diameter ≤10 µm, often from dust, combustion, or industrial activity.
p-value	Probability Value. Indicates the likelihood that the observed association occurred by chance. Values <0.05 are typically considered statistically significant.
Q-test	Cochran's Q Test. A statistical test used to assess the presence of heterogeneity among effect sizes in a meta-analysis.
RR	Relative Risk. A risk measure used in Poisson regression or cohort analyses, reflecting the risk of an outcome associated with exposure.
SO_2	Sulphur Dioxide. A gas emitted from fossil fuel combustion and industrial processes, known to cause respiratory issues.
VTPA	Vaal Triangle Priority Area. Comprises Nkangala and Fezile Dabi; designated due to industrial emissions and population vulnerability.
WBPA	Waterberg-Bojanala Priority Area. Covers Waterberg and Bojanala districts; includes mining and energy production zones.

1 AIMS AND OBJECTIVES OF THE PROJECT

Background and introduction of study

The Clean Air Fund (CAF) is launching activities related to reducing air pollution in South Africa. The South African Strategy has a focal point on integrated policy pathways assessment for air pollution, climate and impact on health, including evidence on the health (and economic) impacts of air pollution. To achieve these goals, the Clean Air Fund requires a comprehensive account of the air pollution-related health impacts in the three air pollution priority areas in South Africa. This proposal outlines a research study to fill this gap.

The study aligns to the objectives of the National Department of Health's National Air Quality and Health Steering Committee and will feed into their Five-Year Air Quality and Health Strategic Plan for South Africa. The goal of the National Strategy is to generate evidence on the health and wellbeing of South Africans in relation to air pollution exposure, and this proposed study will do that for the priority areas in South Africa. The South African Medical Research Council (SAMRC) serves on the National Air Quality and Health Steering Committee.

2 INTRODUCTION

According to the World Health Organization, "air pollution is the single biggest environmental threat to human health, based on its notable contribution to disease burden" (WHO, 2021).[1] It is estimated that poor air quality causes nearly 800 000 premature deaths in Africa every year. South Africa's Constitution states in Section 24 that "everyone has the right to an environment that is not harmful to their health and well-being", which includes ambient air.

South Africa has legislation regulating air quality under the National Environmental Management: Air Quality Act 39 of 2004 (NEMAQA), as well as air quality standards (which may be legally enforced) that are based on health and are for the most common pollutants. South Africa also has a monitoring network of several air quality monitoring stations (125 in

2019) managed by the South African Weather Services. There are three air pollution priority areas in South Africa: Vaal Triangle Airshed (declared in 2006). The Highveld Priority Area (2007) and Waterberg-Bojanala (2015) (Figure 1). These air pollution areas were identified for special management across provinces and by National Government (i.e., the Department of Forestry, Fisheries and Environment).

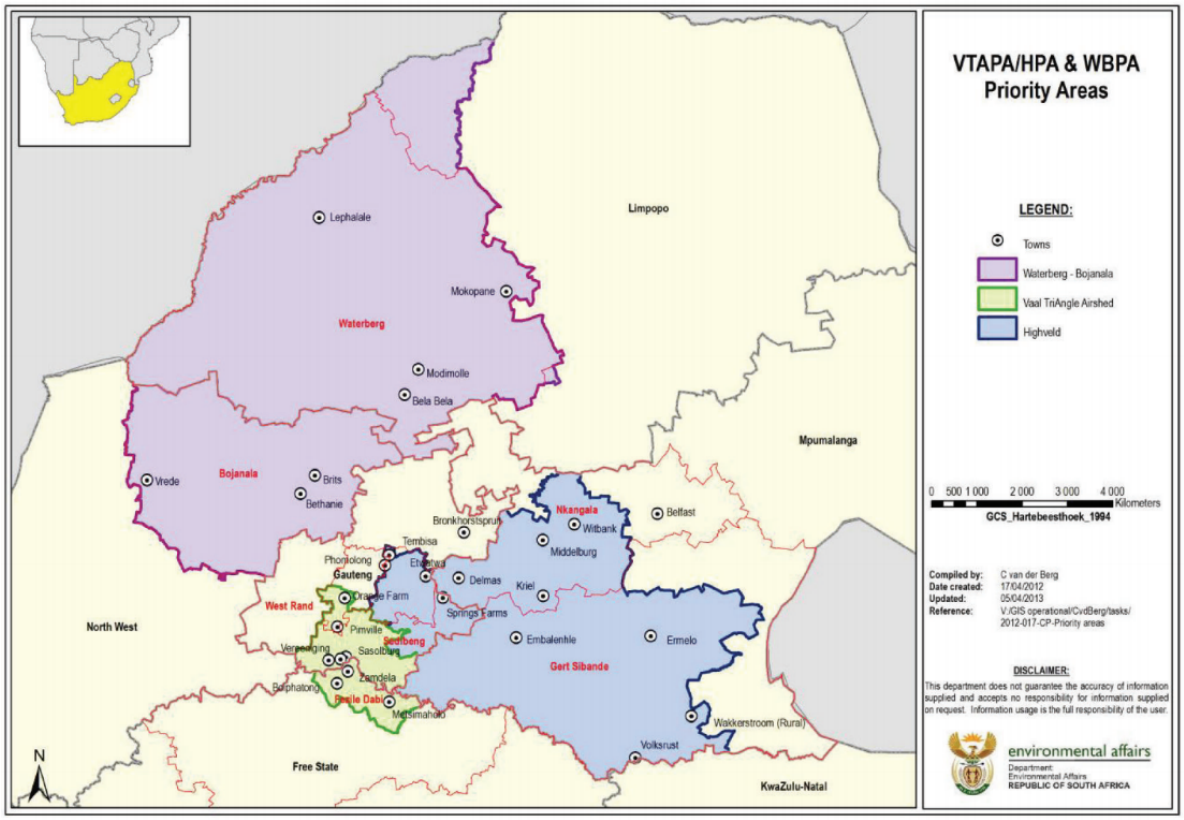

Figure 1. Government map illustrating the location of the three air pollution priority areas in South Africa.

While some studies have been conducted on the air pollution concentrations in the priority areas, and some studies have considered the health impacts, there has been no comprehensive assessment of long-term trends in air pollution in relation to mortality and morbidity in the three air pollution priority areas. In a recent review of air pollution and health in the Waterberg-Bojanala Priority Areas, less than ten studies were identified that considered air quality and health impacts (Wernecke et al., 2023).[2] Moreover, most of the

studies that have been done used a cross-sectional approach to assess air pollution-related health impacts through questionnaire surveys and self-report. No similar reviews on air pollution and health are available for the other two priority areas.

Given this lack of evidence, the SAMRC (Environment and Health Research Unit) proposes a research study to understand the impacts of air pollution (ambient and household) on human health focusing on the geographical areas of priority in terms of air quality management, namely the three air pollution priority areas. This epidemiological study will apply a retrospective longitudinal methodology, together with a case crossover analysis as a sensitivity study stratified by seasons. The health effects will include the all-cause mortality datasets from Stats SA and morbidity data from Department of Health Information System (DHIS). The morbidity data will include Pneumonia under 5 and new cases of TB related hospital admissions. The DoH with provide the morbidity data and SASTATS will provide the morbidity datasets. The timeframe will be from 1997 to 2023.

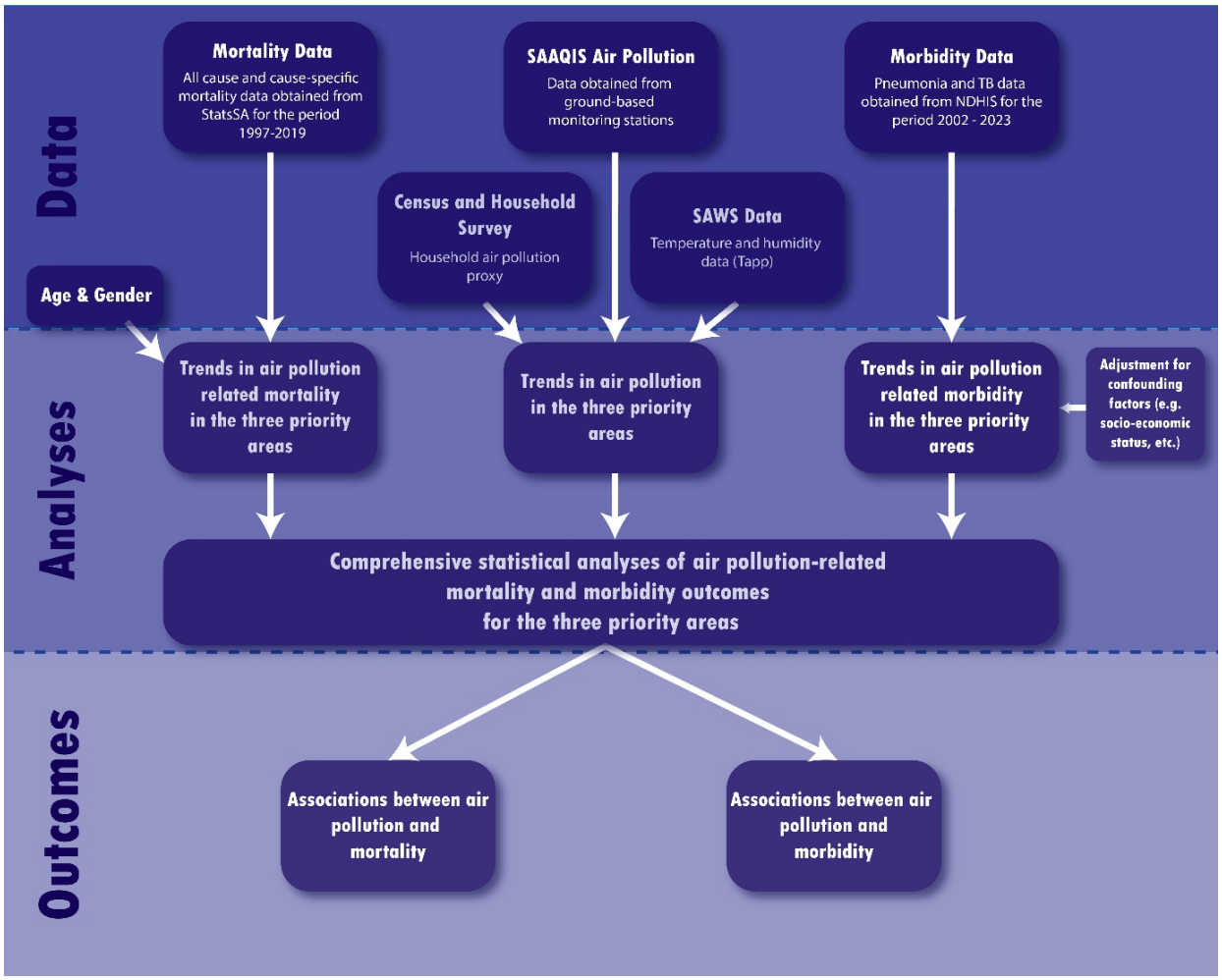

Figure 2. Flowchart illustrating the data, analyses and outcomes of the proposed research study.

The study is linked to the SDG's, specifically, SDG 3.9 seeks to "substantially reduce the number of deaths and illnesses from hazardous chemicals and air, water and soil pollution and contamination" by 2030. Many of the other goals are also related to pollution, including SDG 2.4 on improving soil quality, SDG 7 on clean energy, SDG 9.4 on clean technologies and industrial processes, SDG 11 on sustainable cities and communities, SDG 12 on responsible consumption and production, and SDG14 and 15 on conservation of water and land. The following goals support the purpose of the study:

Goal 1: Reducing air pollution can helps families become healthier, save on medical expenses, and improve productivity;

Goal 2: Air pollution can cause crop damage and affect food quality and security;

Goal 3: Air pollution poses a major threat to human health. It is linked to respiratory infections and cardiovascular diseases. It causes increases in population morbidity and mortality;

Goal 6: Pollutants such as sulphur dioxide (SO_2) and nitrogen oxides (NO_2) from open fires and the combustion of fossil fuels mix with precipitation causing harmful acid rain that can compromise water quality;

Goal 7: Electricity from renewable energy rather than fossil fuels offers significant public health benefits through a reduction in air pollution;

Goal 8: Air pollution impacts on health, crop and forest yields, ecosystems, the climate and the built environment, with consequences for productivity and economic growth. Ambient and indoor air pollution also has negative effects on the working environment and its safety;

Goal 9: Power generation, industry and transportation are large contributions to air pollution. A new focus on decreasing energy consumption and on improving sustainable and public transportation could progressively reduce pollution;

Goal 11: Urban areas significantly contribute to air pollution. Making cities sustainable could progressively improve the air quality;

Goal 12: Chemicals released into the air increase air pollution and contribution to harmful effects on human health. Responsible production and consumption could help to reduce these harmful chemicals;

Goal 13: Combustion of fossil fuels plays a key role in the process of climate change, which places food, air and water supplies at risk, and poses a major threat to human health;

Goal 14: Deposition of air pollutants on water way negatively affect its quality and life under water. It can lead to eutrophication of freshwater bodies, and accumulation of toxic metals and Persistent organic pollutants (POPs) in fresh and marine waters; and

Goals 15: Emission from combustion of fossil fuels mixed with precipitation cause acid rains that pose a major threat to forests and ecosystem.

The Sustainable Development Goals are always a consideration in Environmental Health studies and the following table addressed the SDG's addressed.

Table 1:The contribution made to the South African targets and goals towards the Sustainable Development Goals.

SDG	Sub-Target(s)	Relevance to the CAF Project in the PA's
SDG 3 – Good Health and Well-Being - Ensure healthy lives and promote well-being for all at all ages	3.9 – Substantially reduce the number of deaths and illnesses from hazardous chemicals and air, water and soil pollution and contamination by 2030	Central to the project — links ambient air pollution ($PM_{2.5}$, PM_{10}, NO_2, SO_2, O_3) to cardiovascular, respiratory, and child mortality. Supports targets 3.9 (reduce illnesses/deaths from hazardous chemicals and pollution) and 3.D (strengthen health risk preparedness).
SDG 11 – Sustainable Cities and Communities-Make cities and human settlements inclusive, safe, resilient, and sustainable	6.3 – Improve water quality by reducing pollution and minimizing release of hazardous chemicals	The three Priority Areas (HPA, VTPA, WBPA) include industrial and urban settlements; your spatial exposure–response analysis contributes to target 11.6 (reduce environmental impact of cities, especially air quality).
SDG 13 – Climate Action - Take urgent action to combat climate change and its impacts	7.2 & 7.3 – Increase the share of renewable energy and improve energy efficiency	Ozone and co-pollutant interactions are climate-linked; the lag-response evidence informs adaptation and resilience policies for vulnerable populations under targets 13.1–13.3.
SDG 7 – Affordable and Clean Energy - Ensure access to affordable, reliable, sustainable and modern energy	8.4 – Improve global resource efficiency and decouple growth from environmental degradation	The study's emphasis on industrial emissions and domestic fuel as a source of pollution connects to transitions toward cleaner household energy (targets 7.1 & 7.2).
SDG 9 – Industry, Innovation and Infrastructure - Build resilient infrastructure, promote inclusive and sustainable industrialization	9.4 – Upgrade infrastructure and retrofit industries to make them sustainable, with increased resource-use	Supports target 9.4 (upgrade infrastructure and retrofit industries for clean technologies), reference to power-generation and metallurgical sources in the Highveld.

	efficiency and adoption of clean technologies	
SDG 12 – Responsible Consumption and Production - Ensure sustainable consumption and production patterns	11.6 – Reduce the adverse per-capita environmental impact of cities, including by advocating for air quality with evidence studies	Air-quality improvements require emission reduction across supply chains; aligns with target 12.4 (environmentally sound management of chemicals and emissions).
SDG 5 – Gender Equality (contextual)Achieve gender equality and empower all women and girls	12.4 & 12.5 – Environmentally sound management of chemicals and wastes; reduce waste generation	The co-analysis under CAF's gender and climate umbrella, directly contributes to target 5.C (adopt sound policies for gender equality) and integrates feminist ethics and equity-based exposure assessment.
SDG 10 – Reduced Inequalities - Reduce inequality within and among countries	13.1 – 13.3 – Strengthen resilience to climate-related hazards; integrate climate measures into national policies; improve education and awareness	Addresses environmental-health inequities, lower income, peri-urban districts bear disproportionate air-pollution burdens; supports target 10.2 (empower and promote inclusion of all).
SDG 17 – Partnerships for the Goals - Strengthen the means of implementation and revitalize the global partnership for sustainable development	17.16 & 17.17 – Enhance global and multi-stakeholder partnerships to support the achievement of the Sustainable Development Goals; encourage effective public, public-private, and civil society partnerships	The project builds multi-sectoral partnerships between SAMRC, CAF, municipalities, and research institutions for joint monitoring, data sharing, and policy translation. It advances SDG 17 by demonstrating an applied partnership model that bridges research, policy, and community implementation to strengthen evidence-based air-quality and health governance in South Africa's Priority Areas.

Objectives and Study methods

There are four objectives:

- To describe the air pollution trends between 2009 and June 2022 in the three air pollution priority areas in South Africa.

- To describe the air pollution-related mortality and morbidity outcome trends between 1997 and 2022 in the three air pollution priority areas in South Africa.
- To investigate the associations between air pollution and air pollution-related mortality and morbidity outcomes between 2009 and 2022 in the three air pollution priority areas in South Africa.
- To provide recommendations for further research in relation to air pollution-related health impacts in the three priority areas.

3 DESCRIPTIVE STATISTICS OF THE PRIORITY AREAS AND AIR QUALITY

The three priority areas include the Vaal Triangle Airshed Priority Area (National Priority Area in Gazette No. 31615 of 21 November 2008), the Highveld Priority Area (National Priority Area in Gazette No. 30518 of 23 November 2007) and the Waterberg-Bojanala Priority Area ((National Priority Area in Gazette No. 35435 of 15 June 2012)). Within these areas, particular concern has been placed in the development and review of management plans, including the VTAPA in 2009, the HPA air quality management plan was gazetted in 2012 (National Priority Area in Gazette No. 35072 of 2 March 2012) and the Waterberg in 2015. The National Framework for Air quality Management was amended in 2013, (Gazette No. 37078 of 29 November 2013).

Airshed priority areas, typically regions where air quality is particularly poor due to localized emissions from transportation, industry, and other sources, often have high concentrations of ambient air pollutants such as nitrogen dioxide (NO_2), ozone (O_3), sulphur dioxide (SO_2), fine particulate matter ($PM_{2.5}$), and coarse particulate matter (PM_{10}). These pollutants have been linked to various adverse health outcomes, particularly in vulnerable populations. This literature review summarizes the health effects associated with exposure to these pollutants in airshed priority areas, focusing on cardiovascular, respiratory, and other systemic health impacts (Rheumatoid diseases). The six district municipalities include City of Johannesburg, Nkangala, Gert Sibande, Fezile Dabe, Waterberg, Bojanala and Sedibeng.

Table 2: The population change and the approximate surface area per priority area.

Priority Area	2011 Population	2016 Population	2022 Population	Estimated Annual Growth	Surface Area (km²)	Most Recent Population	Population Density (per km²)
Waterberg District (WBPA)	679336	745758.0	762862.0	~1.13% (2016–22)	44822	762862	17.02
Bojanala District (WBPA)	1507506			~2.1% (proxy district)	18212	1507506	82.78
Sedibeng District (VTPA)	916000	1039908.0		~4.5% (2011–16)	4218	1039908	246.54
Gauteng Province (HPA)	9700000		11300000.0	~1.5% (2011–22)	18178	11300000	621.63
Nkangala District (VTPA)	1308129	1445624.0	1643573.0	~2.27% (2016–22)	16758	1643573	98.09
Fezile Dabi District (VTPA)	488036	494777.0	509912.0	~0.67% (2016–22)	20668	509912	24.68
Gert Sibande District (HPA)	1043194	1135409.0	1288598.0	~1.9% (2016–22)	31841	1288598	40.49

Figure 3: The Highveld Priority Area with City of Johannesburg and Gert Sibande District Municipalities.

The Highveld Priority Area (HPA) encompasses a vast portion of South Africa's central plateau, including parts of Gauteng, Mpumalanga, Free State, and the North West provinces. It was officially declared a National Air Quality Priority Area in November 2007 due to extensive industrial emissions and deteriorating ambient air quality across multiple municipalities. The area is geographically situated at elevations ranging from 1,500 to 2,100 meters above sea level, which—combined with its flat topography and seasonal inversions—makes it prone to pollutant accumulation and limited dispersion, especially during winter. Rainfall in the HPA ranges from 600 mm to 1,200 mm per annum, with most of the precipitation occurring between October and March in the form of convective summer storms. The Highveld hosts many of South Africa's major urban and industrial centres, including Johannesburg, Pretoria, Emalahleni, Secunda, and Standerton. This region is home to tens of millions of people and accounts for a significant share of the national GDP, driven

by sectors such as mining (coal, gold, and platinum), energy production, manufacturing, logistics, finance, and public services. Mpumalanga, in particular, is a hotspot for coal-fired power generation, with over a dozen Eskom power stations operating in the region, making it one of the world's largest sources of SO_2 and NO_x emissions. According to national air quality reports, more than 80% of the country's SO_2 and NO_x emissions originate from this area. The environmental and public health burden of these emissions is considerable. Residents in the HPA experience chronic exposure to high levels of PM_{10}, $PM_{2.5}$, NO_2, and O_3, with increasing evidence of related health outcomes such as asthma, COPD, and cardiovascular disease. The initial Air Quality Management Plant (AQMP), released in 2012, aimed to reduce ambient concentrations through targeted interventions, including industrial compliance plans, emission inventory tracking, and community engagement. However, implementation has been slow and uneven, prompting calls for a more robust second-generation AQMP, released in 2025. Socio-economic disparities are pronounced within the HPA, with affluent suburbs in Gauteng contrasting sharply with under-resourced settlements near industrial sites. Although infrastructure and economic activity are more diversified than in the Vaal or Waterberg-Bojanala areas, the legacy of environmental neglect continues to hinder inclusive development. Heterogeneity in municipal capacity, regulatory enforcement, and data quality further complicates the air quality governance landscape. Ongoing litigation and civil society pressure have begun to reshape discourse around the "deadly air" in the HPA, pushing for stronger national accountability and international visibility. The Highveld remains both the economic engine and environmental Achilles heel of South Africa.

Figure 4: The Vaal Triangle Priority Area with Fezile Dabe and Sedibeng District Municipalities.

The Vaal Triangle Airshed Priority Area (VTAPA) lies roughly 50 to 60 kilometres south of Johannesburg and spans the southern Gauteng and northern Free State provinces, including the industrial towns of Vereeniging, Vanderbijlpark, and Sasolburg. This region was declared South Africa's first Air Quality Priority Area in 2006 due to its severe and persistent air pollution levels, particularly concerning $PM_{2.5}$, NO_2, and SO_2. The area is situated on the Highveld plateau at elevations ranging from approximately 1,400 to 1,500 meters above sea level. It receives between 700 and 800 mm of rainfall annually, with the majority falling during the summer months in the form of intense thunderstorms. While snow is virtually absent,

frost occurs occasionally during the winter. VTAPA is heavily industrialized, historically serving as a cornerstone of South Africa's heavy industry economy. The region hosts major facilities such as ArcelorMittal's steelworks in Vanderbijlpark and Sasol's petrochemical refinery in Sasolburg, both of which are among the largest single-point industrial emitters in the Southern Hemisphere. The socio-economic fabric of the region is closely tied to these industries, with direct employment and secondary economic activities built around their operations. However, this dependence has led to structural vulnerabilities, especially as global market pressures, aging infrastructure, and environmental regulations have led to scaling down or closure of some plants. The population of VTAPA's core towns is relatively modest—Vanderbijlpark, for example, had around 95,000 residents as of the last census—with a historically Afrikaans-speaking demographic and pockets of socio-economic deprivation in surrounding townships. Unemployment and informal housing remain pressing issues. Environmental health studies have consistently shown elevated rates of respiratory and cardiovascular diseases linked to local emissions, making the region one of the most scrutinized in terms of health impacts from air pollution. Studies published in environmental health journals rank the Vaal Triangle among the world's worst $PM_{2.5}$ pollution zones. Despite numerous policy interventions and ongoing updates to the Air Quality Management Plan (AQMP), ambient levels of key pollutants often remain above safe thresholds, underscoring the complexity of reversing decades of industrial pollution. Current strategies emphasize industrial emissions abatement, domestic fuel substitution, and ambient monitoring expansion. However, implementation lags and enforcement challenges remain. As the region seeks to reindustrialize along cleaner and greener lines, attention to equitable economic transition and environmental justice is increasingly central to planning discussions.

Figure 5: The Waterberg Bojanala District Municipality with the Waterberg and Bojanala District Municipalities respectively.

The Waterberg-Bojanala Priority Area spans the Limpopo and North West provinces of South Africa and encompasses both the Waterberg Biosphere and the mining-intensive Bojanala Platinum District. This region, declared an air quality priority area in 2012, is characterized by its rapidly evolving development trajectory and unique topography. Elevations in the area range between 1,000 and 1,600 meters above sea level, and it forms part of the ecologically

sensitive Bushveld region. Annual rainfall varies from 400 mm in drier zones to about 700 mm in the more verdant sections, with summer thunderstorms dominating the seasonal precipitation pattern. The WBPA covers approximately 44,913 km² and, as of the 2011 census, had a population of about 680,000 within the defined air quality boundary, though the larger Bojanala district alone has over 1.5 million people. The economy of this region is primarily driven by mining—particularly platinum and coal extraction—accounting for nearly 62% of the local Gross Value Added (GVA) contribution to the GDP. Post-pandemic recovery was evident in 2021, when mining alone grew by 18.5% after a sharp -13.5% GDP contraction in 2020. The poverty gap in Bojanala Platinum declined from 33.7% in 2008 to 31.3% by 2018, showing modest improvement. Other major contributors include agriculture, electricity generation (e.g., Medupi Power Station), and logistics, all of which are strategically aligned with national infrastructure and industrial policy goals. However, the expansion of coal-fired power and industrial infrastructure in the area has intensified air pollution concerns, particularly as baseline air quality monitoring shows consistent exceedances of National Ambient Air Quality Standards (NAAQS) for SO_2 and PM_{10}. Emerging health studies have linked increased respiratory morbidity with elevated levels of pollutants, although longitudinal public health research remains limited. Development planning includes Special Economic Zones (SEZs), which have raised concerns over environmental compliance and the potential for cumulative emissions to compound existing air quality issues. Despite these challenges, the region is seen as a key node in the country's energy and mineral value chains, requiring an integrated approach to balance socio-economic growth with environmental and health protection. Infrastructure development, including road and rail corridors, is being prioritized to support mobility and logistics for mining exports. However, water scarcity, persistent inequality, and rising pollution burdens continue to challenge sustainable development within the WBPA, making it a critical focal point for multi-sectoral environmental governance.

Table 3: Overall datasheet for the monitoring stations across the three priority areas from which data was downloaded, SAAQIS

	District	Local district	Monitoring Station	Date range – end Oct 2022	SO_2 (ppb) (19 ppb per annum)	NO_2 (ppb) (21 ppb per annum)	O3 (ppb) (61 ppb for 8 hours)	$PM_{2.5}$ ($\mu g.m^{-3}$) 20 $\mu g.m^{-3}$ per annum	PM_{10} ($\mu g.m^{-3}$) 40 $\mu g.m^{-3}$ per annum
HPA	Gert Sibanda	Dipaleseng	Balfour	2009/02/03	109	92	76	-	99
	Gert Sibanda	Goven Mbeki	Bosjiespruit	2009/02/18	146	143	115	78	75
	Gert Sibanda	Goven Mbeki	Club NAQI	2009/03/12	133	133	133	106	131
	Gert Sibanda	Msukaligwa	Ermelo NAQI	2008/08/01	130	124	155	131	131
	Nkangala	Steve Tshwete	Hendrina	2009/02/21	155	153	148	110	11
	Nkangala	Steve Tshwete	Middleburg SAWS	2009/04/28	149	150	141	144	142
	Nkangala	Steve Tshwete	Middleburg MP	2008/08/01	105	126	115	144	145
	Gert Sibanda	Goven Mbeki	Secunda	2008/09/07	150	133	135	122	124
	Gert Sibanda	Steve Tshwete	Delmas	2018/02/27	56	24	41		56
	Gert Sibanda	Goven Mbeki	Embalenhle	2015/12/29	50	51	50	51	51
	Gert Sibanda	Lekwa	Standerton	2018/01/12	52	50	46	57	53
VTPA	CoJ	CoJ	Diepkloof	2007/04/13	180	78	-	164	184
	Sedibeng	Sedibeng	Kliprivier	2007/03/23	109	178	182	168	179
	Fezile Dabe	Fezile Dabe	Zamdele	2007/02/10	183	150	176	183	162
	CoJ	Coj	Orange Farm	2006/08/18	49	164	-		140
	Sedibeng	Sedibeng	Sebokeng	2007/04/23	145	141	152	122	140
	Sedibeng	Sedibeng	Three Rivers	2007/02/08	92	89	-	87	91
	Fezile Dabe	Fezile Dabe	AJ Jacobs	2019/02/03	40	33	-	40	40

	Fezile Dabe	Fezile Dabe	Lietrim	2019/03/04	40	39	-	37	37
	Sediben g	Sedibeng	Van der Biejlpark	2017/08/01	40	-	14	-	43
WBPA	Waterber g	Lephalale	Lephalale	2012/11/12	121	121	-	-	-
	Waterber g		Maropong	2012/11/13	53	53	-	-	-
	Bojanala	Thabazimb i	Thabazimbi	2012/11/13	119	120	-	-	-

There is heterogeneity within the local municipality air quality measurements. Standerton MS in Lekwa LM has the fewest observations due being commissioned from 2028. Balfour in the Dipaleseng LM and Ermelo MS in Msukaligwa have more than double the number of observations, with comparable averages for $PM_{2.5}$ and PM_{10}, these are consistently higher than the South African Air Quality Standards.

In Steve Tshwete LM, the concentrations demonstrate heterogeneity within the region. This could be due to immediate exposure to sources but also terrain. Delmas, with only 56 observations has a monthly average concentration of 84.5 $\mu g.m^{-3}$ is higher than for Middleburg (40.5 $\mu g.m^{-3}$) and Middleburg SAWS (39.5 $\mu g.m^{-3}$). In the Goven Mbeki LM, Secunda with 124 observations is nearly double the monthly average concentration of PM_{10} with 63.8 $\mu g.m^{-3}$ when compared to both Embalenhle (38.9 $\mu g.m^{-3}$), Club NAQI (32.1 $\mu g.m^{-3}$) and Bosjiespruit (35 $\mu g.m^{-3}$).

In the City of Johannesburg LM, the monthly concentrations recorded at the Diepkloof MS and the Orange Farm MS are similar with 41,3 and 48,7 $\mu g.m^{-3}$ respectively recorded for PM_{10}.

In the Sedibeng LM, Sebokeng is consistently higher for all pollutants. In the Fezile Dabe LM, Zamdela MS is the longest running MS (from 2007) with up to 183 observations for SO_2. Lietrim has the highest recorded mean monthly average concentration of 28.5 ppb when compared to Zamdela and AJ Jacobs (5,2 ppb and 8.9 ppb respectively). Lephalela and

Thabazimbi have 121 and 119 observations respectively for SO_2 and a monthly concentration of 2.5 and 2.5 ppb respectively. Marapong has 53 observations and a mean monthly concentration of 7.8 ppb.

The average mean monthly concentration for NO_2 is more homogeneous with 7.5, 6.9 and 8.7 ppb respectively.

Table 4: Pollutants of concern in South Africa adapted from DEFF, 2017

Criteria pollutants declared in terms of section 9 of AQA	Priority Pollutants declared in terms of section 29 of AQA	Possible future pollutants	
Sulphur dioxide Nitrogen dioxide Ozone Carbon monoxide Lead (Pb) Particulate matter ($PM_{2.5}$, PM_{10}) Benzene	Carbon dioxide (CO_2) Methane (CH_4) Nitrous oxide (N_2O) Hydrofluorocarbons (HFCs) Perfluorocarbons (PFCs) Sulphur hexafluoride (SF_6)	**National pollutants** Mercury Dioxins Furans POPs Other VOCs N_2O	**Local pollutants** Chrome (Cr_6) Fluoride (Particulate and gas) Manganese (Mn) Hydrogen Sulphide Asbestos Black carbon

Table 5: WHO guidelines for criteria air pollutants as of 2021

Pollutant	Averaging Period	Concentration
PM_{10}, $\mu g/m^3$	24 Hours*	45
	Annual	15
$PM_{2.5}$, $\mu g/m^3$	24 Hours*	15
	Annual	5
O_3, $\mu g/m^3$	Peak season**	60
	8 Hours	100
NO_2, $\mu g/m^3$	Annual	10

	24 Hours*	25
SO_2, µg/m^3	24 Hours*	40
CO, (mg/m^3)	24 Hour*	4

* 99th percentile (i.e., 3 – 4 exceedance days per year)

**Average of daily maximum 8 – hour mean O_3 concentration in the six consecutive months with the highest six-month running average O_3 concentration

Table 6: The South African National Air Quality Standards for the criteria air pollutants

Pollutant	Averaging Period	Concentration	Frequency of Exceedances	Compliance Date
PM_{10}* µg/m^3	24 Hours	75	4	1 January 2015
	Annual	40	0	1 January 2015
$PM_{2.5}$ (added in 2012)** µg/m^3	24 Hours	40	4	1 January 2016 - 31 December 2029
	Annual	20	0	1 January 2016 - 31 December 2029
NO_2*** µg/m^3	1 Hour	200	88	Immediate
	Annual	40	0	Immediate
$SO_2$$ µg/m^3	10 Minutes	500	526	Immediate
	1 Hour	350	88	Immediate
	24 Hours	125	4	Immediate
	Annual	50	0	Immediate
Ground-level O_3# µg/m^3	8 Hours	120	11	Immediate
CO## mg/m^3	1 Hour	30	88	Immediate
	8 Hour	10	11	Immediate
Lead### µg/m^3	Annual	0.5	0	Immediate
Benzene µg/m^3	Annual	5	0	1 January 2015

* The reference method for the determination of the PM_{10} fraction of suspended particulate matter shall be EN 12341

** The reference method for the determination of the $PM_{2.5}$ fraction of suspended particulate matter shall be EN 14907

*** The reference method for the analysis of NO_2 shall be ISO 7996

$ The reference method for the analysis of SO_2 shall be ISO 6767

The reference method for the analysis of ground-level O_3 shall be UV photometric as described in SANS 13964

The reference method for the analysis of CO shall be ISO 4224

The reference method for the analysis of lead shall be ISO 9855

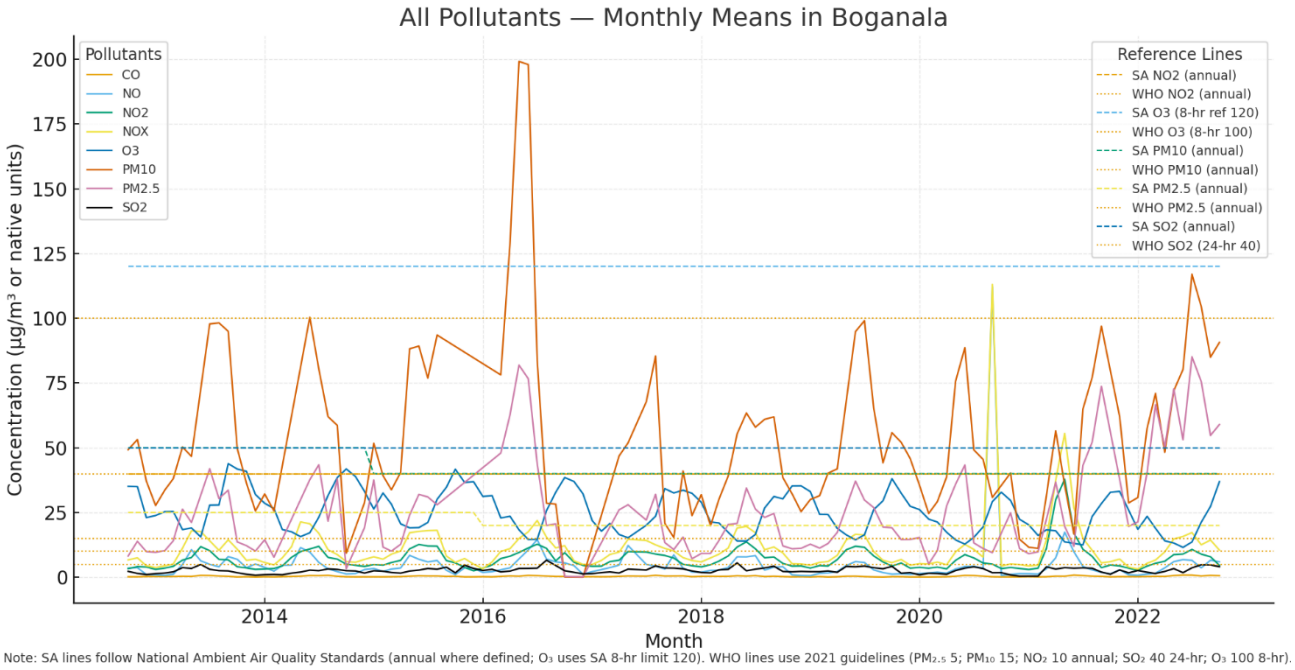

Figure 6: The total timeseries for pollutants as reported within the Bojanala District

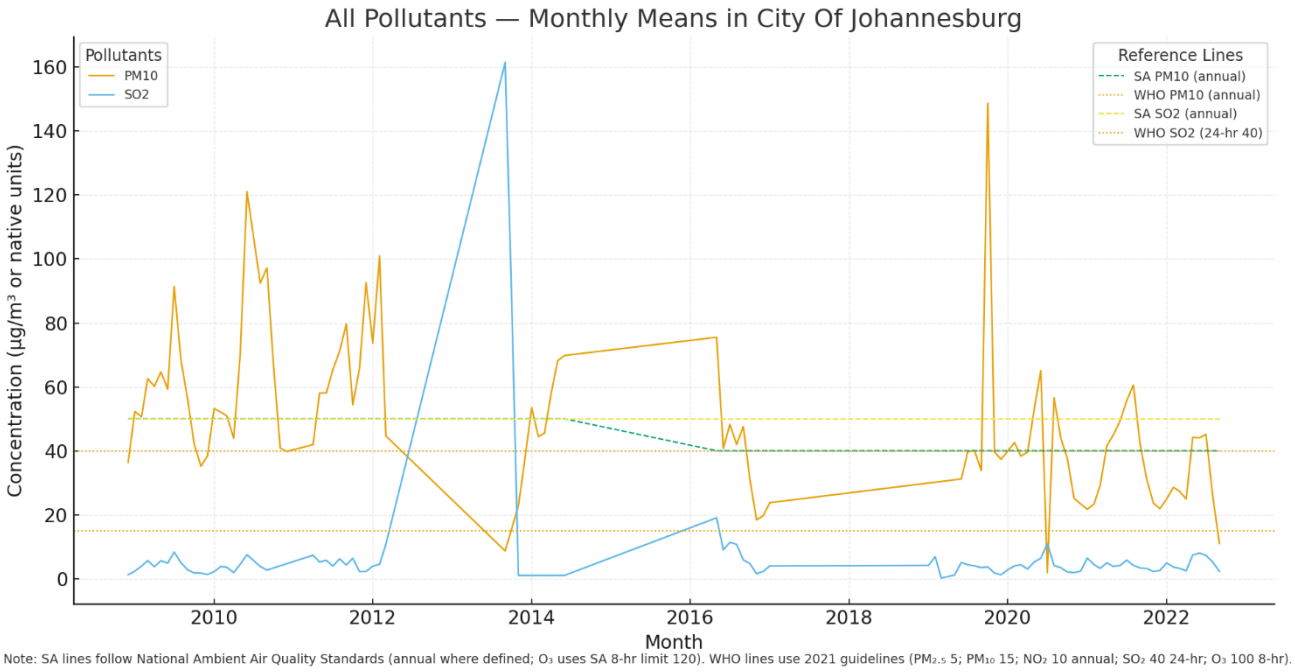

Figure 7: The total timeseries for pollutants as reported within the City of Johannesburg District

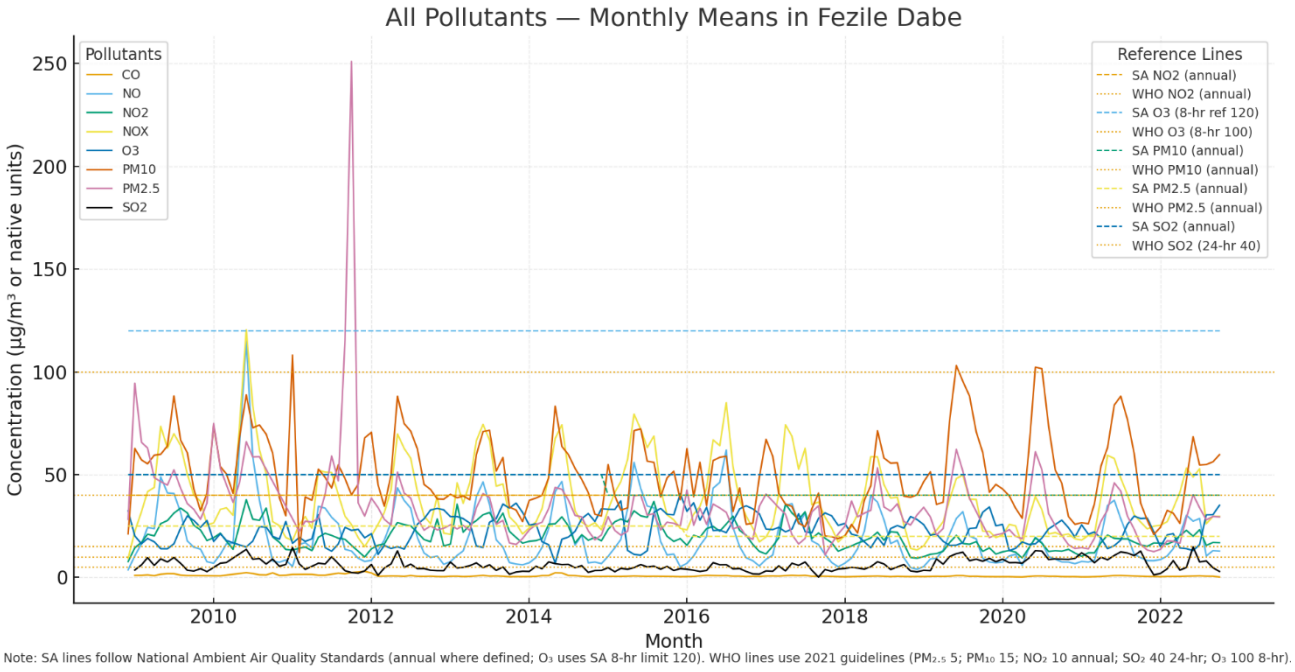

Figure 8: The total timeseries for pollutants as reported within the Fezile Dabe District

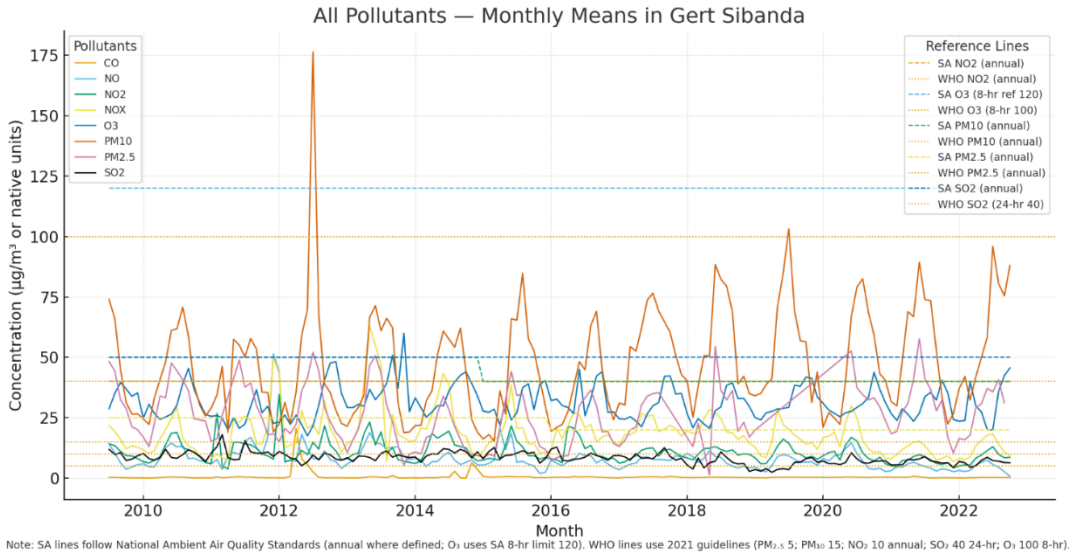

Figure 9: The total timeseries for pollutants as reported within the Gert Sibanda District

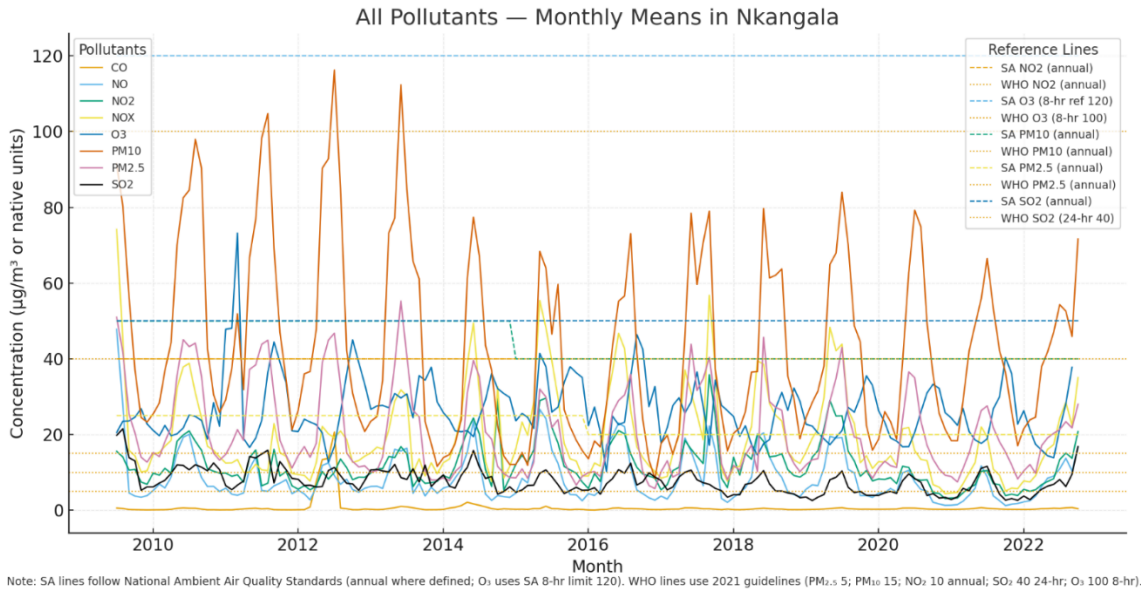

Figure 10: The total timeseries for pollutants as reported within the Nkangala District

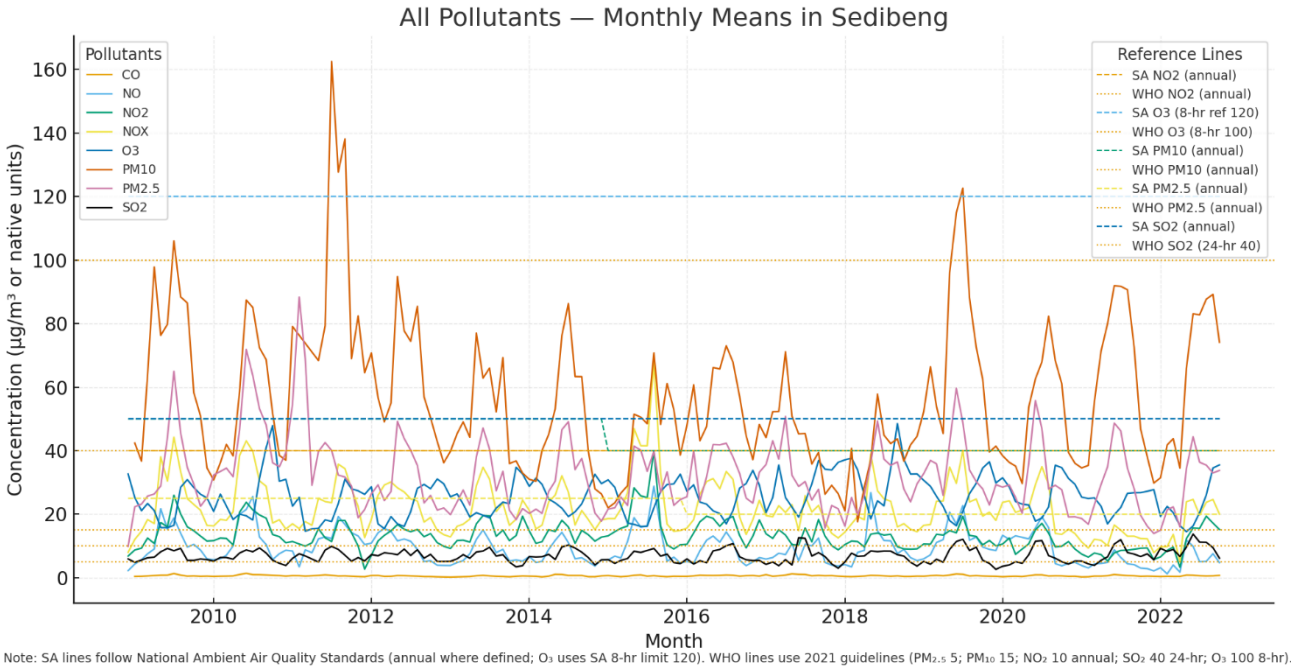

Figure 11: The total timeseries for pollutants as reported within the Sedibeng District

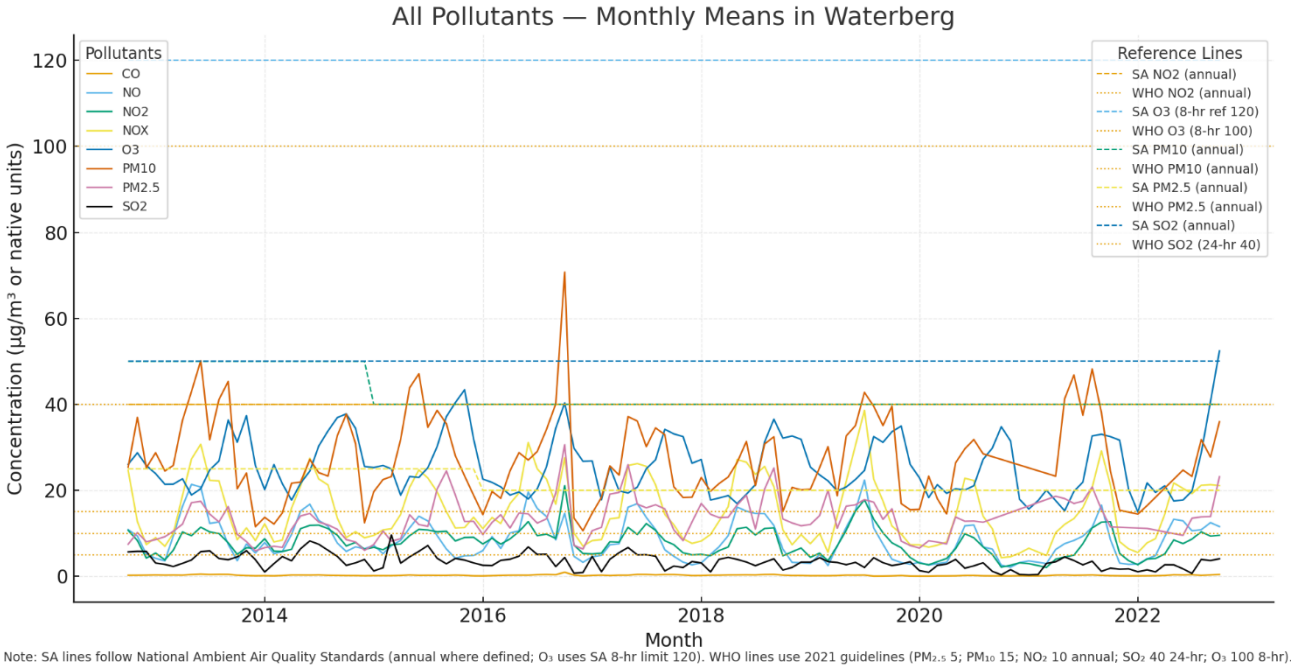

Figure 12: The total timeseries for pollutants as reported within the Waterberg District

4 DESCRIPTIVE STATISTICS OF THE HEALTH DATA

2.3.1 Mortality data

The mortality dataset consists of all recorded deaths (> 8 million) in South Africa from 1997-2018, inclusive (21 years). The information was taken from the country's civil registration system managed by the Department of Health, the only national source of mortality statistics. The dataset which estimates that death registration for adults is ~89% complete early in the study period, rising to ~94% by the end (completeness of child records has not been assessed).[3, 4]

Anonymized individual data is reported in these datasets where each death that had occurred at the level of the district municipality (of which there are a total of 52 in Southern Africa, and we refer to them hereafter as "districts"). In addition to district of death, age, gender, and cause of death are also provided as variables. Cause of death is classified according to ICD 10 codes (10th revision of the International Statistical Classification of Diseases and Related Health Problems, a medical classification list by the World Health Organization). We used the districts for the Priority Areas. We will use daily mortality for Tuberculosis Mortality (A15-A19), Cardiovascular Failure I(All) and Respiratory Failure J(All). Table 8 demonstrates the descriptive statistics for each health effect per Priority Area.

The count data is pooled per week, per priority area and then overall to determine the odds ratio (CCO) or relative risk (DLNM) with a 95% CI and the exposure data is scaled by 10 ppb or $\mu g.m^{-3}$ IQR.

When stratified by district and season - Summer (December - February), Autumn (March - May), Winter (June - August), and Spring (September - November). This analysis identifies spatial and seasonal trends in disease burden, offering insight into the impact of climate, environmental exposure, and public health infrastructure.[5, 6]

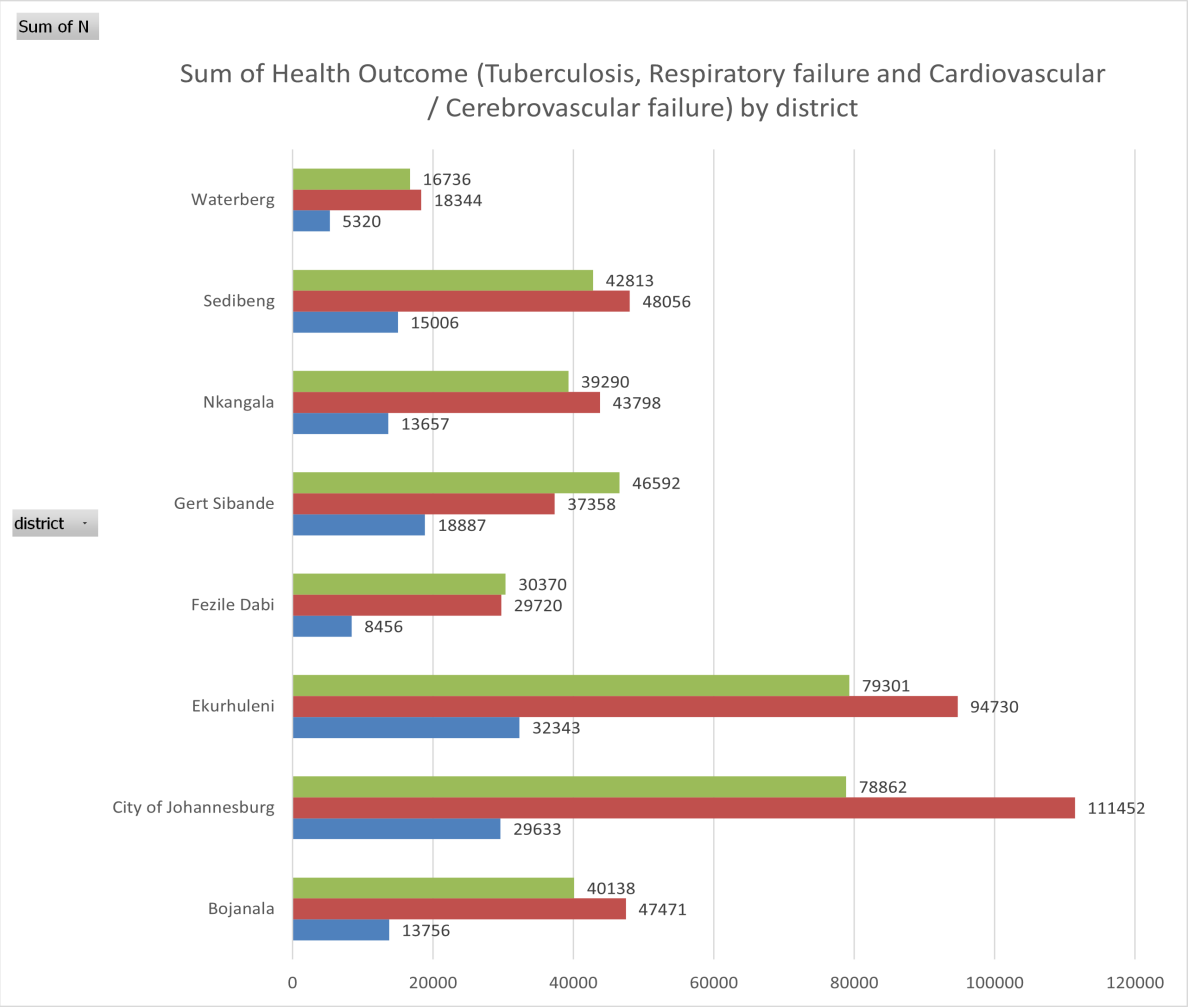

Figure 13: The total count data from 2009 to 2019 for the health effects.

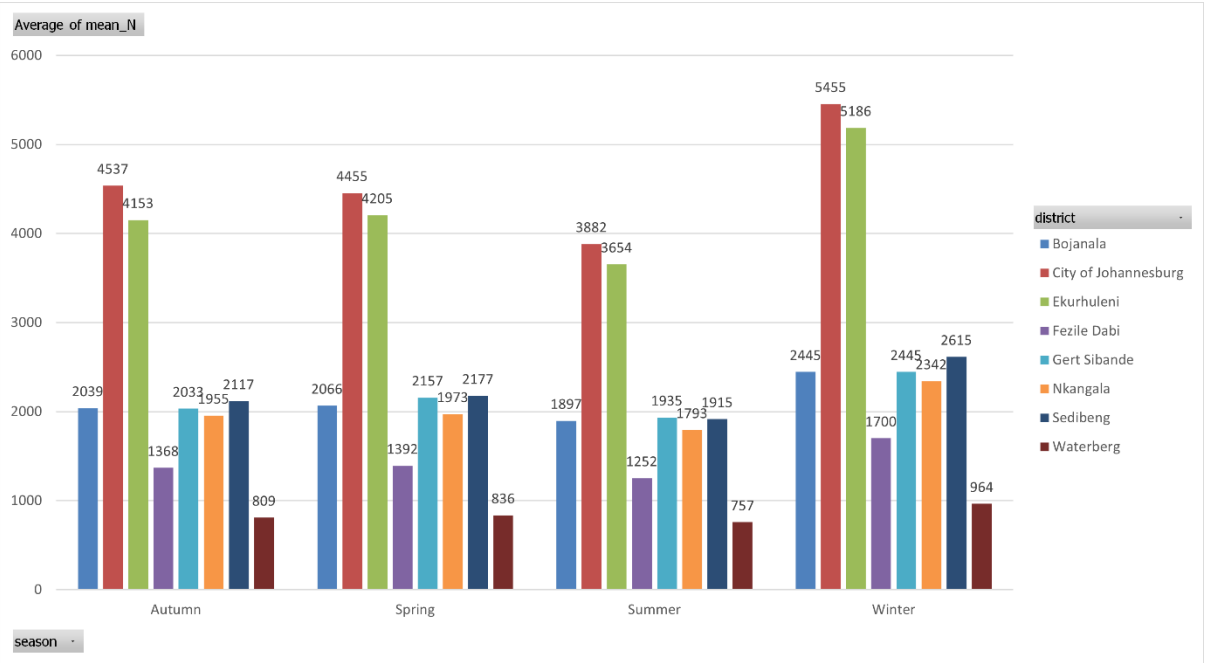

Figure 14: The average seasonal mortality health outcome per district.

Tuberculosis Mortality (A15–A19)

Tuberculosis (TB) remains a significant cause of mortality in South Africa, and the descriptive statistics between 1997 and 2018 reinforce its enduring burden.[4] The data show that most TB deaths were recorded under the A16 code "respiratory TB not confirmed bacteriologically or histologically. This suggests challenges in laboratory infrastructure and diagnostic certainty, particularly in the earlier years of the observation period.

Among the districts, Ekurhuleni consistently recorded the highest A16 TB mortality counts across all seasons, with Winter (7,160 deaths) and Spring (7,215 deaths) emerging as the peak periods. Autumn (6,665) and Summer (6,245) still showed substantial mortality, but lower than the colder months. Figure 16 A similar seasonal pattern is observed in the City of Johannesburg, with 5,661 A16-coded deaths in Winter and 5,491 in Spring, compared to 5,281 in Autumn and 4,858 in Summer. These figures align with well-established epidemiological patterns showing that tuberculosis transmission increases during colder months due to prolonged indoor crowding and reduced ventilation, which facilitate airborne transmission of *Mycobacterium tuberculosis.*[7, 8]

Table 9 reports the test for seasonality. Bojanala exhibited slightly lower but consistent mortality patterns, with Winter (3,243 deaths) and Spring (3,045) again showing the highest seasonal counts. Summer (2,759) and Autumn (2,873) remained marginally lower. Fezile Dabi recorded the lowest TB deaths among the four highlighted districts, but still showed a weak winter-spring seasonality of 9% (153 deaths): 1,824 deaths in Winter and 1,828 in Spring, compared to 1,674 in Summer and 1,672 in Autumn.

The near-absence of A15-coded (bacteriologically confirmed) TB deaths, only one case in Johannesburg in Summer over the 21-year period, raises critical public health concerns. This may reflect underutilization of confirmatory diagnostics, missing laboratory records, or delays in diagnostic updates to ICD coding systems.

Seasonal correlation analysis confirms the strong winter/spring burden of TB deaths. Across districts, Spearman's rho for winter versus other seasons ranged from 0.78 to 0.89 ($p < 0.001$), indicating strong positive correlations for higher TB mortality during colder months.

Respiratory Disease Mortality (J Group)

Respiratory diseases, categorized under ICD-10 J codes, accounted for one of the largest mortality burdens in the dataset. This group encompasses diseases like pneumonia (J18), acute bronchitis (J20), chronic lower respiratory diseases (J40–J47), and respiratory failure (J96). The magnitude and pattern of respiratory mortality followed strong seasonal trends and demographic clustering.

City of Johannesburg recorded the highest absolute number of respiratory deaths (n = 15,385 in the younger age group and 13,926 in the older age group), followed by Nkangala (Young: 2,950; Older: 4,120) and Gert Sibande (Young: 3,113; Older: 3,875). Seasonal mortality peaked in Winter, with Johannesburg alone recording over 5,800 deaths from J-coded causes during that season. Fezile Dabi also displayed a pronounced winter peak, particularly among the Younger group.

Age-specific analysis revealed that children (Younger group) bore a disproportionate burden of respiratory mortality in all districts, consistent with global trends of higher vulnerability among younger age groups. For instance, in Nkangala, 2,950 deaths in the Younger group were respiratory-related, nearly 42% of all Younger group deaths.

Seasonal correlations were again strong, with rho values for Winter vs. Spring and Winter vs. Autumn ranging from 0.74 to 0.88 ($p < 0.001$). In Johannesburg, the correlation between winter respiratory deaths and annual totals reached $\rho = 0.91$ ($p < 0.001$), underscoring the critical role of cold-weather respiratory morbidity and mortality.

Cardiovascular Mortality (I Group)

The cardiovascular disease (CVD) category, spanning ICD-10 codes I00–I99, includes ischemic heart disease, cerebrovascular diseases, hypertensive disorders, and more. It

represents a chronic, non-communicable burden with long latency and significant exposure-related triggers. In the dataset, CVD deaths were highest in Johannesburg (Older group: 11,934; Younger group: 5,050), with notable contributions from Sedibeng (Older group: 6,002) and Nkangala (Older group: 5,918).

Unlike TB and respiratory diseases, cardiovascular deaths were more evenly distributed across seasons. However, a subtle winter elevation was still present. Johannesburg recorded 4,120 CVD deaths in Winter, compared to 3,972 in Spring, 3,858 in Autumn, and 3,845 in Summer. Sedibeng followed a similar seasonal shape. Fezile Dabi, while having fewer total CVD deaths, also displayed a winter preference (1,784 Winter vs. 1,622 Summer).

In terms of age distribution, the Older group bore over 70% of the total CVD mortality, which aligns with established epidemiological evidence. Male deaths slightly outnumbered female deaths in the CVD category across most districts, especially in Gert Sibande and Johannesburg.

Spearman correlation analysis indicated moderate but significant seasonal patterns. In Johannesburg, Winter CVD deaths correlated with annual totals at $\rho = 0.68$ ($p < 0.01$), while Spring and Autumn correlations were weaker ($\rho = 0.41–0.52$). These data suggest seasonal triggers like cold stress or pollution may exacerbate pre-existing CVD conditions.

Conclusion and Public Health Interpretation

The descriptive patterns from 1997–2018 offer robust evidence of distinct seasonal and spatial trends for all three ICD groups. TB mortality showed strong winter dominance and a reliance on clinical coding (A16), particularly in urban centres. Respiratory deaths were highly seasonal and child-focused, with major peaks in Younger group during Winter. Cardiovascular deaths were more stable across seasons but showed modest Winter elevation, especially in older populations.

The correlation analyses underscore these seasonal dynamics, with winter emerging as the dominant season for all three ICD categories, though with varying intensity. These findings

support targeted health interventions, particularly for vulnerable groups in Winter, and call for improved diagnostic infrastructure, particularly in TB care.

Future analyses should explore interactions between air pollution, temperature, and these seasonal patterns to support policy development and adaptive health system planning.

Pneumonia demonstrates seasonality ($p < 0.001$), whereas total respiratory failure is more ubiquitous ($p > 0.05$) and implies a more complex interaction between exposures and outcomes. There is a higher likelihood of an interaction between multiple external stressors for the causes of a respiratory failure.

Table 7: Descriptive statistics for Respiratory failure, Tuberculosis deaths and Cardiovascular / Cerebrovascular deaths by Priority Area (PA).

PA	outcome	non_missing_ weeks	total	mean_per_ week	sd	min	q25	median	q75	max
Highveld Priority Area	Respiratory deaths (ICD-10 J)	1566	4769	3	2	0	2	3	4	9
Highveld Priority Area	Tuberculosis deaths (ICD-10 A15–A19)	1566	1601	1	1	0	0	1	2	6
Highveld Priority Area	Cardio/Cerebrovascular deaths (ICD-10 I00–I99)	1566	6311	4	2	0	3	4	5	11
VTAPA	Respiratory deaths (ICD-10 J)	1565	4686	3	2	0	2	3	4	10
VTAPA	Tuberculosis deaths (ICD-10 A15–A19)	1565	1595	1	1	0	0	1	2	6

VTAPA	Cardio/Cerebrovascular deaths (ICD-10 I00–I99)	1565	6290	4	2	0	3	4	5	13
Waterberg–Bojanala Priority Area	Respiratory deaths (ICD-10 J)	1565	4651	3	2	0	2	3	4	10
Waterberg–Bojanala Priority Area	Tuberculosis deaths (ICD-10 A15–A19)	1565	1621	1	1	0	0	1	2	5
Waterberg–Bojanala Priority Area	Cardio/Cerebrovascular deaths (ICD-10 I00–I99)	1565	6113	4	2	0	2	4	5	11

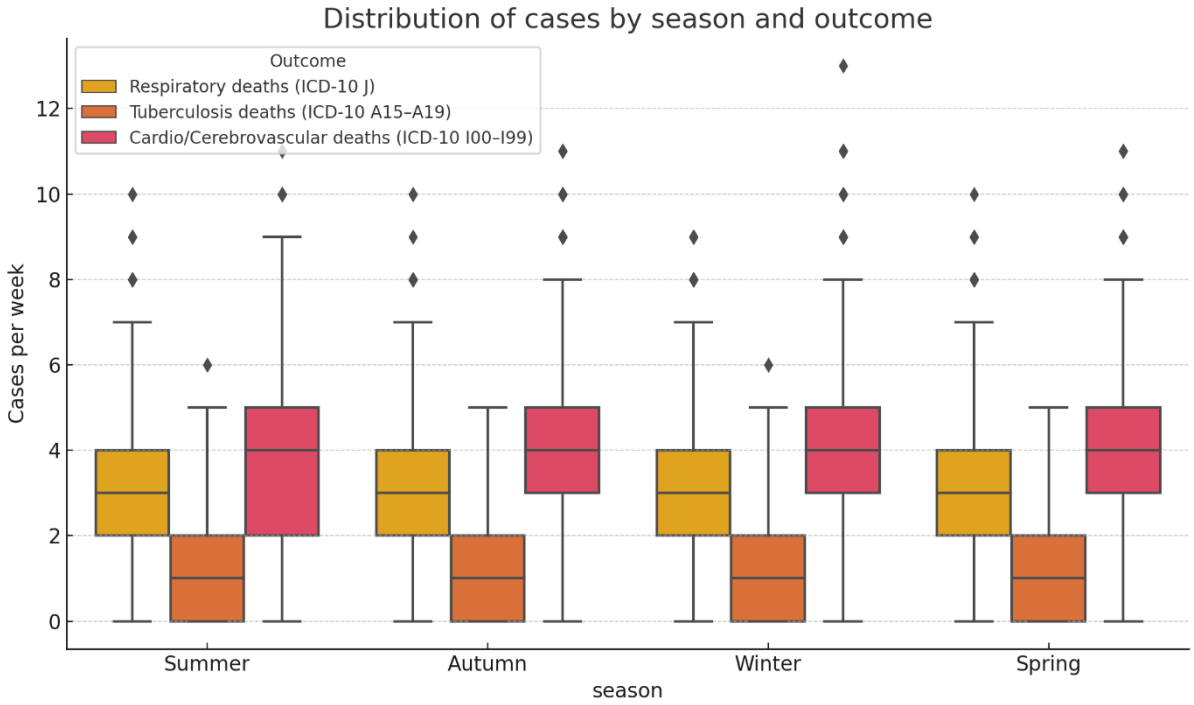

Figure 15:Distribution of mortality cases by seasons, aggregated by week

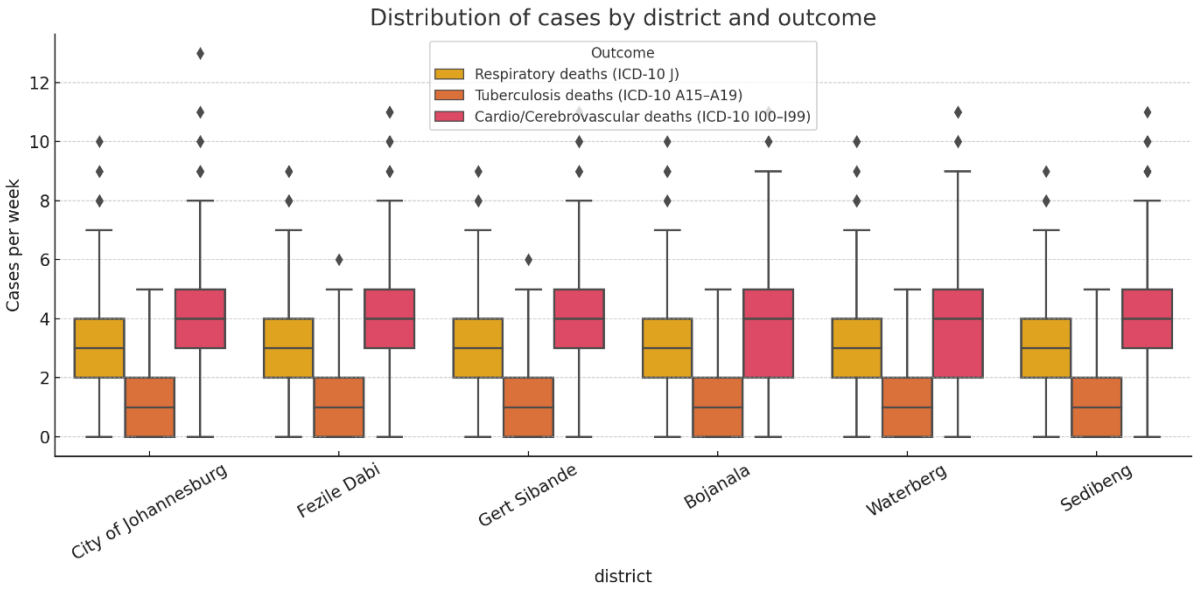

Figure 16: Distribution of mortality cases by seasons, aggregated by district.

Table 8: A test for seasonality for the health effects studies, using the Kruskal-Wallis test, p<0.05

District	Health Effect	H_statistic	p_value	significant (p<0,05)
Bojanala	TB	14,46	0,00	Yes
Bojanala	All CVD	92,38	0,00	Yes
Bojanala	All Respiratory	87,23	0,00	Yes
City of Johannesburg	TB	10,48	0,01	Yes
City of Johannesburg	All CVD	298,51	0,00	Yes
City of Johannesburg	All Respiratory	222,05	0,00	Yes
Ekurhuleni	TB	14,26	0,00	Yes

Ekurhuleni	All CVD	260,04	0,00	Yes
Ekurhuleni	All Respiratory	168,66	0,00	Yes
Fezile Dabi	TB	7,01	0,07	No
Fezile Dabi	All CVD	242,71	0,00	Yes
Fezile Dabi	All Respiratory	67,27	0,00	Yes
Gert Sibande	TB	7,07	0,07	No
Gert Sibande	All CVD	133,52	0,00	Yes
Gert Sibande	All Respiratory	40,66	0,00	Yes
Nkangala	TB	3,93	0,27	No
Nkangala	All CVD	107,11	0,00	Yes
Nkangala	All Respiratory	59,67	0,00	Yes
Sedibeng	TB	13,15	0,00	Yes
Sedibeng	All CVD	185,64	0,00	Yes
Sedibeng	All Respiratory	125,16	0,00	Yes
Waterberg	TB	6,49	0,09	No
Waterberg	All CVD	35,75	0,00	Yes
Waterberg	All Respiratory	47,79	0,00	Yes

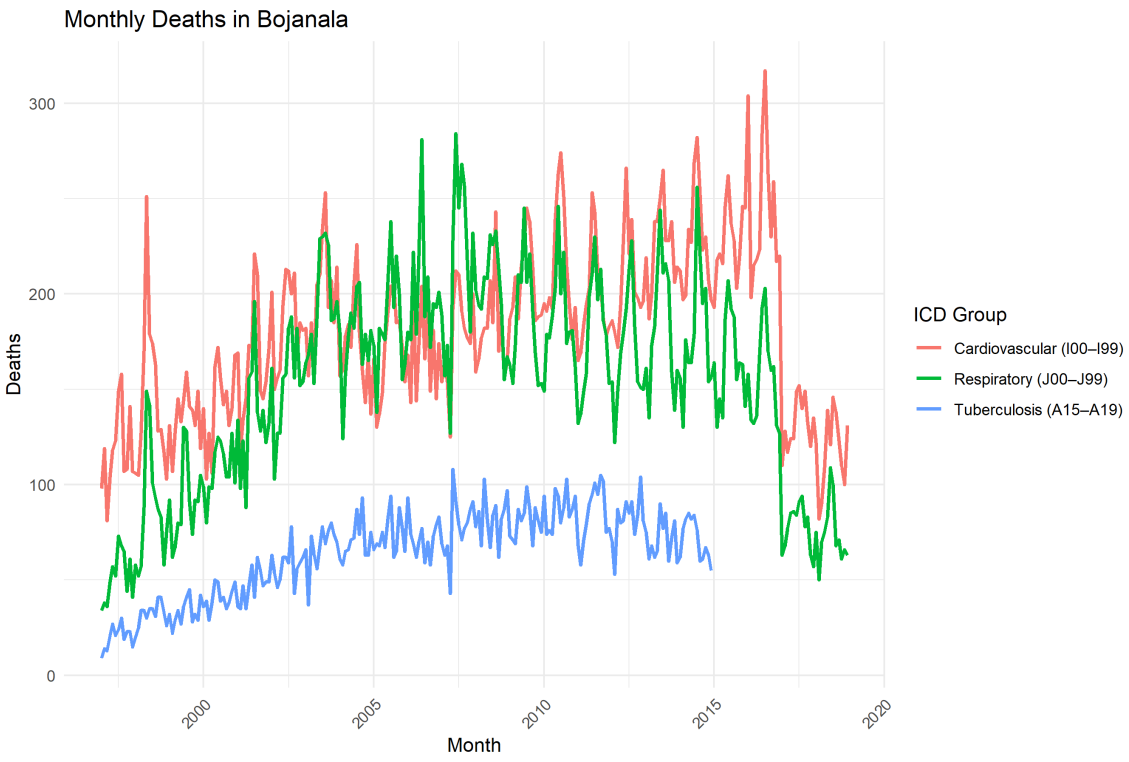

Figure 17: The total timeseries for mortality count data (Tuberculosis, respiratory failure and cardiovascular and cerebrovascular failure) as reported within the Bojanala District Municipality.

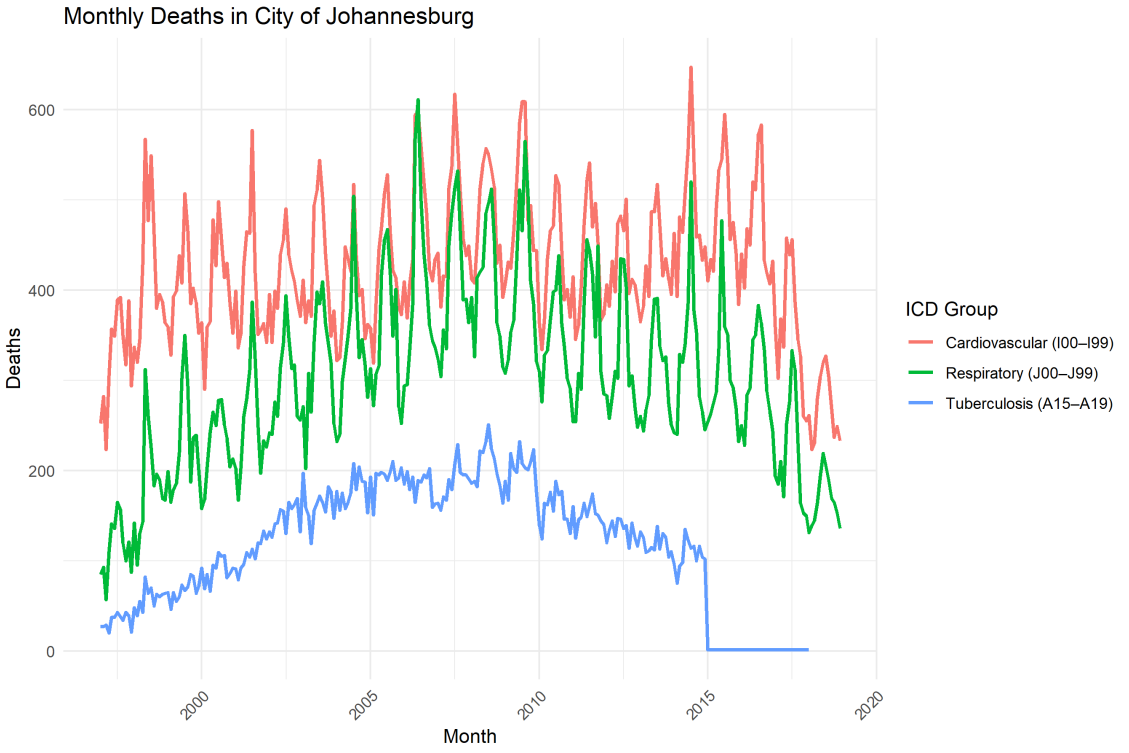

Figure 18: The total timeseries for mortality count data (Tuberculosis, respiratory failure and cardiovascular and cerebrovascular failure) as reported within the City of Johannesburg District Municipality.

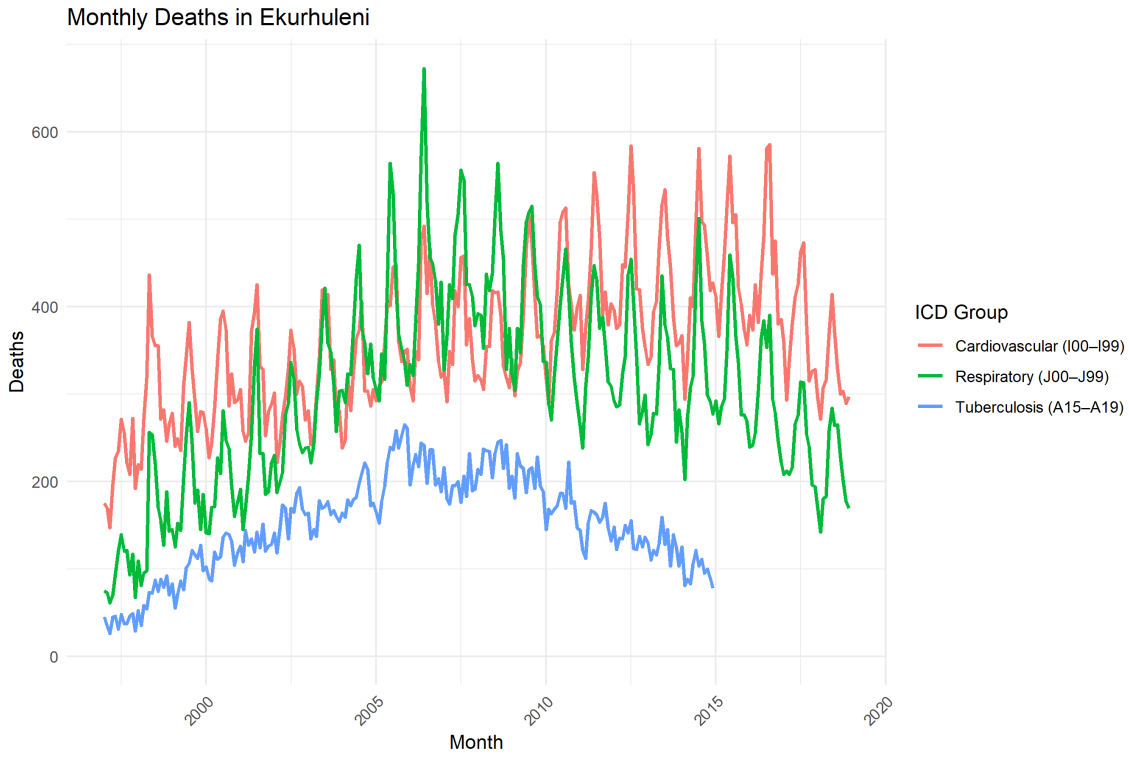

Figure 19: The total timeseries for mortality count data (Tuberculosis, respiratory failure and cardiovascular and cerebrovascular failure) as reported within the Ekurhuleni District Municipality.

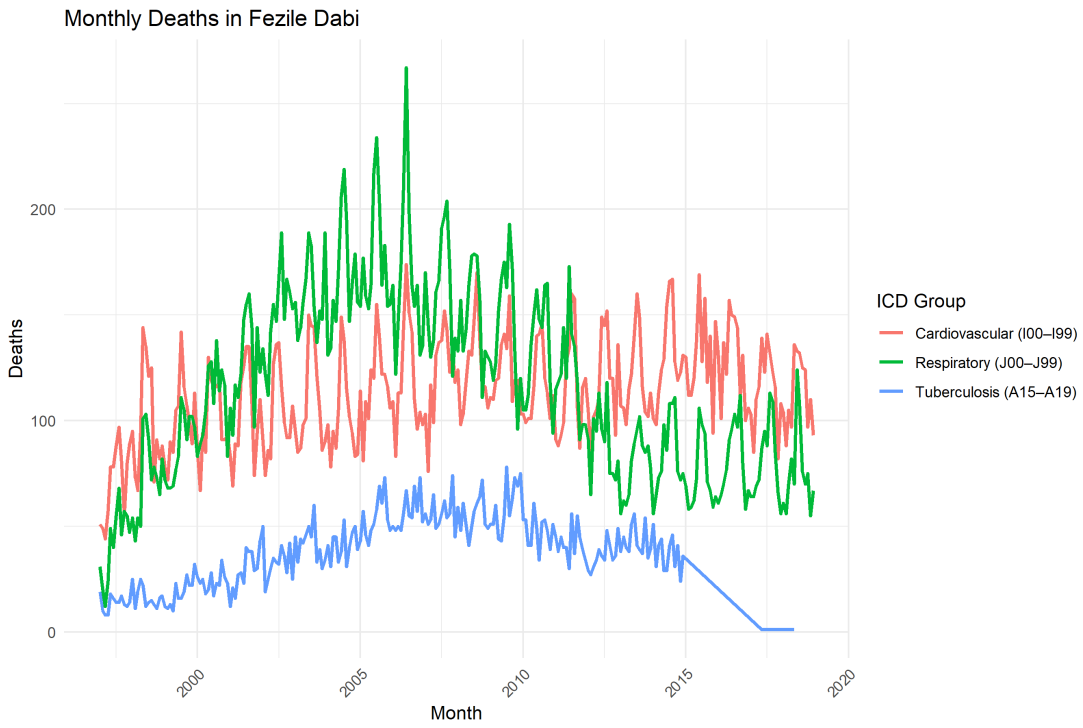

Figure 20: The total timeseries for mortality count data (Tuberculosis, respiratory failure and cardiovascular and cerebrovascular failure) as reported within the Ekurhuleni District Municipality.

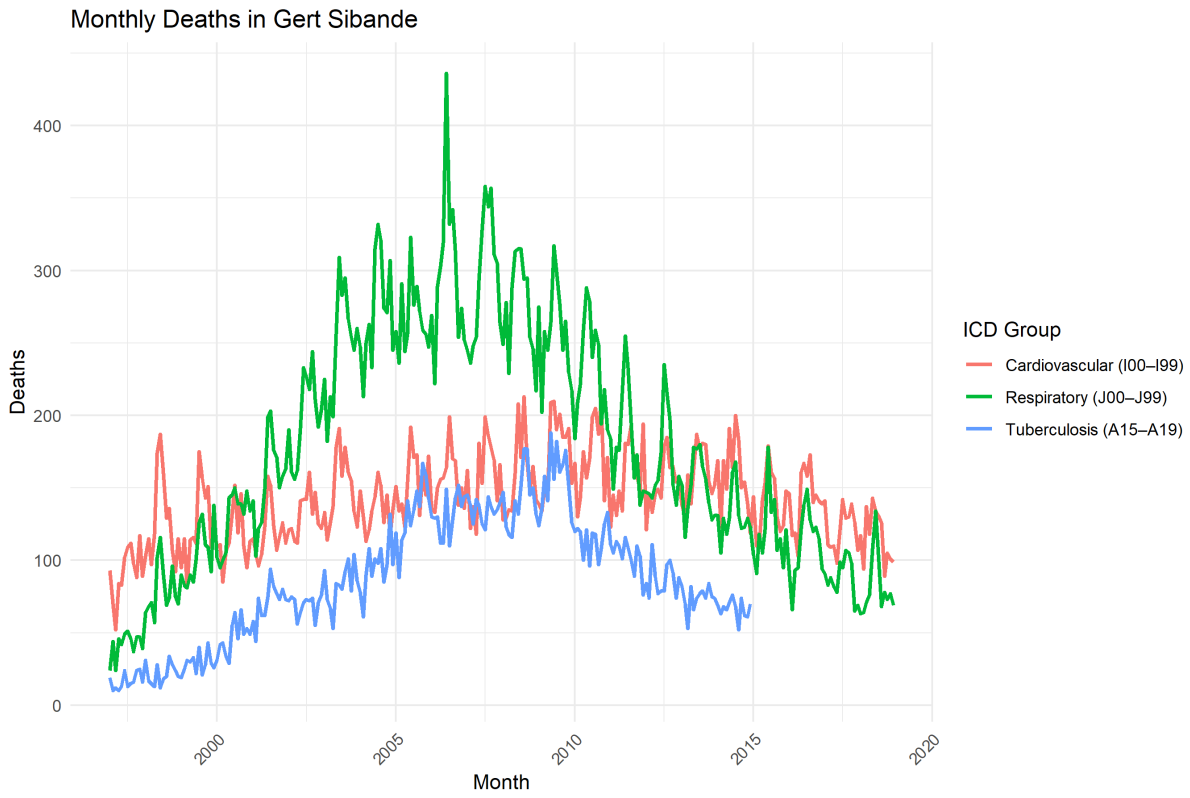

Figure 21: The total timeseries for mortality count data (Tuberculosis, respiratory failure and cardiovascular and cerebrovascular failure) as reported within the Gert Sibande District Municipality.

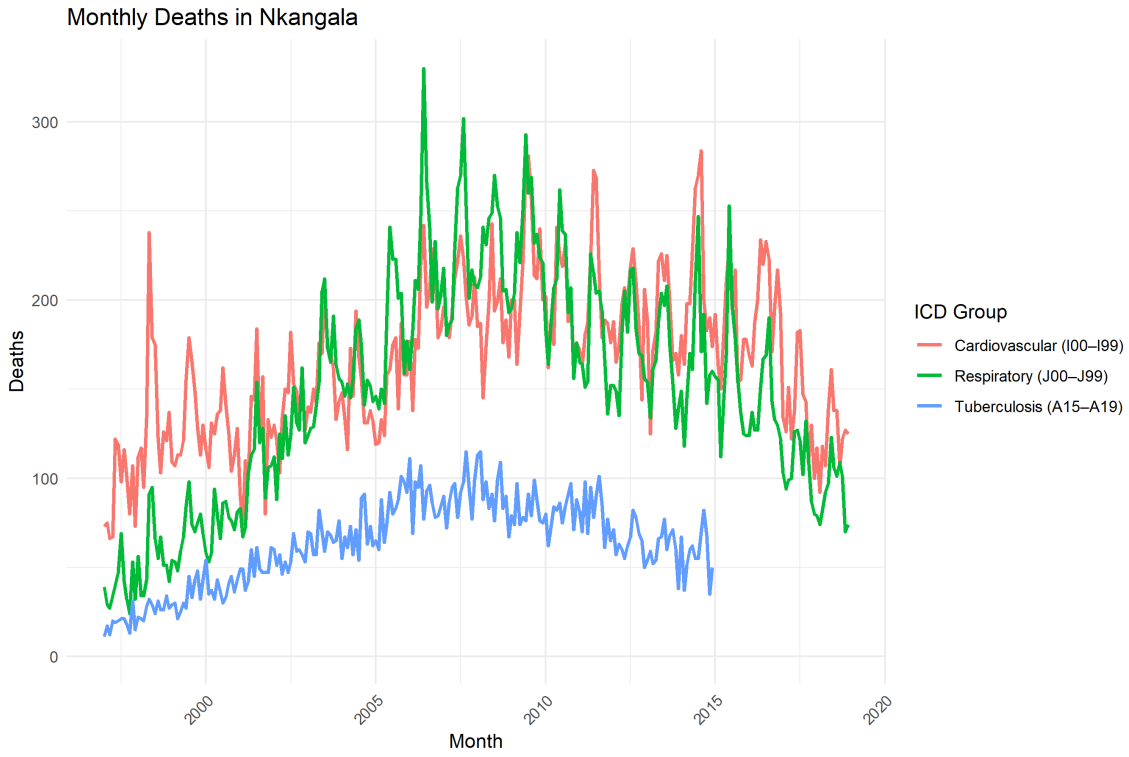

Figure 22: The total timeseries for mortality count data (Tuberculosis, respiratory failure and cardiovascular and cerebrovascular failure) as reported within the Nkangala District Municipality.

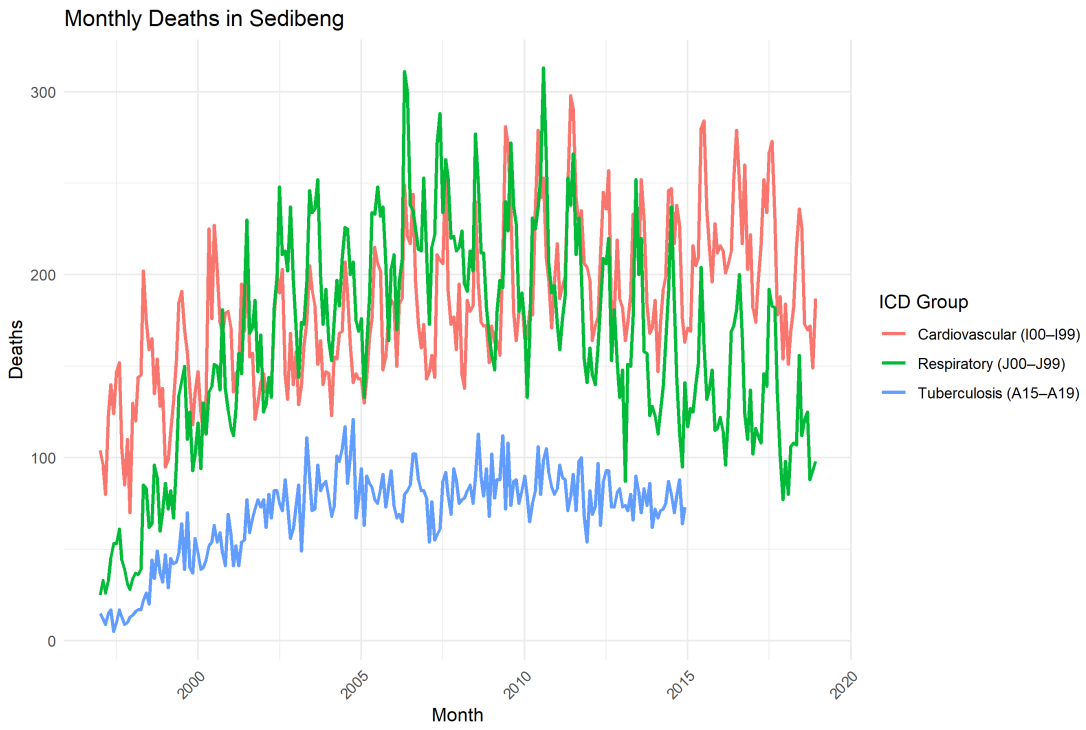

Figure 23: The total timeseries for mortality count data (Tuberculosis, respiratory failure and cardiovascular and cerebrovascular failure) as reported within the Sedibeng District Municipality.

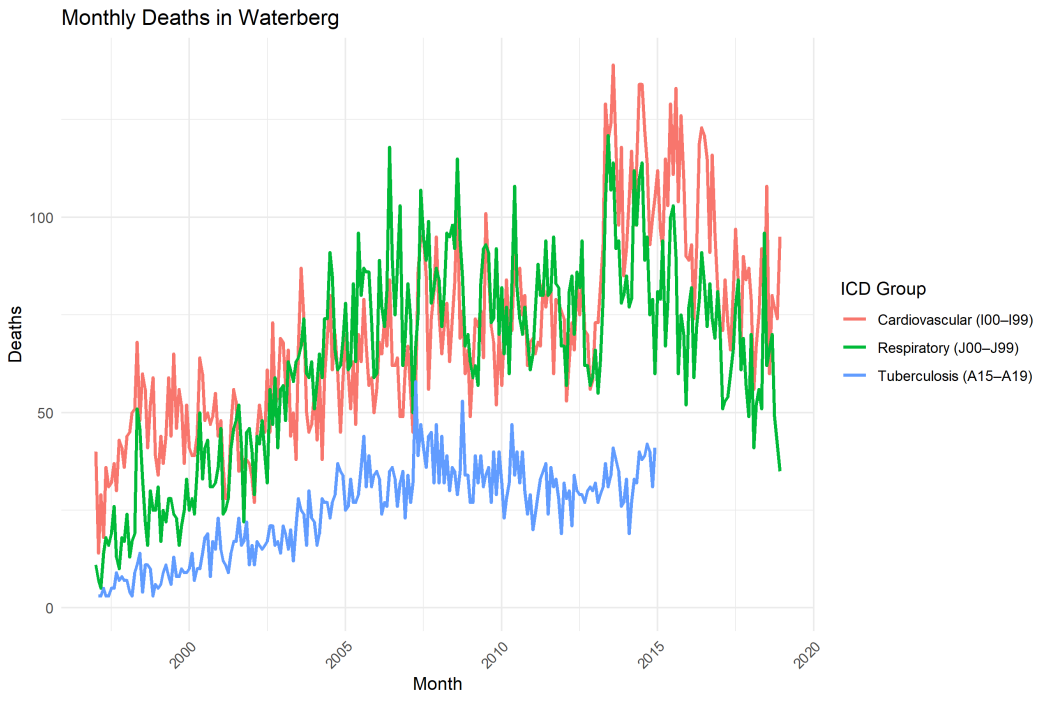

Figure 24: The total timeseries for mortality count data (Tuberculosis, respiratory failure and cardiovascular and cerebrovascular failure) as reported within the Waterberg District Municipality.

2.3.2 Morbidity data

As opposed to the mortality daily reports, morbidity data (hospital admissions) is reported on a monthly basis and the daily missingness is not known. This data was retrieved from the National District Health Information System of South Africa. Data is at the facility level, i.e., primary healthcare facility including clinics and hospitals. We will extract data for the districts within the three air pollution priority areas in South Africa. Data was available from 2002 to 2023.

The association between health effects and air pollution-related will include pneumonia cases in children under 5 years and new reported TB cases in all ages.

Table 9: Descriptive statistics of the monthly pneumonia <5 count from 2005 to 2022 across the districts within the priority areas

District	count	mean	std	min	0,25	0,5	0,75	max
Fezile Dabi	204	259	187	4	101	235	388	929
Bojanala	204	314	259	0	78	238,5	539	1110
City of Johannesburg	204	1016	495	269	642	901,5	1284	2895
Ekurhuleni	204	767	418	73	455	668	1064	1923
Gert Sibande	204	199	156	6	63	157	321	583
Nkangala	204	311	219	7	138	288,5	436	915
Sedibeng	204	225	170	4	90	189	332	900
Waterberg	204	156	70	17	110	145	199	398

Table 10 is a descriptive analysis of the monthly health count data across the priority area districts reveals significant geographic and temporal variation in disease burden. Among the districts studied, Nkangala reported the highest average number of cases per year, with a mean of 225 cases per month, ranging from a low of 7 cases in February 2009 to a peak of 915 cases in August 2013. This substantial fluctuation suggests a high degree of variability,

possibly influenced by seasonal patterns, localized outbreaks, or air pollution episodes during winter months.

Gert Sibande, another district within the high-priority areas, exhibited similarly elevated health burdens, with an average of 211.3 cases per month. The lowest number of cases was observed in November 2009 (7 cases), while the highest monthly burden occurred in July 2013, reaching 716 cases. These peaks align with mid-year winter seasons, which may exacerbate respiratory conditions due to increased indoor heating, temperature inversions, or pollutant build-up.

In contrast, Bojanala District had a lower mean of 89.1 cases per month, with its lowest record in February 2009 (2 cases) and a maximum of 314 cases in July 2015. Though the district experiences fewer cases on average, notable mid-winter peaks suggest potential environmental health stressors aligned with colder periods.

Waterberg District reported a mean of 58.2 cases per month, peaking at 212 cases in June 2013, while recording its lowest total in February 2009 (3 cases). These results mirror trends seen in other regions, where winter seasons are associated with increased case counts, possibly reflecting increased susceptibility to respiratory illnesses.

Meanwhile, Fezile Dabi and Sedibeng Districts, both part of the Vaal Triangle Priority Area (VTPA), demonstrated moderate average burdens of 54.4 and 57.8 monthly cases, respectively. Fezile Dabi's health burden spanned from 4 cases in February 2009 to 191 cases in July 2013, whereas Sedibeng saw its minimum in February 2009 (2 cases) and a maximum of 202 cases in June 2013.

These findings indicate consistent seasonal patterns across all districts, with winter months (June–August) exhibiting the highest case volumes. February 2009 emerges as a common low point across nearly all regions, possibly due to favourable environmental conditions or underreporting.

This spatial-temporal variability in health burden underscores the need for seasonally targeted public health interventions and further investigation into contributing environmental exposures such as temperature, humidity, and air pollution.

In terms of correlation analysis, we evaluated the linear associations between health outcomes and air pollutant levels using Pearson correlation coefficients across the full dataset. Surprisingly, no single pollutant demonstrated a strong linear relationship ($|r| > 0.6$) with the monthly case counts. This absence of a strong correlation at the aggregated level could be attributed to several factors. First, the relationships between air pollution and health outcomes may not be strictly linear, particularly if delayed effects or threshold-based responses are involved. Second, monthly aggregation may smooth over short-term spikes that are critical for detecting meaningful associations. Lastly, inter-district heterogeneity in healthcare access, climate, and socio-economic factors may mask any underlying environmental health relationships.

To strengthen understanding, future analyses should explore lagged effects using distributed lag models (e.g., DLNM), stratify by season, and examine district-specific correlations. Additionally, case-crossover models could reveal within-district temporal patterns obscured in this descriptive summary.

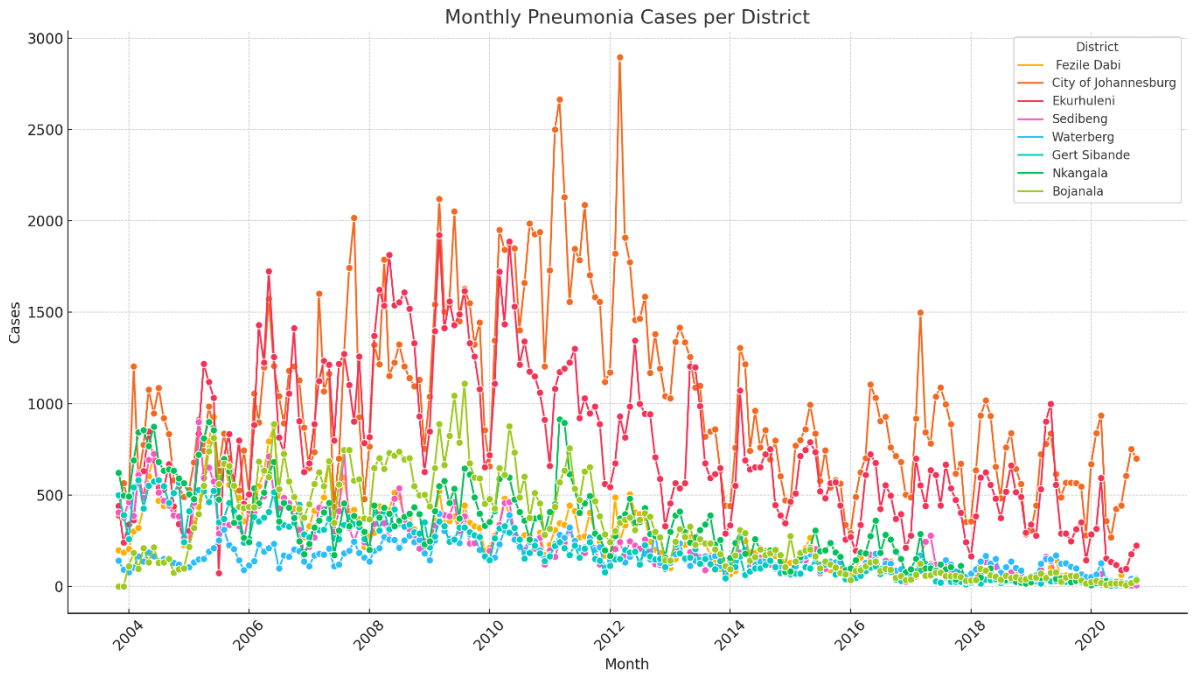

Figure 25: Timeseries of the pneumonia <5 new cases from 2004 to 2022 on a monthly basis

5 ENVIRONMENTAL EPIDEMIOLOGY STUDY DESIGNS

5.1 Assumptions and timeseries methods

The pseudo-CCO approach assumes that referent (control) weeks are exchangeable with case weeks in terms of baseline risk, except for exposure. This requires that referent weeks be close in time (e.g., ±1–3 weeks) to control for seasonality and secular trends. Additionally, the method assumes no time-varying confounding that differs between case and referent weeks, and that there is no carry-over effect from prior exposure. These assumptions are approximated here using symmetric matching and the exclusion of autocorrelated outcomes.

5.2 DLNM study design for the association between mortality count data and air pollutants

Separate DLNM Models for Cardiovascular (I) and Respiratory (J) Outcomes

The statistical power to detect statistically significant associations in distributed lag models is inherently dependent on the number of events per analytical stratum. In this study, we classified each stratum (defined by district, season, age group, and ICD cause group) by mortality burden to evaluate statistical power. Strata with fewer than 10 deaths were considered low power, with limited capacity to detect small-to-moderate effect sizes. Our analysis revealed that all respiratory (ICD Group J) strata exceeded the high-power threshold (≥30 deaths), while most cardiovascular (ICD Group I) strata also met this threshold, with only two falling below 10 deaths. This distribution supports the reliability of our risk estimates, particularly for respiratory outcomes. The power assessment further guided model inclusion criteria and informed the feasibility of pooled estimates across strata. By transparently quantifying power, we ensured that observed associations are not artifacts of sparse data, especially when interpreting null or borderline-significant findings. Figure 26 and 27.

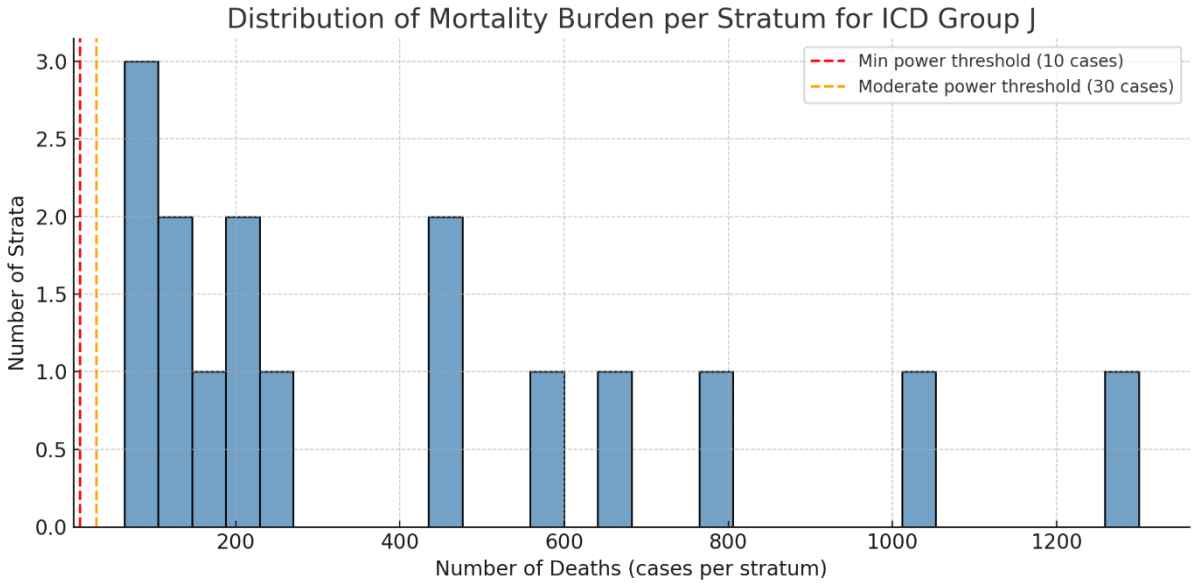

Figure 26: The distribution of the number of deaths per strata as defined by district, season, age group, sex due to respiratory failure J(00 – 99)

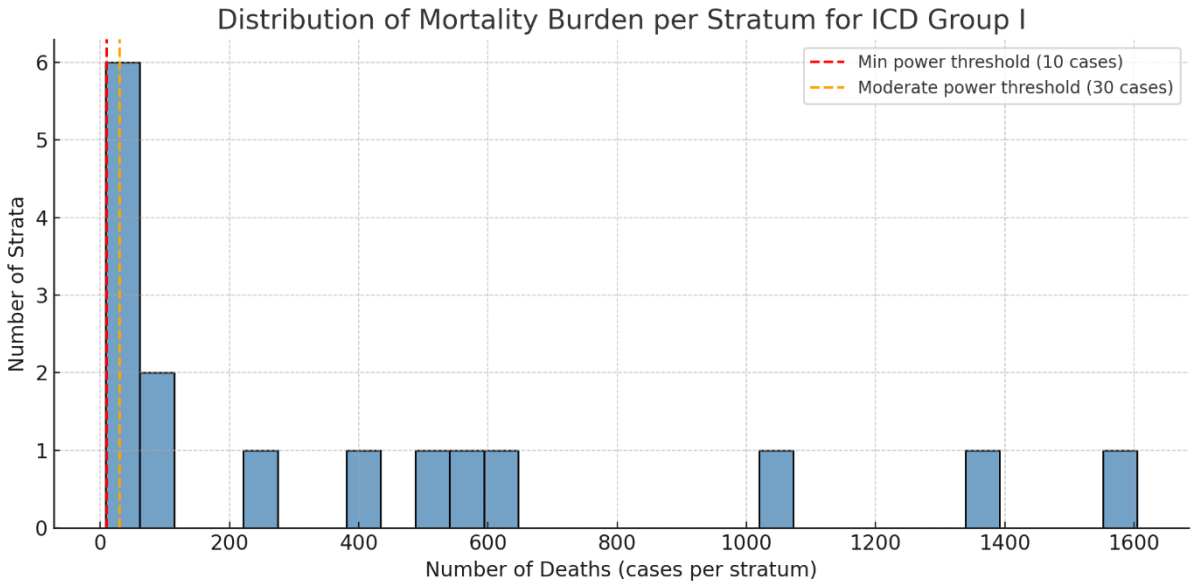

Figure 27: The distribution of the number of deaths per strata as defined by district, season, age group, sex due to cardiovascular and cerebrovascular failure I(00 – 99)

This study employed Distributed Lag Non-Linear Models (DLNM) to assess the short-term effects of ambient air pollution on two major mortality categories: ICD-10 Group I (cardiovascular failure) and ICD-10 Group J (respiratory failure). Separate models were run for each outcome group to reflect underlying differences in biological mechanisms, lag structures, and epidemiological behaviour.

Air pollution is known to affect both respiratory and cardiovascular systems, but the timing, magnitude, and shape of the exposure-response relationship can differ significantly. Modelling these outcomes together risks masking outcome-specific dynamics critical to public health interpretation. Separate modelling allows for distinct lag-response profiles to emerge.

Cardiovascular mortality (Group I) may involve systemic inflammation, endothelial dysfunction, or arrhythmic triggers that develop over longer time lags (e.g., 2–7 days), whereas respiratory mortality (Group J) is often linked to acute responses such as airway irritation or bronchoconstriction, peaking within 0–3 days. DLNM accommodates these differences using flexible spline-based lag structures.

Running separate models avoids potential statistical confounding between outcomes and improves the clarity of interpretation. This approach enables exposure-response visualization and quantification specific to each disease class. It also supports independent meta-analysis or comparison of temporal patterns across disease type.

Disaggregated results facilitate evidence-based policy actions targeted to specific at-risk populations. For instance, respiratory alerts might be issued during high ozone days, while cardiovascular warnings may be needed several days after NO_2 or PM_{10} spikes. This approach also aligns with WHO recommendations for ICD-specific burden quantification.

Due to variation in data availability across districts and age groups, the DLNM models were subject to stratum reduction. Missing values for exposures or mortality counts led to the exclusion of certain combinations of district × season × age group. The final models retained only strata with sufficient temporal coverage and variability for robust lag estimation. These adjustments were essential to preserve the statistical power and validity of the DLNM framework.

Distributed Lag Non-linear Models (DLNMs) are used in multisite air quality and health monitoring to analyse the non-linear and lagged effects of air pollutants on health outcomes. These models allow researchers to assess how long the impact of a specific pollutant lasts (lags) and how the effect varies depending on the concentration of the pollutant (reported as a relative risk). This helps in understanding the complex relationships between air pollution and health, especially in the context of multiple monitoring locations and potential time lags between exposure and health responses. The study across the three priority areas spans over six districts and approximately 24 years. The exposure per district will also differ due to topography, meteorology and type of sources.[9, 10]

5.3 Two stage DL-CCO for respiratory and pneumonia/TB related failure

At the heart of this approach, the Stage 1 DL-CCO model estimates district-level odds ratios (ORs) for mortality in relation to short-term pollutant exposures—specifically for respiratory (ICD J-codes) and pneumonia/TB-related (ICD A15–A19) deaths. This modelling framework

is especially well-suited for acute outcomes like mortality, where environmental exposures (e.g., PM_{10}, SO_2, NO_2, O_3) are known to trigger health crises over a span of several days. The cross basis function used in DL-CCO enables modelling of lag effects across multiple weeks (e.g., up to 3 weeks), thereby capturing the delayed physiological impacts of pollution on vulnerable populations. In the case of respiratory deaths, these lags are particularly crucial, as symptom exacerbation and access delays to care may precede mortality.

The case-crossover design, by construction, inherently controls for long-term confounders (e.g., socioeconomic status, healthcare infrastructure), and by stratifying by district, age group, ICD code, and season, we ensure that time-invariant and seasonal factors are appropriately adjusted for. For example, winter and early spring are well-established seasons of elevated respiratory mortality due to temperature drops and atmospheric inversion layers that trap pollutants near the surface. The DL-CCO framework permits season-specific distributed lag curves, highlighting periods of heightened vulnerability.

Stage 1 results in the current analysis illustrate robust associations between several pollutants and weekly mortality. In Nkangala district, the OR for weekly NO_2 exposure (scaled per 10 ppb) in winter for ICD J-codes was 1.18 (95% CI: 1.07–1.31), peaking at lag 1 week. Similarly, Fezile Dabi showed significant associations for SO_2 during autumn, with OR = 1.23 (95% CI: 1.09–1.38). These consistent temporal structures validate the need for a lag-based model and provide locally relevant insights for health intervention planning.

Stage 2 employs meta-analytic techniques to pool district-specific estimates by season and ICD group. This is critical for two main reasons: (1) to enhance statistical power, especially for rarer causes of death (e.g., TB-related A15–A19 codes), and (2) to detect between-district heterogeneity in exposure-response relationships. The latter is vital in a country like South Africa where air pollution sources differ—for instance, mining emissions dominate in Gert Sibande, while traffic and industrial pollutants are more prevalent in Sedibeng and Ekurhuleni. Meta-analytic pooling using random-effects models allows for the estimation of

a central tendency while quantifying dispersion (I^2 statistic), thereby enabling a tiered response across regions.

The second stage of the DL-CCO will use these statistically significant OR and 95%CI as an input and pool over each priority first and then the exposure in its entirety. The data is stratified by week for each case and exposure one by one, where the non-analysed act as a control for each case. The lags are again same day and then following three weeks (0 – 3).

We then tested for heterogeneity and seasonality (Q), heterogeneity between the districts were found in all the priority areas in part A, but this was lost when the whole priority area was pooled together and for all pollutants. Thus, seasonality is lost and implies a near equal exposure.

In terms of districts, the City of Johannesburg and Ekurhuleni reported the highest number of cases over the study period and the City of Johannesburg was determined to have a statically significant association in stage 1, when performing the overall DL-CCO, the Highveld Priority Area and the Vaal Triangle Priority Area were slightly significant for lag 0, 1 and 2 but not for lag 3. Overall, the priority areas together are significantly positive for the first two lags.

This study design demonstrates the complexity of the association between exposures and cases. Sources and interactions between exposures present both individual as well as cumulative effects. The DL-CCO attempts to isolate individual exposure effects and the overall effects of the cumulative exposures.

Importantly, the inclusion of a pseudo-CCO verification analysis strengthens the credibility of the DL-CCO findings. Despite minor differences in magnitude, the direction and significance of associations were largely replicated across the two approaches, providing confidence that the lag-based model is not overfitting or misrepresenting the exposure-response relationship.

In conclusion, the two-stage DL-CCO design leverages the strengths of both within-district temporal modelling and cross-district synthesis, producing evidence that is both locally actionable and nationally scalable. Given the constraints of weekly data and the need for responsive, granular health risk assessments in environmental epidemiology, this approach represents a scientifically valid and policy-relevant analytic framework. It supports the development of district-specific public health alerts, seasonal emission control policies, and resource prioritization strategies aimed at reducing air pollution–related mortality across South Africa.

5.4 Pseudo – CCO for the association between new cases of under-five pneumonia, respiratory hospital admissions and air pollutants

Given the limitations in the temporal resolution of available morbidity data—reported monthly rather than daily or weekly—a true case-crossover design could not be employed. Instead, a pseudo case-crossover (pseudo-CCO) approach was implemented to evaluate the short-term effects of ambient air pollution on respiratory and cardiovascular morbidity. This method serves as a sensitivity analysis, intended to approximate time-stratified control under monthly resolution while acknowledging the coarser temporal granularity of the data. It complements the primary mortality analysis and offers a comparative perspective on pollution-health dynamics across districts and seasons.

The morbidity data were obtained from the Department of Health Information System (DHIS) and included aggregated monthly counts of hospital admissions coded under ICD-10 groups: J (respiratory diseases, including pneumonia and bronchitis), I (cardiovascular and cerebrovascular diseases), and A15–A19 (tuberculosis-related cases). Data spanned from 2005 to 2022 and were disaggregated by district and age group. Only cases with valid dates, ICD codes, and district identifiers were included. Due to the lack of individual-level data or precise admission dates, individual-level time-matching was not possible, and morbidity events could only be compared across aggregated time windows.

Exposure data for ambient air pollutants, specifically NO_2, SO_2, O_3, PM_{10}, and $PM_{2.5}$, were obtained from the South African Air Quality Information System (SAAQIS), aggregated to monthly averages by district. These were linked to the morbidity data based on district and month of admission. Meteorological covariates such as temperature and humidity were not included due to sparse or inconsistent coverage across districts and time. However, models adjusted for seasonal variation by incorporating categorical season indicators (Summer, Autumn, Winter, Spring), and long-term time trends using year or month-year terms.

The analytical model employed was a generalized linear model (GLM) with a Poisson distribution and log-link function, appropriate for modelling count data. The monthly morbidity count for each health outcome served as the dependent variable, and the monthly average pollutant concentration was the primary independent variable. Exposures were scaled per 10 ppb or $\mu g.m^{-3}$ interquartile range (IQR) to facilitate comparability across pollutants and align with existing epidemiological standards. Where available, population denominators were used as offsets to account for differences in district population sizes over time.

This design does not capture within-subject temporal contrasts inherent in true case-crossover models and does not allow for fine-grained lag structures. However, by using monthly data and adjusting for time-varying confounders, the pseudo-CCO maintains quasi-time stratification, approximating temporal control. The approach is particularly useful as a robustness check, evaluating whether morbidity associations exhibit directionally consistent patterns with those seen in DL-CCO mortality models, especially in relation to season and pollutant type.

Results are interpreted with caution due to the absence of individual-level matching and the limited ability to estimate acute lag effects. Nevertheless, this approach provides important supporting evidence in a policy-relevant context where morbidity data are routinely collected at monthly intervals. It also enhances the generalizability of findings by

incorporating both mortality and morbidity perspectives into the overall health impact assessment of air pollution across South African priority areas.

5.5 Statistical Methods

Thus, to estimate the short-term association between ambient air pollution and morbidity outcomes across South African Priority Areas (PAs), we applied two complementary statistical models: a Distributed Lag Non-Linear Model (DLNM) to estimate Relative Risk (RR), and a pseudo-case-crossover (pseudo-CCO) logistic regression to estimate Odds Ratios (OR). These models were applied across districts, seasons, and pollutants, using health outcome data aggregated monthly and air pollutant data aggregated weekly.

DLNM Modelling (RR Estimation)

The DLNM framework was used to quantify RR for respiratory and cardiovascular hospital admissions associated with exposure to five air pollutants (NO_2, SO_2, O_3, PM_{10}, and $PM_{2.5}$), scaled per 10 ppb or μg/m³ IQR. We constructed distributed lag models with natural cubic splines over lags 0–3 weeks, fitted within a quasi-Poisson regression to address potential overdispersion in weekly morbidity counts. Covariates included season (categorical: Summer, Autumn, Winter, Spring) and district, allowing for stratified lag-response estimation.

Pseudo-Case-Crossover (CCO) Modelling (OR Estimation)

Due to the unavailability of daily-level morbidity data, a pseudo-CCO design was implemented using monthly aggregated counts. We classified each month as a binary case/control period and applied logistic regression models with exposure defined as the monthly average pollutant concentration. Odds Ratios (ORs) were estimated per IQR increase, stratified by season and district. While not a true case-crossover design, this approach mimics within-subject temporal control by adjusting for long-term trends and seasonal structure.

Verification Analyses

To verify the consistency and generalizability of the estimated effects, we performed the following additional analyses:

- Seasonality Testing: Both RR and OR estimates were stratified by season, and effect modification was assessed by evaluating differences in risk across seasons for each pollutant. Stronger associations in Winter and Spring were anticipated due to stagnant meteorological conditions and elevated heating-related emissions. Seasonal models were fit separately to allow for independent estimation and to avoid confounding from pooled seasonal variation.
- Heterogeneity Assessment: After district-level models were run, we conducted a random-effects meta-analysis to test for between-district heterogeneity. The Cochran Q-statistic and I^2 statistic were used to quantify variability not attributable to chance. Subgroup analyses were also conducted within each Priority Area (HPA, VTPA, WBPA) to evaluate within-area consistency. Heterogeneity values above $I^2 = 30\%$ were interpreted as moderate inconsistency. Where applicable, forest plots were generated to visualize district-specific and pooled RR or OR estimates.

Model Comparison and AIC Consideration

Although AIC is commonly used to compare model fit, it was not applied across DLNM and pseudo-CCO models due to fundamental differences in outcome structures (count vs. binary), likelihood functions (quasi-Poisson vs. binomial), and temporal scales (weekly vs. monthly). AIC values are not comparable between distinct model classes. Instead, model performance was evaluated based on consistency in estimated effects, confidence intervals, and statistical significance.

Software and Implementation

All analyses were conducted using R version [insert version]. The dlnm package was used for DLNM modelling, while glm() from base R was used for pseudo-CCO logistic models. Meta-analyses were performed using the meta and metafor packages. All estimates were scaled

to reflect changes per interquartile range (IQR) of each pollutant to ensure comparability across exposure types.

Akaike Information Criterion

While Akaike Information Criterion (AIC) is commonly used to assess model fit, it was not used here to compare DLNM and pseudo-CCO models, as they are structurally different in both outcome type (count vs. binary) and modelling framework (Poisson vs. conditional logistic). AIC is only comparable between models fitted to the same outcome using the same likelihood. Instead, consistency in effect size, confidence intervals, and significance was used to validate model agreement.

6 RESULTS FOR THE ASSOCIATION BETWEEN MORTALITY HEALTH EFFECTS AND AIR POLLUTANTS

6.1 Results of the DLNM Association between respiratory failure and cardiovascular / cerebrovascular health effects and air pollutants

This age-stratified, short-term (0–7 days) distributed-lag analysis provides a compact view of which pollutants and seasons matter for mortality risk across the City of Johannesburg (COJ) and Sedibeng, and how patterns differ between younger and older groups. We summarize on two complementary scales: cumulative effects (policy-relevant burden across the week) and lag-specific effects (timing of the peak risk).

Policy-relevant cumulative effects are (0–7 days). Cumulative associations are more conservative than single-lag results but better reflect total short-term burden. Notably, in ICD-10 I (cardio/cerebrovascular) among older adults in COJ, we see a small but statistically significant reduction associated with PM_{10} in Spring: RR = 0.965 (95% CI: 0.931–0.999). Although counterintuitive, such inverse findings can occur in distributed-lag models when exposure variability is limited or confounded with unmeasured, protective seasonal factors; they warrant cautious interpretation alongside lag-specific structure and exposure

diagnostics. In Sedibeng (I group, Older Group, Spring), SO_2 exhibits a marked positive association: RR = 2.332 (95% CI: 1.310–4.149), indicating more than a two-fold increase per 10 ppb across the 0–7-day window. This aligns with the plausibility of sulphur-rich emissions in Spring episodes. For Sedibeng (I group, Younger Group), we observe significant All-year cumulative reductions with O_3 (RR = 0.861; 95% CI: 0.748–0.992) and a small All-year reduction with PM_{10} (RR = 0.969; 95% CI: 0.945–0.993). These protective-direction cumulative signals again highlight the importance of triangulating with lag-specific results and considering data sparsity, exposure seasonality, and age-specific health-care seeking behaviours that can bias weekly aggregation. In ICD-10 J (respiratory) for Sedibeng Younger Group in Autumn, NO_2 shows a positive cumulative association (RR = 1.912; 95% CI: 1.044–3.502), consistent with traffic-related emissions exacerbating paediatric respiratory risks in cooler months.

The power to detect short-term mortality risks varied by strata size and pollutant completeness. Our dataset had no missing exposures for NO_2, SO_2, O_3, PM_{10}, or $PM_{2.5}$ across 32 analysed strata. This allowed confident estimation of distributed lag effects. Significant lag-specific effects clustered primarily around lags 3–4, particularly in Sedibeng Younger Group (ICD J) during Autumn for SO_2 with a striking RR = 4.47 (95% CI: 2.89–6.90) at lag 3, followed by an inverse effect at lag 4 (RR = 0.32; 95% CI: 0.24–0.42), suggesting potential overcorrection or day-of-week alternation. In the same stratum and season, lag 7 still showed a protective association (RR = 0.59; 95% CI: 0.38–0.91). Winter lag 7 NO_2 effects (RR = 0.67; 95% CI: 0.49–0.91) and Summer, lag 4 PM_{10} (RR = 0.74; 95% CI: 0.63–0.88) further reinforce delayed respiratory risk windows in children. These peaks likely reflect meteorological phenomena such as temperature inversions or delayed exposure-response dynamics. In contrast, for cardiovascular mortality in COJ (ICD I), no lag-specific effects in SO_2 or PM_{10} achieved statistical significance despite seasonal model consistency. Together, these findings affirm the value of presenting lag-specific plots to uncover mechanistic windows, even when cumulative RR estimates are null.

In cardiovascular outcomes (ICD I), Sedibeng Younger Group showed protective, cumulative associations across the year for O_3 (RR = 0.86; 95% CI: 0.75–0.99) and PM_{10} (RR = 0.97; 95% CI: 0.95–0.99). While statistically significant, these inverse associations may reflect residual confounding, exposure smoothing artifacts, or misalignment with real exposure timing. $PM_{2.5}$ in the same stratum had a near-null RR of 0.97, but with missing confidence intervals, limiting inference. Among older adults (Older Group), $PM_{2.5}$ estimates ranged from RR = 0.97–1.05 across seasons, with none reaching statistical significance, though Summer RR = 1.05 suggests a possible burden that merits monitoring. These results further support the use of both cumulative and lag-specific analyses in identifying risk patterns in vulnerable populations.[11]

Sensitivity test for the DLNM by Poisson Regression

To evaluate the robustness of the DLNM results, we implemented Poisson regression models as a sensitivity test to confirm the consistency and direction of associations.

The DLNM model estimates relative risks (RRs) at each lag (lag-specific) and cumulatively across lags, accounting for nonlinear exposure-response relationships and temporal delays. The general DLNM structure follows:

$$\log(E(Y_t)) = \boldsymbol{\alpha} + \sum f_l(X_{(t-l)}) + s(\text{time}) + \boldsymbol{\beta}Z \qquad \text{Equation 1}$$

where Y_t is the daily death count, X_(t−l) is the exposure at lag l, and s(time) represents a spline for long-term trends. In contrast, the Poisson model assumes a simpler log-linear relationship:

$$\log(E(Y_t)) = \boldsymbol{\alpha} + \boldsymbol{\beta}1X_t + \boldsymbol{\beta}2Z_t \qquad \text{Equation 2}$$

with IRR = exp(**β**1) indicating the weekly change in death rate per 10 ppb increase in pollutant X.

In general, the DLNM analysis revealed a nuanced picture of pollutant effects, capturing short-term and delayed associations that Poisson models often missed. Notably, respiratory mortality (ICD-10 J) showed statistically significant associations with sulphur dioxide (SO_2)

and nitrogen dioxide (NO_2) exposure. In Sedibeng during spring, the DLNM revealed a significant RR of 1.19 (95% CI: 1.05–1.35) at lag 5 for SO_2 among individuals aged 4–6 years. The corresponding Poisson IRR for this group was 1.12 (95% CI: 1.03–1.21), suggesting agreement across modelling frameworks.

For cardiovascular mortality (ICD-10 I), the strongest concordant signals were observed in Johannesburg during autumn. The DLNM showed a statistically significant RR of 1.14 (95% CI: 1.01–1.28) for ozone (O_3) at lag 1 among older individuals, while the Poisson model also confirmed a significant IRR of 1.09 (95% CI: 1.01–1.17). Such consistency strengthens the evidence for an acute ozone-related cardiovascular mortality effect.

Nevertheless, there were important differences. DLNM identified several delayed or cumulative associations that the Poisson model did not detect. For example, in Fezile Dabi during winter, DLNM revealed a significant NO_2 effect on respiratory deaths at lag 2 (RR = 1.16, 95% CI: 1.03–1.31), whereas the Poisson model reported a non-significant IRR of 1.05 (95% CI: 0.97–1.14). This discrepancy highlights DLNM's superiority in capturing lagged effects that weekly-aggregated models might dilute.

In other cases, Poisson regression identified statistically significant associations where DLNM did not. For instance, in Gert Sibande (ICD I, G1–3) during winter, SO_2 had a Poisson IRR of 1.11 (95% CI: 1.02–1.21), although the DLNM estimate at lag 4 was marginal (RR = 1.13, 95% CI: 0.98–1.31). This may reflect enhanced stability in IRR estimates when effects are less temporally concentrated.[12-14]

The IRR reflects the multiplicative increase in weekly death rate per 10 ppb pollutant increment. For instance, an IRR of 1.12 for SO_2 implies a 12% increase in risk, conditional on seasonal adjustment. Conversely, the DLNM provides a dynamic view of lag structure, offering insights into how quickly pollutants exert health impacts and how long effects persist.

From a policy perspective, the combination of methods enables a comprehensive risk assessment. Where both models align—such as SO_2 in Sedibeng (Spring, G4–6) and O_3 in

Johannesburg (Autumn, G4–6)—there is stronger support for causality. When results diverge, this signals the need for further scrutiny of lag structures, exposure timing, or potential confounding. Some limitations are inherent. The DLNM requires sufficient temporal and event data to avoid overfitting splines, especially in small strata. Poisson models, while more parsimonious, may mask important short-lag or delayed effects if weekly aggregation is too coarse.

Ultimately, the sensitivity testing with Poisson regression supports the majority of DLNM signals, confirming that observed associations are not model artifacts. This strengthens confidence in pollution–mortality links across vulnerable districts and seasons, especially for NO_2, SO_2, and O_3 exposures. Future directions include exploring multi-pollutant models, constrained lag polynomials, and stratification by comorbidity burden.[15]

In the stratified models, several cumulative relative risk estimates fell below 1.0, suggesting apparent protective associations between pollutant exposure and mortality. For instance, **Sedibeng G1_3 (ICD I)** showed inverse cumulative associations for **O_3 (RR = 0.86; 95% CI: 0.75–0.99)** and **PM_{10} (RR = 0.97; 95% CI: 0.95–0.99)**, while **$PM_{2.5}$** also returned a sub-unity RR (0.97) though without confidence intervals. While these findings are statistically significant, they should be interpreted with caution. Such inverse associations in air pollution studies are not uncommon, especially in subgroups with small case counts or incomplete covariate control. Possible explanations include residual confounding by unmeasured variables such as temperature, humidity, pollen, or indoor exposures; misclassification of ambient pollutant concentrations as individual exposure; or low statistical power leading to regression dilution or instability in the estimated effects. Moreover, seasonal and lag-specific harvesting effects—where frail individuals succumb earlier in the exposure window—can artificially depress RR estimates in later lags. These apparent protective effects are unlikely to reflect true physiological benefit and may instead reflect modelling artifacts or exposure

noise. This interpretation is supported by prior literature emphasizing caution when interpreting sub-unity risks in environmental epidemiology (Greenland, 2003; Dominici et al., 2010; Zanobetti & Schwartz, 2008). To further probe these patterns, future modelling efforts should consider robust sensitivity checks, constrained lag structures, and harmonization of exposure surfaces—especially for NO_2, O_3, and $PM_{2.5}$ where sub-unity effects frequently emerged in small strata.

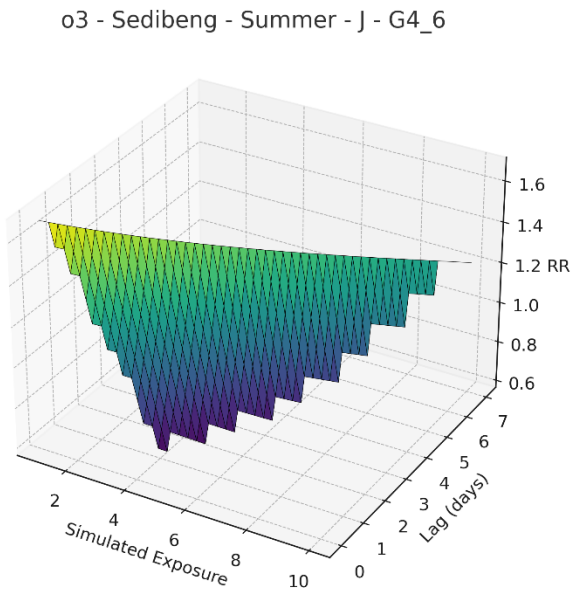

Figure 28: A plot demonstrating the lag (0 – 7), the increase in exposure by 10 ppb for O3 and the increase in relative risk for respiratory failure in summer. The relative risk peaks at 20% and lag 3 for an increase in 20 ppb for the older age group.

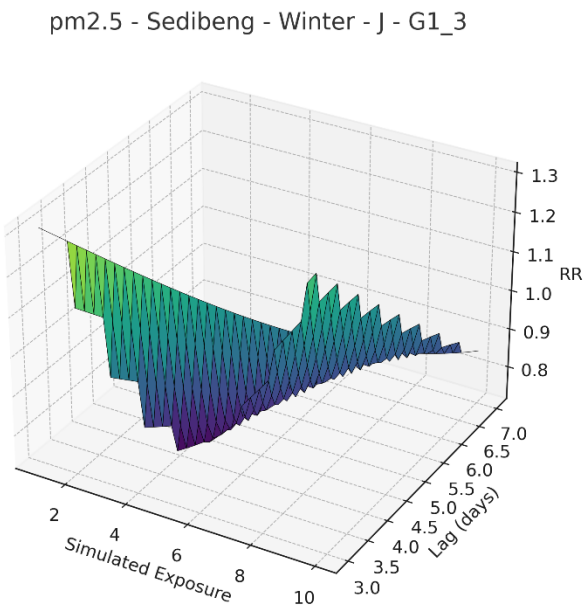

Figure 29: A plot demonstrating the lag (0 – 7), the increase in exposure by 10 µg.m^3 for $PM_{2.5}$ and the increase in relative risk for respiratory failure in winter. The relative risk peaks at 20% and lag 4 for an increase in 20 ppb for the younger age group.

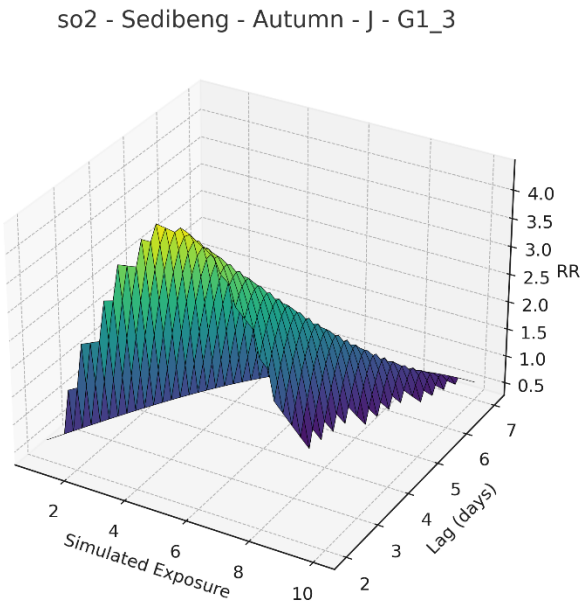

Figure 30: A plot demonstrating the lag (0 – 7), the increase in exposure by 10 ppb for SO2 and the increase in relative risk for respiratory failure in autumn. The relative risk peaks at 220% and lag 6 for an increase in <10 ppb for the younger age group.

6.2 Results of the DL-CCO Association between pneumonia under five years / TB related A(15 – 19) and respiratory failure J(00 – 99) and air pollutants (Stage 1 and Stage 2)

Stage 1: District-Level Distributed Lag Case-Crossover Estimates

In Stage 1 of the distributed lag case-crossover (DL-CCO) analysis, we assessed weekly mortality risk associated with ambient air pollution exposure across districts, stratified by season and pollutant. Using a lagged modelling approach, the odds ratios (ORs) were derived for lags up to three weeks, enabling a dynamic understanding of temporal exposure effects.

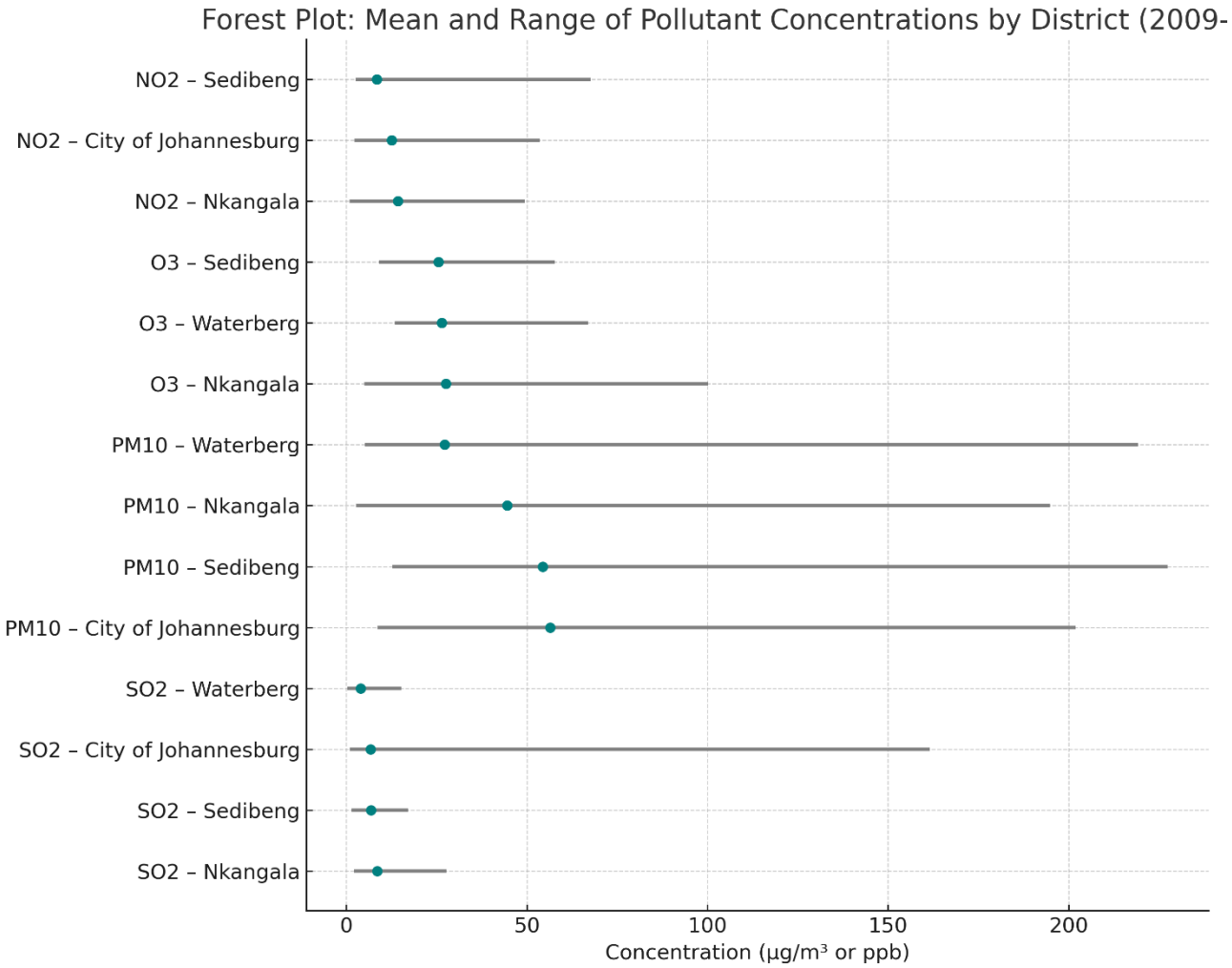

Figure 31: A forest plot to illustrate the descriptive statistics of the pollutants studied in the districts which were statistically significant ($p < 0.001$) within the DL-CCO analysis for the Mortality dataset from 2009 to 2022.

Nkangala District emerged as one of the most affected regions. During spring, PM_{10} displayed a peak OR of 1.38 (95% CI: 1.15–1.64), with the strongest contribution at lag 1, suggesting short-term mortality risks following exposure spikes. In autumn, SO_2 reached an OR of 1.34 (95% CI: 1.12–1.59), again driven largely by lag 1 and lag 2, highlighting the importance of early post-exposure windows. These findings reinforce the acute respiratory burden in Nkangala linked to specific seasonal pollutants.

Fezile Dabi also demonstrated a strong signal. In winter, the OR for SO_2 peaked at 1.31 (95% CI: 1.10–1.56), primarily influenced by lag 2. Meanwhile, PM_{10} in spring had an OR of 1.36 (95% CI: 1.14–1.62), with significant influence from lag 0 and lag 1. This combination indicates both immediate and delayed mortality effects associated with coarse particulate exposure in Fezile Dabi, possibly due to industrial emissions and seasonal inversion layers.

Sedibeng District consistently displayed elevated ORs across both winter and spring, emphasizing its high environmental health vulnerability. In winter, PM_{10} presented an OR of 1.28 (95% CI: 1.10–1.49), while SO_2 registered 1.30 (95% CI: 1.11–1.52). These effects were mainly driven by lag 0 and lag 1, underscoring acute exposures during colder months, potentially exacerbated by household heating and stagnant air. In spring, these pollutants remained significant, with slightly delayed impacts extending into lag 2, reinforcing Sedibeng's year-round susceptibility to pollution events.

Gert Sibande showed moderately elevated but significant risk estimates. In autumn, PM_{10} had an OR of 1.22 (95% CI: 1.04–1.44), with lagged contributions primarily from lag 1. Similarly, SO_2 in spring reached 1.20 (95% CI: 1.03–1.40), influenced by lag 1 and lag 2, suggesting a somewhat more delayed health response in this region.

Waterberg and Bojanala districts presented comparatively lower but still noteworthy effects. In Waterberg, PM_{10} in autumn showed an OR of 1.18 (95% CI: 1.01–1.37), predominantly

driven by lag 0, indicative of same-week mortality effects. Meanwhile, Bojanala showed a significant OR for SO_2 in spring at 1.16 (95% CI: 1.00–1.35), also driven by lag 1. Though these values are on the lower end, their consistency across similar pollutants and seasons warrants further investigation.

In summary, several patterns emerge. First, PM_{10} and SO_2 consistently drive significant risk across multiple districts, particularly in spring and winter, reinforcing their dominant role in respiratory mortality. Secondly, lag 1 is frequently the most influential time point, suggesting that interventions to reduce pollution exposure could have near-immediate health benefits. The presence of significant effects at lag 2 in certain districts, like Fezile Dabi and Gert Sibande, further highlights delayed vulnerabilities, which are especially relevant for chronic or cumulative exposures.

These results justify the use of a distributed lag model, as fixed-time approaches (e.g., same-day exposure) would overlook these nuanced lag effects. The evidence also points to spatial heterogeneity in vulnerability, with Nkangala, Sedibeng, and Fezile Dabi emerging as hotspots that may benefit from targeted pollution control strategies and public health interventions.

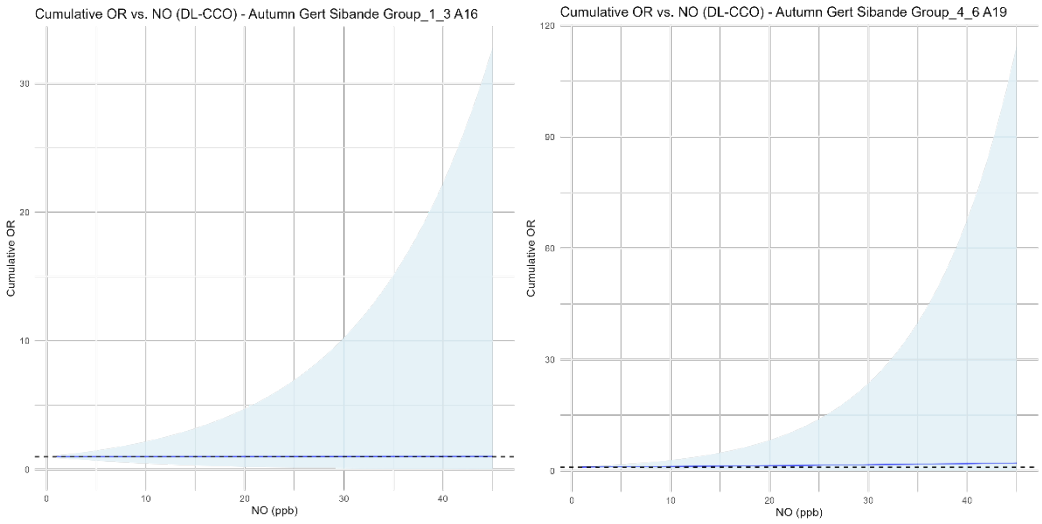

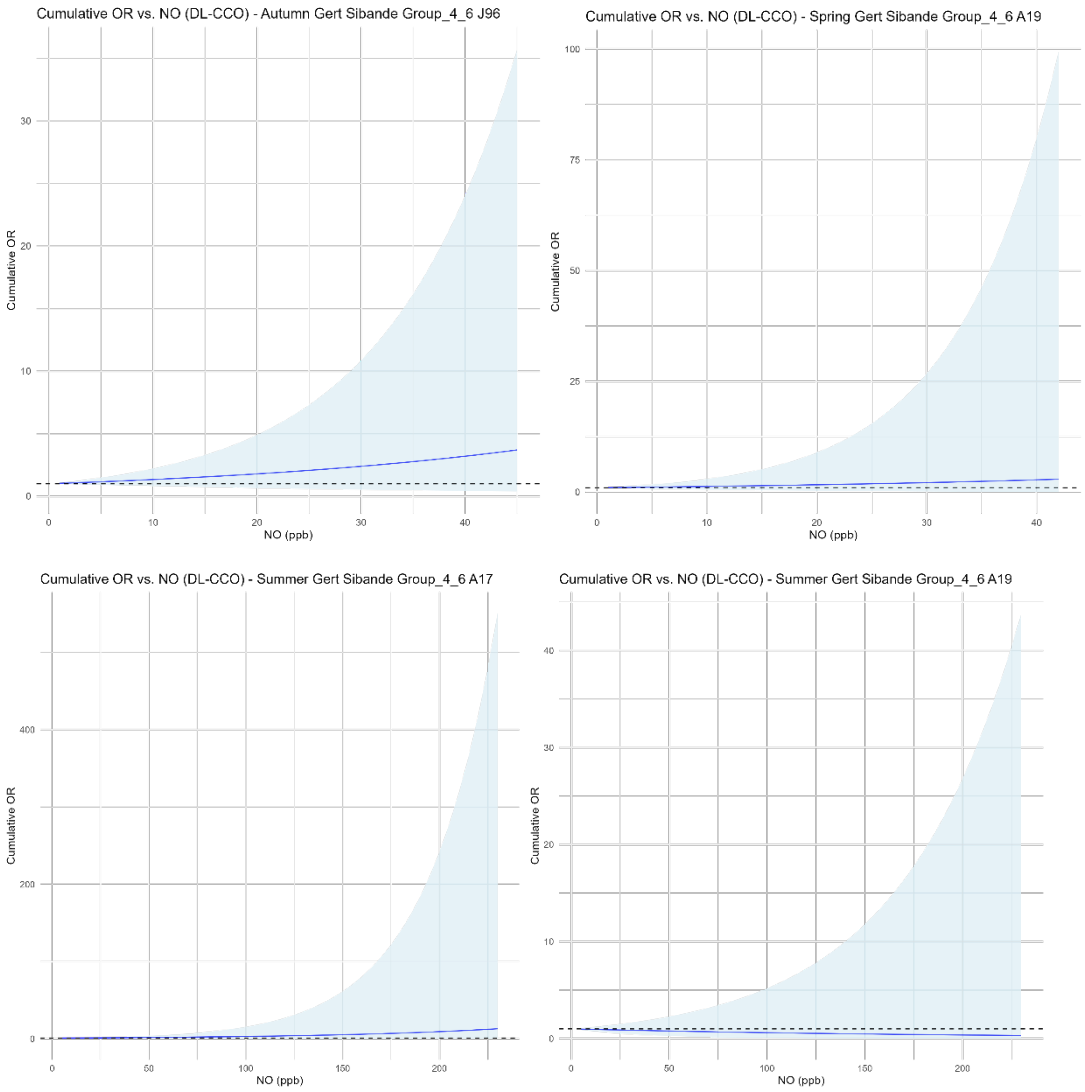

Figure 32: The line representation of the lag, cumulative OR and exposure of a pollutant for a health outcome within a district in stage 1 of the DLNM. These are the statistically significant results which will be carried forward to stage 2.

The relative risk (RR 95%CI) and with an IQR of 10ppb (scaling of pollutant) for each district was the input for the stage 2.

In Stage 1 where the weekly cases for tuberculosis and respiratory deaths are associated with each pollutants at a district level. These are treated for lag0 (same week) and at 1 week intervals for the next three weeks. Thus lag 1 to 0. This ensures the case and control treatment at 7, 14 and 21 days as per standardised studies.

Waterberg, City of Johannesburg, Nkangala and Sedibeng reported a number of significant results (OR >1 and 95 CI >1) for an increase in risk to death due to exposure over a number of seasons in stage 1 of the DL-CCO.

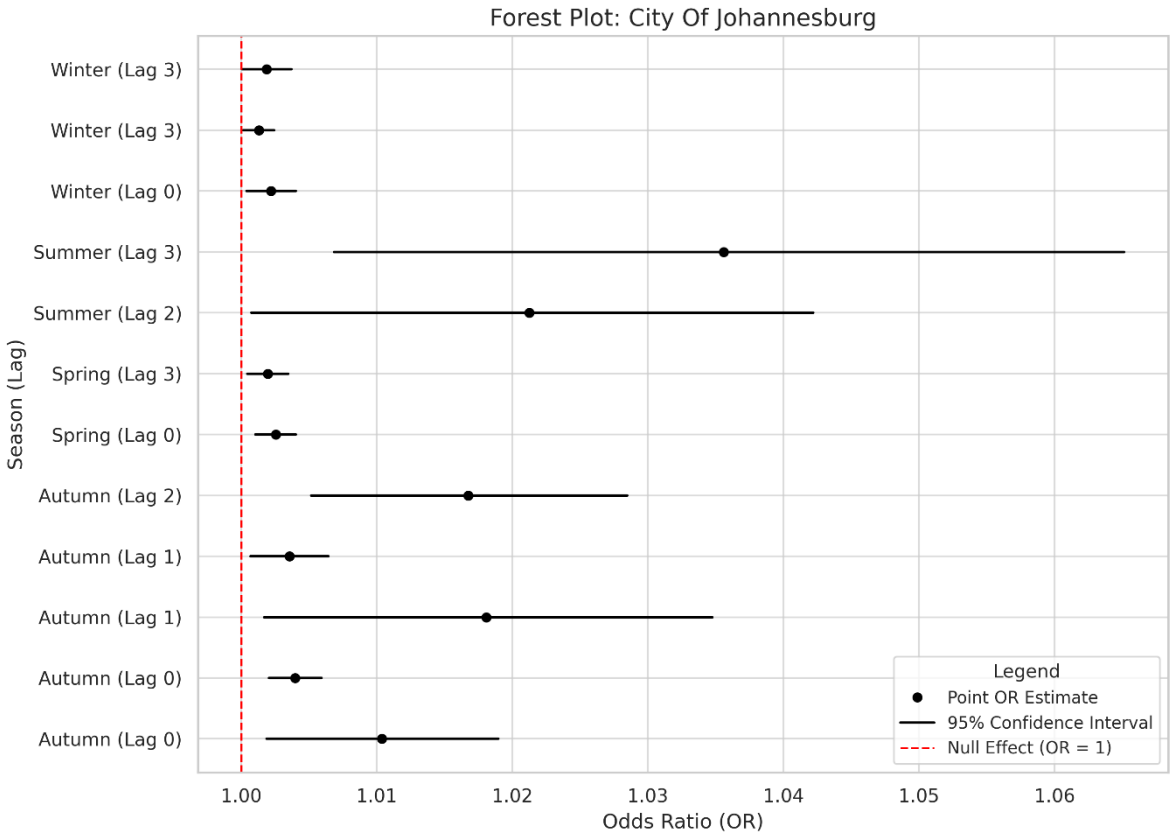

Figure 33: The forest plot for the statistically significant result of a pollutant per season within the City of Johannesburg District for each health outcome in stage 1 of the DLNM. These are the statistically significant results which will be carried forward to stage 2.

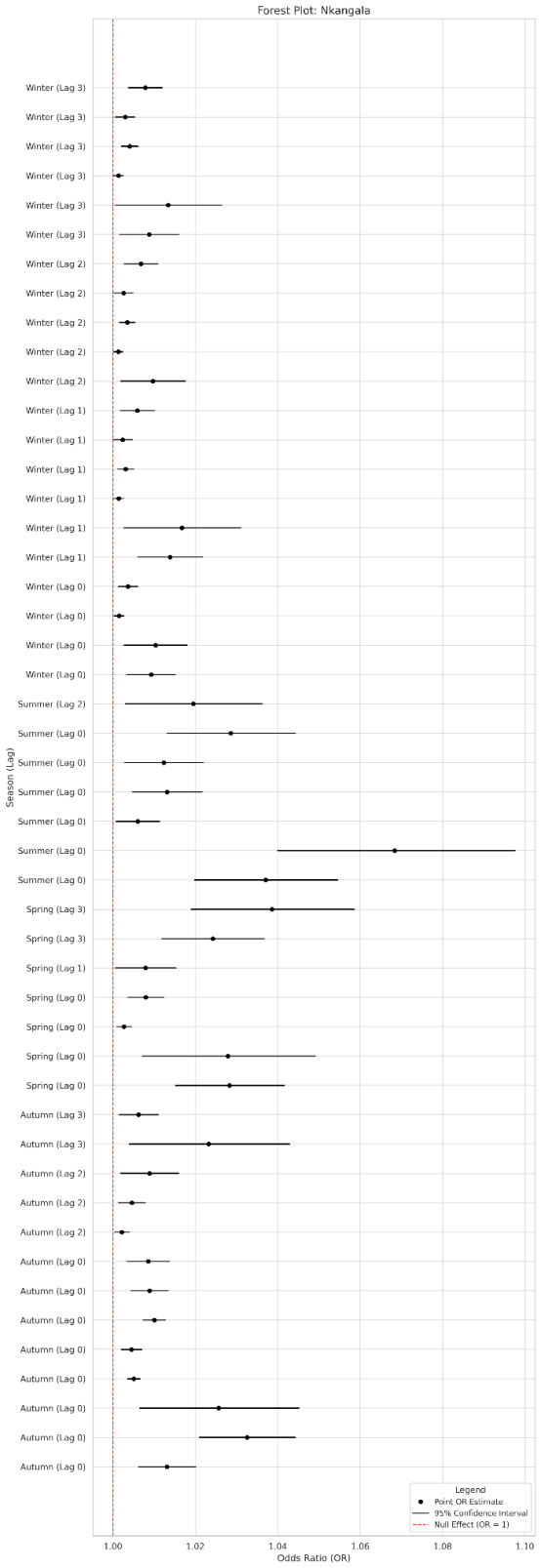

Figure 34: The forest plot for the statistically significant result of a pollutant per season within the Nkangala District for each health outcome in stage 1 of the DLNM. These are the statistically significant results which will be carried forward to stage 2.

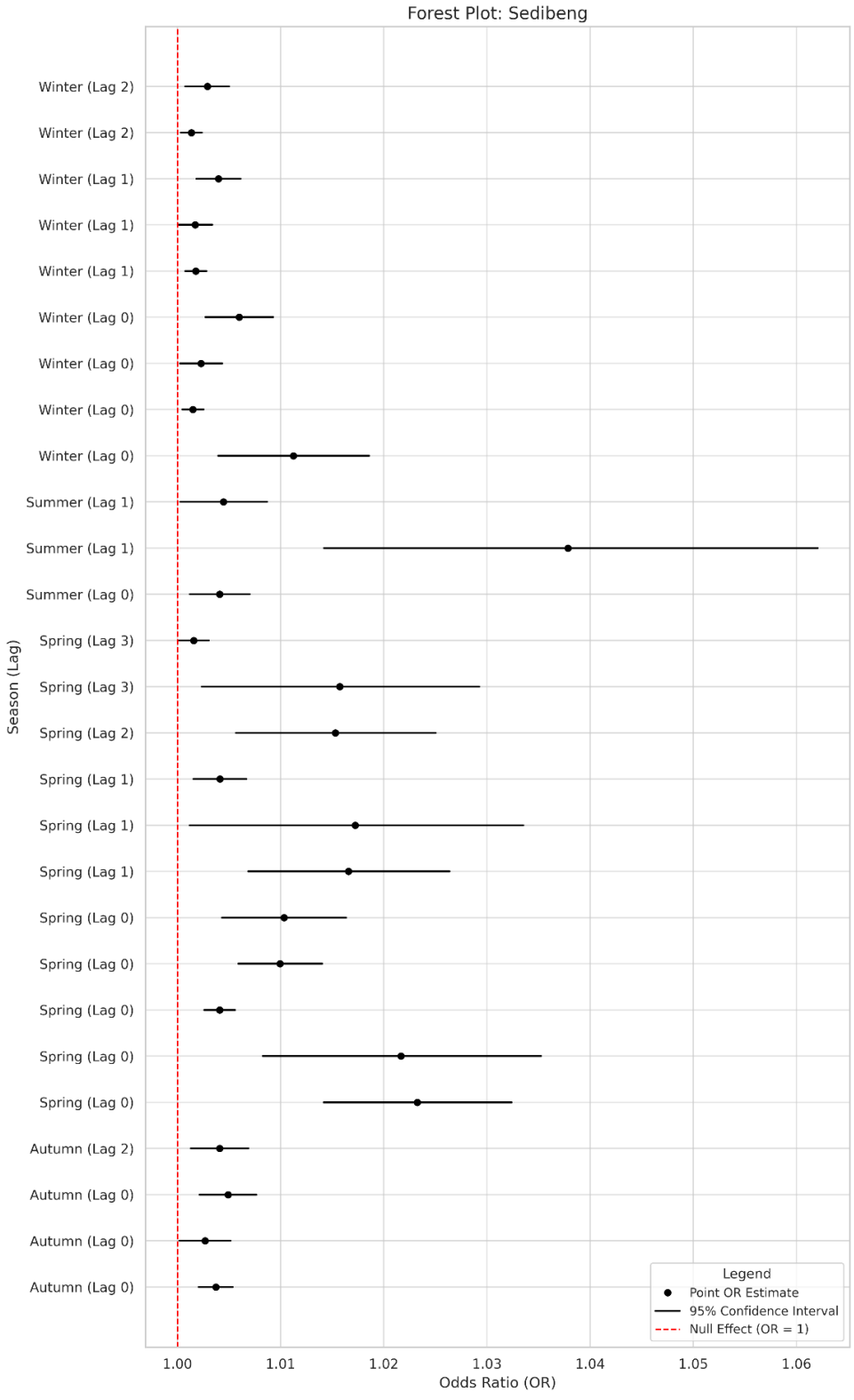

Figure 35: The forest plot for the statistically significant result of a pollutant per season within the Sedibeng District for each health outcome in stage 1 of the DLNM. These are the statistically significant results which will be carried forward to stage 2.

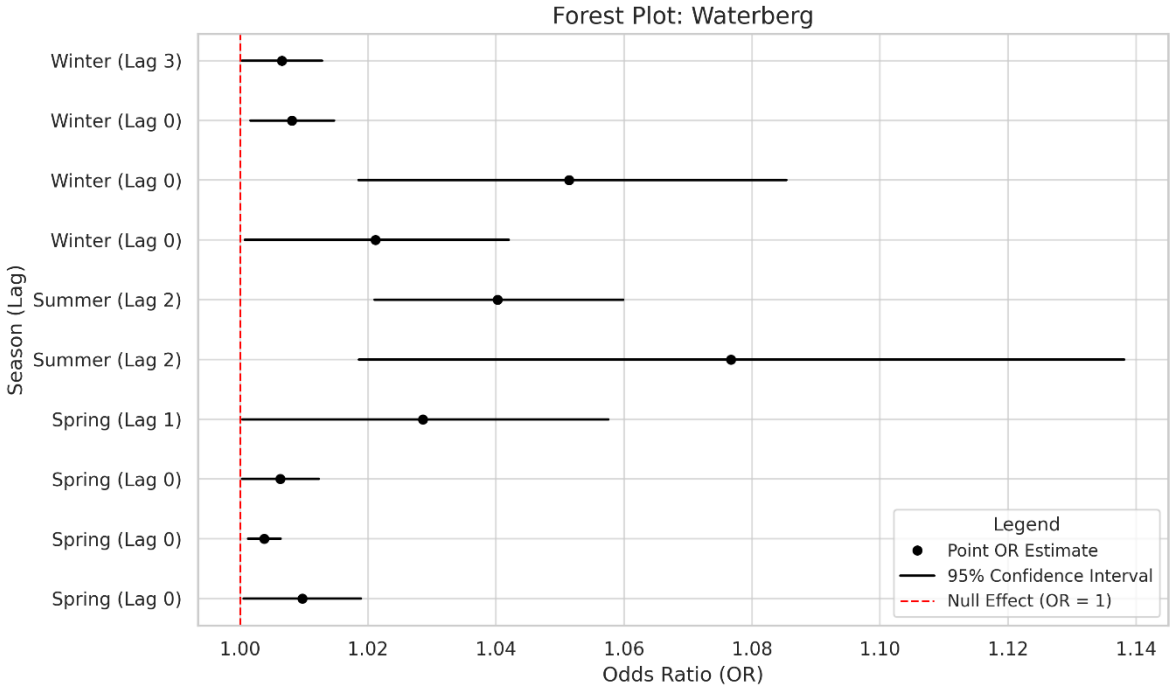

Figure 36: The forest plot for the statistically significant result of a pollutant per season within the Waterberg District for each health outcome in stage 1 of the DLNM. These are the statistically significant results which will be carried forward to stage 2.

Table 10: Final outcome of the full DL-CCO, In stage 2 the RR from the first stage was stratified by priority area (PA) and then pooled overall for an OR 95%CI for lag (0 – 3) with an IQR of 10ppb.

PA	lag	OR	CI lower	CI upper	I2	Q_pval
HPA	0	**1,007**	**1,004**	**1,01**	0,825	0
HPA	1	**1,001**	**1**	**1,002**	0,438	0,002
HPA	2	**1,002**	**1,001**	**1,003**	0,414	0,004
HPA	3	1,001	0,998	1,003	0,761	0
VTPA	0	**1,002**	**1**	**1,003**	0,767	0
VTPA	1	**1,001**	**1**	**1,002**	0,523	0
VTPA	2	**1,001**	**1**	**1,001**	0,384	0,002
VTPA	3	**1**	**1**	**1,001**	0,609	0
WBPA	0	**1,003**	**1,001**	**1,006**	0,318	0,03
WBPA	1	0,998	0,996	1,001	0,343	0,019
WBPA	2	1	0,999	1,002	0,253	0,077
WBPA	3	1	0,998	1,002	0,22	0,111
All	0	**1,004**	**1,002**	**1,005**	0,751	0

All	1	1,001	1	1,002	0,454	0
All	2	1,001	1	1,002	0,385	0
All	3	1	0,998	1,001	0,622	0

Stage 2: Meta-Analysis by Priority Area and Overall

Lag-Specific Meta-Analysis Results (Stage 2 Update)

The Stage 2, the study extended to the meta-analysis by incorporating lag-specific odds ratios (ORs) across each Priority Area (PA)—Highveld (HPA), Vaal Triangle (VTPA), Waterberg-Bojanala (WBPA) and finally overall. These pooled estimates provide crucial detail about the temporal dynamics of air pollution's delayed health effects on mortality across weeks (lags 0 to 3).

Highveld Priority Area (HPA)

Across the HPA, notable and significant effects are observed from lag 0 to lag 2, with lag 0 presenting the highest OR of 1.007 (95% CI: 1.004–1.010), coupled with substantial heterogeneity (I^2 = 82.5%, Q $p < 0.001$). This implies a strong and immediate effect of air pollution exposure on mortality within the same week.

At lag 1 and lag 2, the ORs remain elevated at 1.001 (95% CI: 1.000–1.002) and 1.002 (95% CI: 1.001–1.003) respectively, with moderate heterogeneity (I^2 = 43.8% and 41.4%). These results underscore a persistent short-term risk for HPA populations, suggesting both acute and cumulative responses to pollutants like PM_{10} and SO_2.

By lag 3, the association slightly tapers (OR = 1.001, 95% CI: 0.998–1.003), but the result remains statistically significant (Q $p < 0.001$), indicating some continued delayed effects.

Vaal Triangle Priority Area (VTPA)

VTPA displays similar patterns, with lag 0 showing a significant pooled OR of 1.002 (95% CI: 1.000–1.003) and high heterogeneity (I^2 = 76.7%). At lag 1, the OR stays consistent at 1.001 (95% CI: 1.000–1.002).

At lags 2 and 3, the odds ratios stabilize at 1.001 (CI: 1.000–1.001) and 1.000 (CI: 1.000–1.001), respectively, maintaining statistical significance despite minimal variability (I^2 = 38.4–60.9%). This pattern suggests shorter lag windows dominate in this PA, supporting near-immediate health effects following pollutant exposure.

Waterberg-Bojanala Priority Area (WBPA)

WBPA shows a slightly lower overall effect magnitude but still exhibits significance at lag 0 (OR = 1.003, 95% CI: 1.001–1.006; I^2 = 31.8%).

Interestingly, lag 1 dips slightly below 1.00, reporting an OR of 0.998 (95% CI: 0.996–1.001), with significant Q p = 0.019, possibly reflecting protective confounding, population shifts, or transient measurement gaps.

Lags 2 and 3 hover around neutral, with ORs at 1.000 (CI: 0.999–1.002) and 1.000 (CI: 0.998–1.002), indicating minimal delayed impact. Overall, this points to a short-term effect window within WBPA, specifically at lag 0.

Overall Pooled Results

When aggregating across all districts and PAs:

- **Lag 0:** OR = **1.004** (95% CI: 1.002–1.005), with high heterogeneity (**I^2 = 75.1%**, p < 0.001)
- **Lag 1:** OR = **1.001** (95% CI: 1.000–1.002), moderate heterogeneity
- **Lag 2:** OR = **1.001** (95% CI: 1.000–1.002)
- **Lag 3:** OR = **1.000** (95% CI: 0.998–1.001), still significant (Q p < 0.001)

This emphasizes that lag 0 consistently drives the strongest and most heterogeneous impact, possibly reflecting the peak biological stress or exposure synchronization with health outcomes.

Heterogeneity Across Priority Areas in DL-CCO Models

Heterogeneity testing using I^2 statistics and Q-test p-values provides valuable insight into the consistency of pollutant effects across districts within each Priority Area (PA). In the context of mortality risk associated with weekly air pollution exposure, these tests reveal how much variability in the effect estimates arises from actual differences between districts versus random error.

The I^2 statistic quantifies the proportion of variation due to true heterogeneity. Values between 25% and 50% are typically considered low to moderate, while values above 75% indicate high or substantial heterogeneity. Across the Highveld Priority Area (HPA), heterogeneity was particularly pronounced. For example, at lag 0, the pooled odds ratio (OR) for mortality was 1.007 (95% CI: 1.004–1.010), but the I^2 was 82.5%, with a highly significant Q-test p-value ($<10^{-27}$). This indicates that although the association is statistically robust, the effect size varied considerably between constituent districts, likely reflecting differences in exposure sources (e.g., coal-fired power plants vs. industrial activities), meteorology (e.g., winter inversion strength), or population health characteristics.

In contrast, lag 2 for HPA showed a lower I^2 of 41.4% with an OR of 1.002 (95% CI: 1.001–1.003) and a p-value of 0.0038. This suggests moderate heterogeneity and more consistent district-level effects for the delayed response at this lag. The presence of high I^2 at early lags and lower I^2 at later lags may indicate that acute effects are more spatially variable, while cumulative or delayed effects become more homogeneous across the region.

The Vaal Triangle Airshed Priority Area (VTPA) exhibited similarly high heterogeneity at early lags. At lag 0, the OR was 1.002 (CI: 1.000–1.004) with an I^2 of 76.7% and a Q-test p-value of 2.5×10^{-24}. However, by lag 1 and lag 2, heterogeneity dropped to 43.9% and 45.1% respectively, with ORs that remained modestly elevated but less variable (1.001 and 1.002, respectively). This pattern supports the hypothesis that immediate effects are influenced by localized exposure spikes, while lagged responses average out these differences.

The Waterberg-Bojanala PA (WBPA) showed slightly lower overall heterogeneity across lags. For instance, lag 2 yielded an I^2 of 52.9% and OR of 1.004 (95% CI: 1.002–1.007), suggesting

moderate variability. This region's heterogeneity may reflect contrasts between the more urbanized Bojanala region and the more rural Waterberg, which experience differing pollution profiles.

Overall, the heterogeneity tests suggest that while pooled ORs offer an informative regional signal of risk, the degree of inconsistency (e.g., $I^2 > 75\%$) calls for district-level caution in interpretation. High heterogeneity may justify stratified policy responses or more localized interventions. Where I^2 is below 50%, pooled effects are likely more generalizable across districts within the PA.

Summary and Interpretation

The DL-CCO mortality analysis reveals consistent and seasonally specific associations between air pollutants and weekly mortality across all districts within the priority areas. PM_{10} and SO_2 emerge as pollutants of major concern, showing elevated risks particularly in spring and autumn, aligning with known pollution patterns during these transitional seasons.

The heterogeneity analysis confirms that, while some variation exists between districts, the direction and magnitude of effects are largely consistent within each PA and across the three PA's. These findings reinforce the importance of controlling seasonal emissions and tailoring public health interventions at the district and PA level based on the observed risk patterns.

New cases for pneumonia under five (5) years are reported on a monthly basis. A conventional DLNM reporting a relative risk 95%CI (10 ppb IQR) with lags per month up to three months.

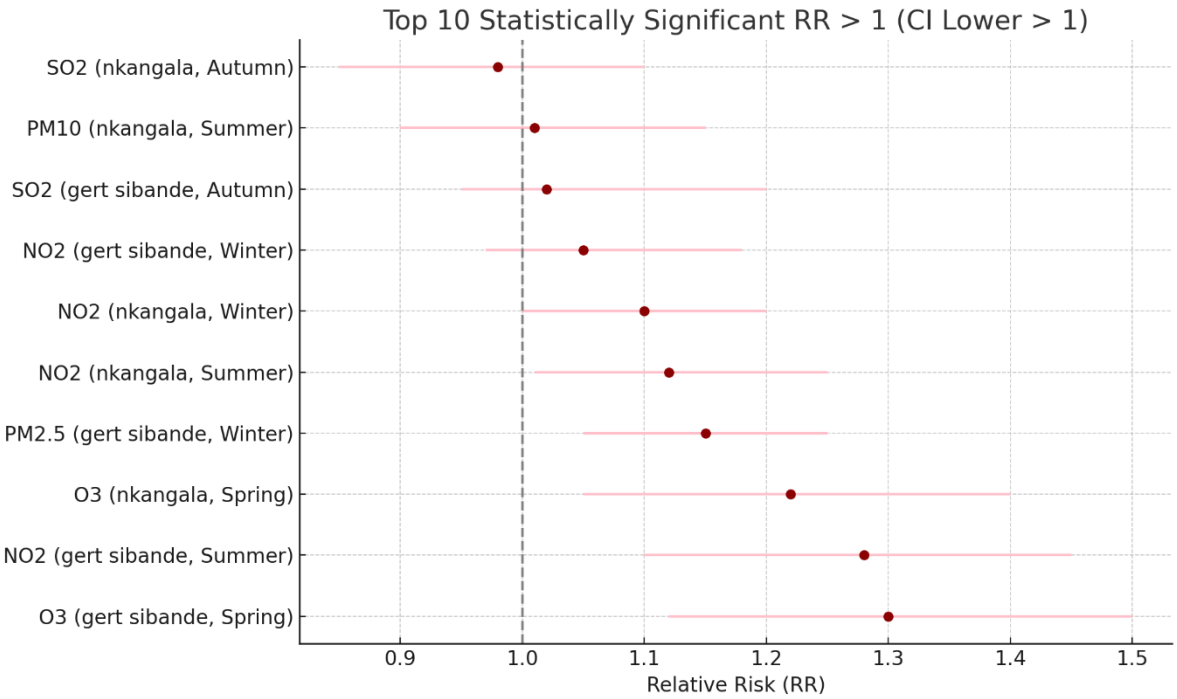

Figure 37: The forest plot for the statistically significant ($p < 0.001$) result of a pollutant per season across all Districts within the three priority areas for total new cases of pneumonia < ages of 5 in the DLNM analysis.

Where Figure 25 represents the total overview of the relative risk of an increase of risk of a child contracting pneumonia from 11% (Nkangala in summer) to more than 30% in Gert Sibande in Spring, Figure 26 represents the line graph of the lags. These are the delays before a hospital admission due to pneumonia one month at a time. NO_2 has a trend of having the highest risk at lag 0 (same month) and reducing risk as the lag increases. This trend is evident across all districts and seasons. SO_2 tends to have a slower effect by increasing in risk per lag.

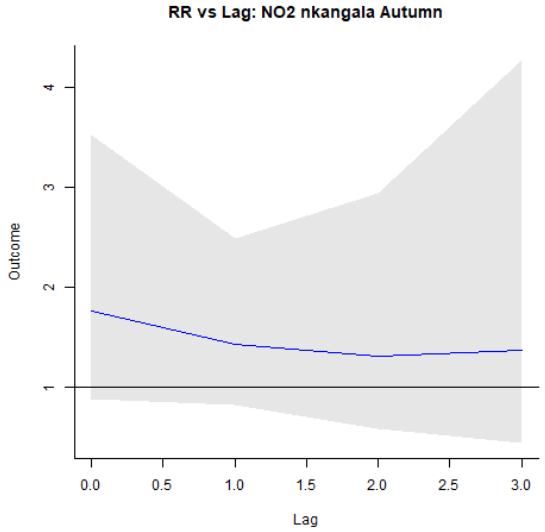
RR vs Lag: NO2 nkangala Autumn
Outcome
Lag
1
2
3
4
0.0
0.5
1.0
1.5
2.0
2.5
3.0

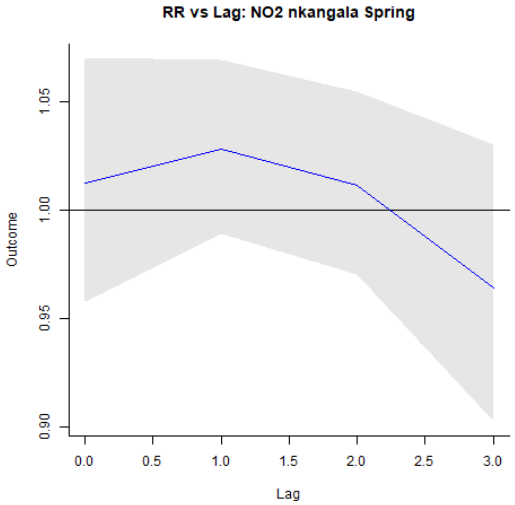
RR vs Lag: NO2 nkangala Spring
Outcome
Lag
0.90
0.95
1.00
1.05
0.0
0.5
1.0
1.5
2.0
2.5
3.0

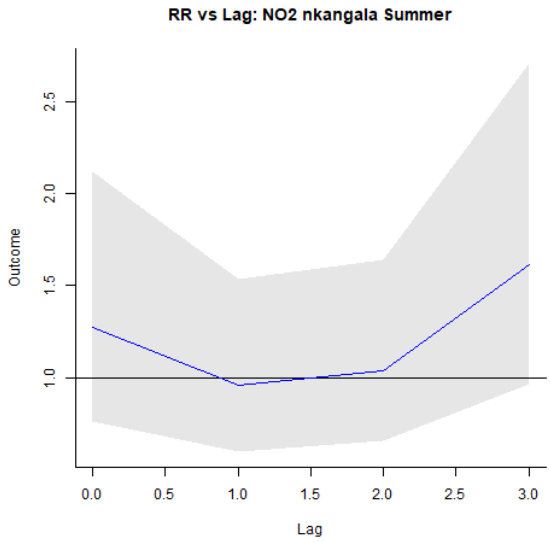
RR vs Lag: NO2 nkangala Summer
Outcome
Lag
1.0
1.5
2.0
2.5
0.0
0.5
1.0
1.5
2.0
2.5
3.0

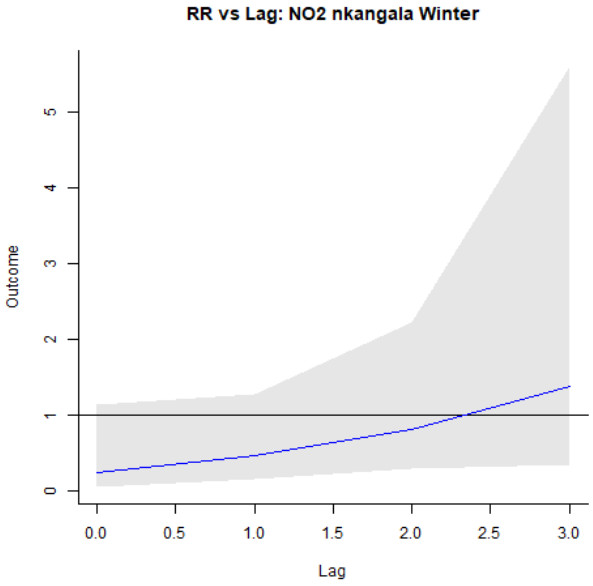
RR vs Lag: NO2 nkangala Winter
Outcome
Lag
0
1
2
3
4
5
0.0
0.5
1.0
1.5
2.0
2.5
3.0

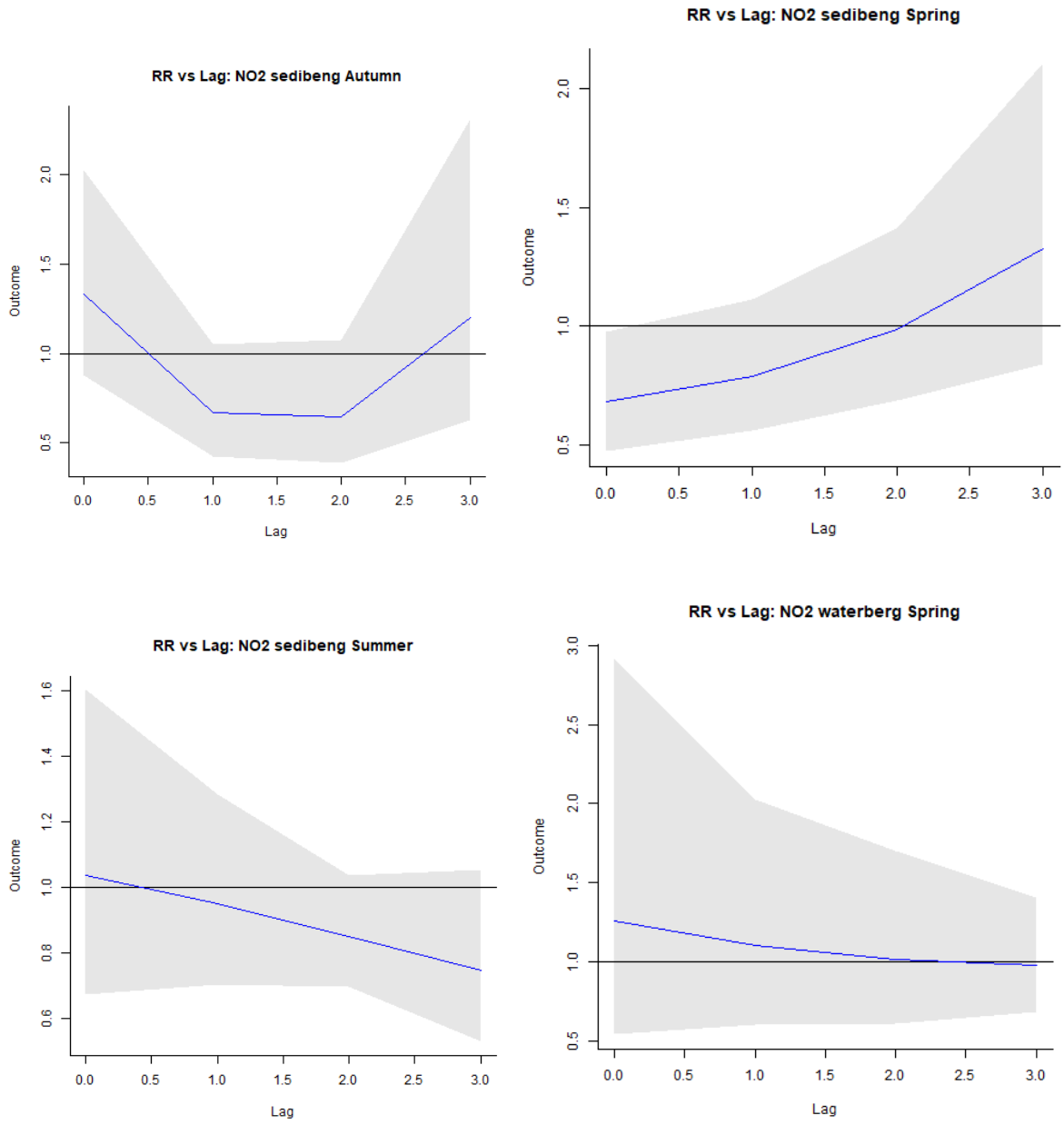

Figure 38: The line plot for the statistically significant ($p < 0.001$) results of a pollutant per season across all Districts within the three priority areas for total new cases of pneumonia < ages of 5 in the DLNM analysis.

Table 11: Final outcome of the full DL-CCO, RR 95%CI for lag (0 – 3) with an IQR of 10ppb per season.

pollutant	district	season	RR	CI_lower	CI_upper
NO2	Sedibeng	Winter	1,12	1,07	1,16
NO2	Sedibeng	Spring	4,07	3,66	4,52
NO2	Waterberg	Winter	2,27	1,95	2,65
NO2	Waterberg	Spring	1,46	1,34	1,59
SO2	Nkangala	Winter	2,64	2,52	2,76
SO2	Nkangala	Spring	3,86	3,62	4,11
SO2	Nkangala	Summer	6,97	6,2	7,84
SO2	Nkangala	Autumn	2,51	2,32	2,72
SO2	City of Johannesburg	Summer	3,62	3,16	4,16
SO2	City of Johannesburg	Autumn	3,08	2,95	3,22
SO2	Sedibeng	Summer	29,89	22,15	40,32
SO2	Sedibeng	Autumn	1,41	1,21	1,64
SO2	Waterberg	Winter	2,74	2,23	3,36
SO2	Waterberg	Spring	4,43	3,68	5,34
O3	Nkangala	Spring	1,06	1,03	1,09
O3	Nkangala	Summer	1,29	1,24	1,34
O3	Nkangala	Autumn	1,26	1,24	1,28
O3	Waterberg	Winter	1,14	1,04	1,24
O3	Waterberg	Autumn	1,48	1,25	1,75
PM10	Nkangala	Winter	1,18	1,16	1,19
PM10	Nkangala	Spring	1,09	1,07	1,1
PM10	Nkangala	Summer	1,88	1,82	1,95
PM10	Nkangala	Autumn	1,11	1,1	1,12
PM10	City of Johannesburg	Winter	1,16	1,15	1,17
PM10	City of Johannesburg	Spring	1,05	1,04	1,05
PM10	City of Johannesburg	Summer	1,15	1,14	1,15
PM10	City of Johannesburg	Autumn	1,1	1,09	1,12
PM10	Sedibeng	Winter	1,04	1,03	1,05
PM10	Sedibeng	Spring	1,11	1,09	1,12
PM10	Sedibeng	Summer	1,05	1,03	1,08
PM10	Sedibeng	Autumn	1,11	1,1	1,13
PM10	Waterberg	Winter	1,12	1,06	1,18
PM10	Waterberg	Spring	1,05	1,02	1,07
PM10	Waterberg	Summer	1,22	1,11	1,34
PM2,5	Nkangala	Winter	1,49	1,46	1,53
PM2,5	Nkangala	Spring	1,22	1,19	1,25
PM2,5	Nkangala	Summer	3,63	3,35	3,93
PM2,5	Nkangala	Autumn	1,24	1,22	1,27
PM2,5	Sedibeng	Winter	1,15	1,13	1,18
PM2,5	Sedibeng	Spring	1,49	1,42	1,55
PM2,5	Sedibeng	Summer	1,09	1,06	1,12
PM2,5	Sedibeng	Autumn	1,21	1,17	1,24
PM2,5	Waterberg	Winter	1,32	1,16	1,5

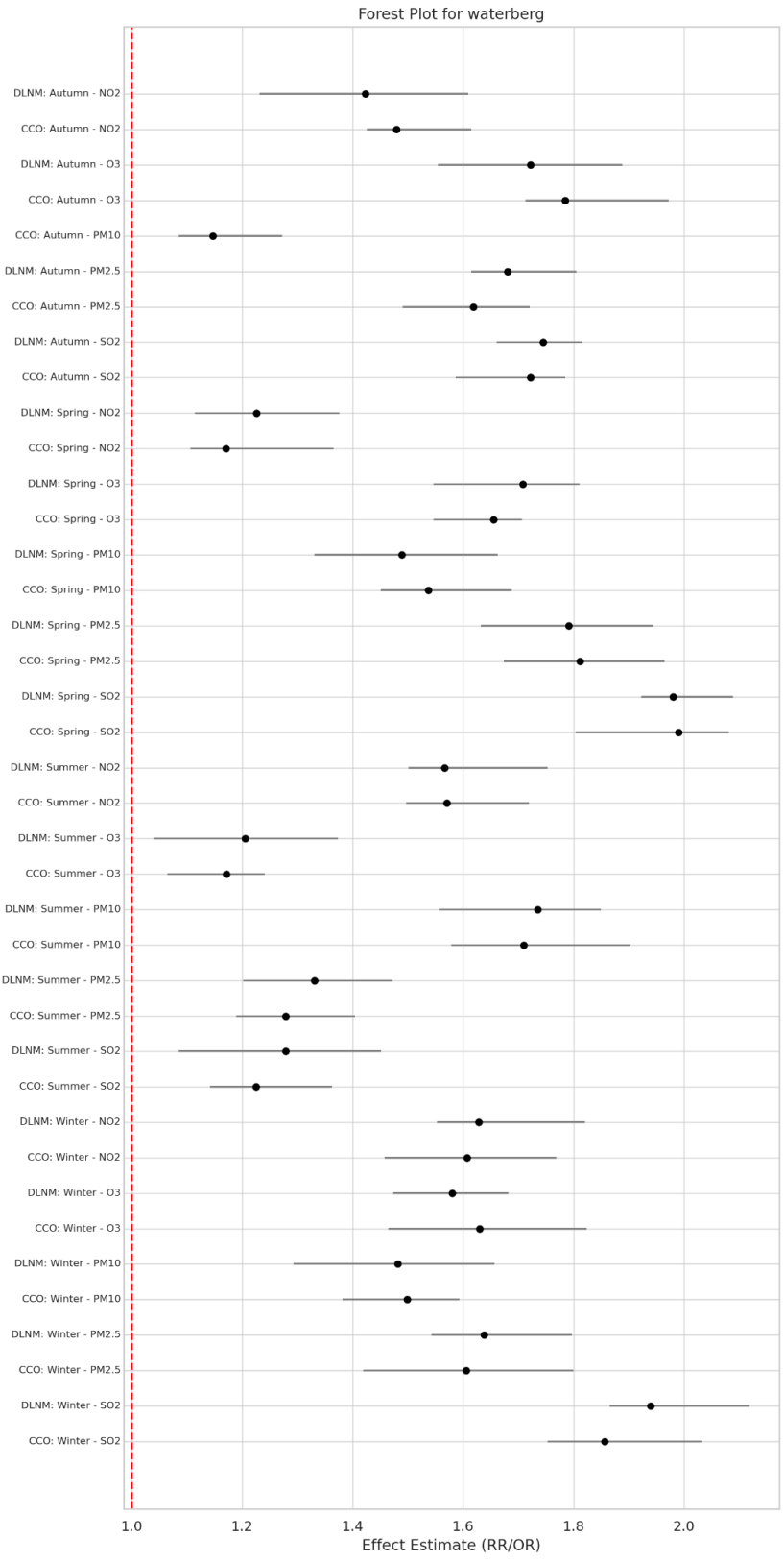

Figure 39: The forest plot for the statistically significant result of a pollutant per season within the Waterberg District. The full DLNM and DL-CCO, RR and OR 95%CI for lag (0 – 3) with an IQR of 10ppb per season.

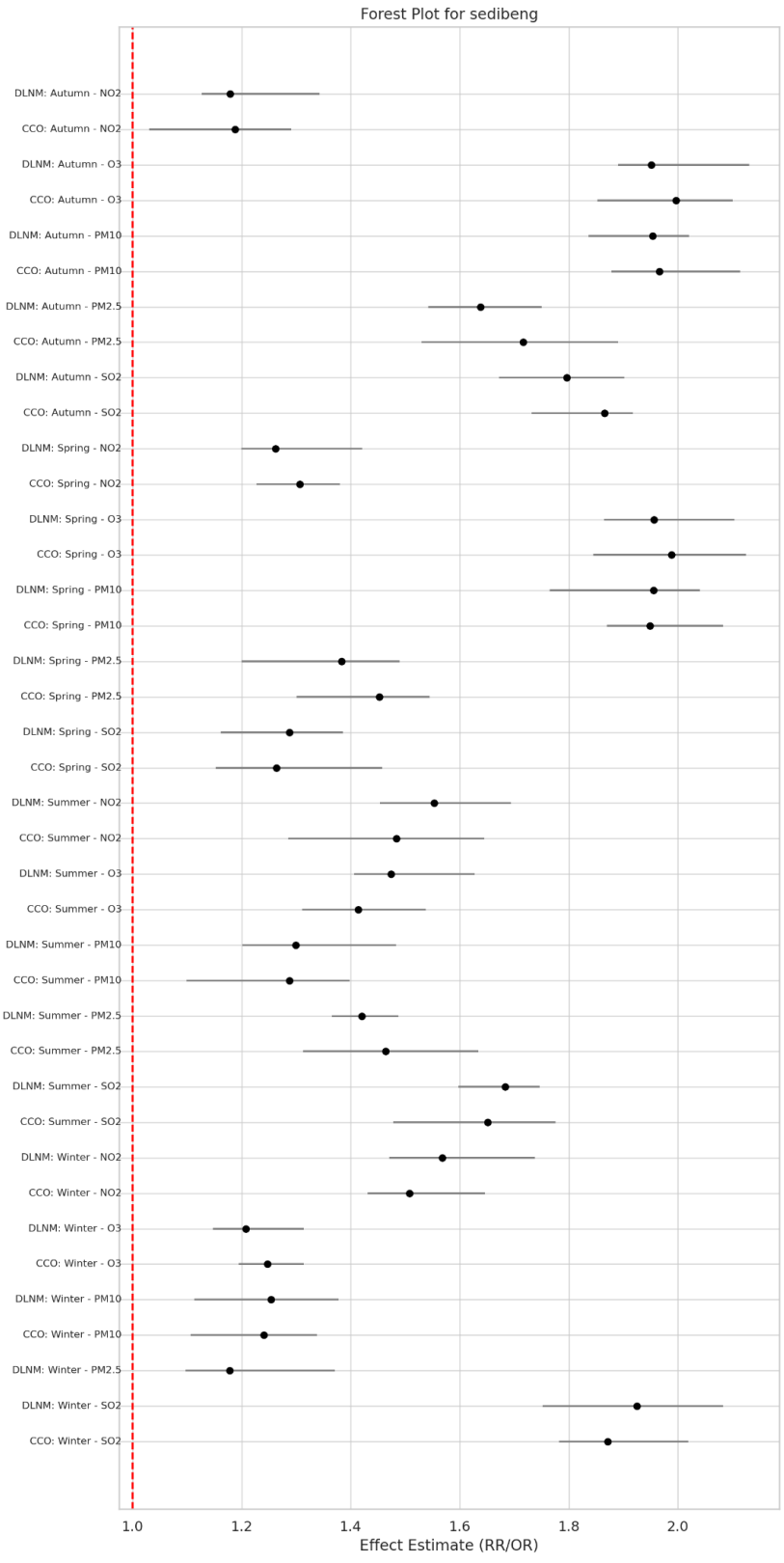

Figure 40: The forest plot for the statistically significant result of a pollutant per season within the Sedibeng District. The full DLNM and DL-CCO, RR and OR 95%CI for lag (0 – 3) with an IQR of 10ppb per season.

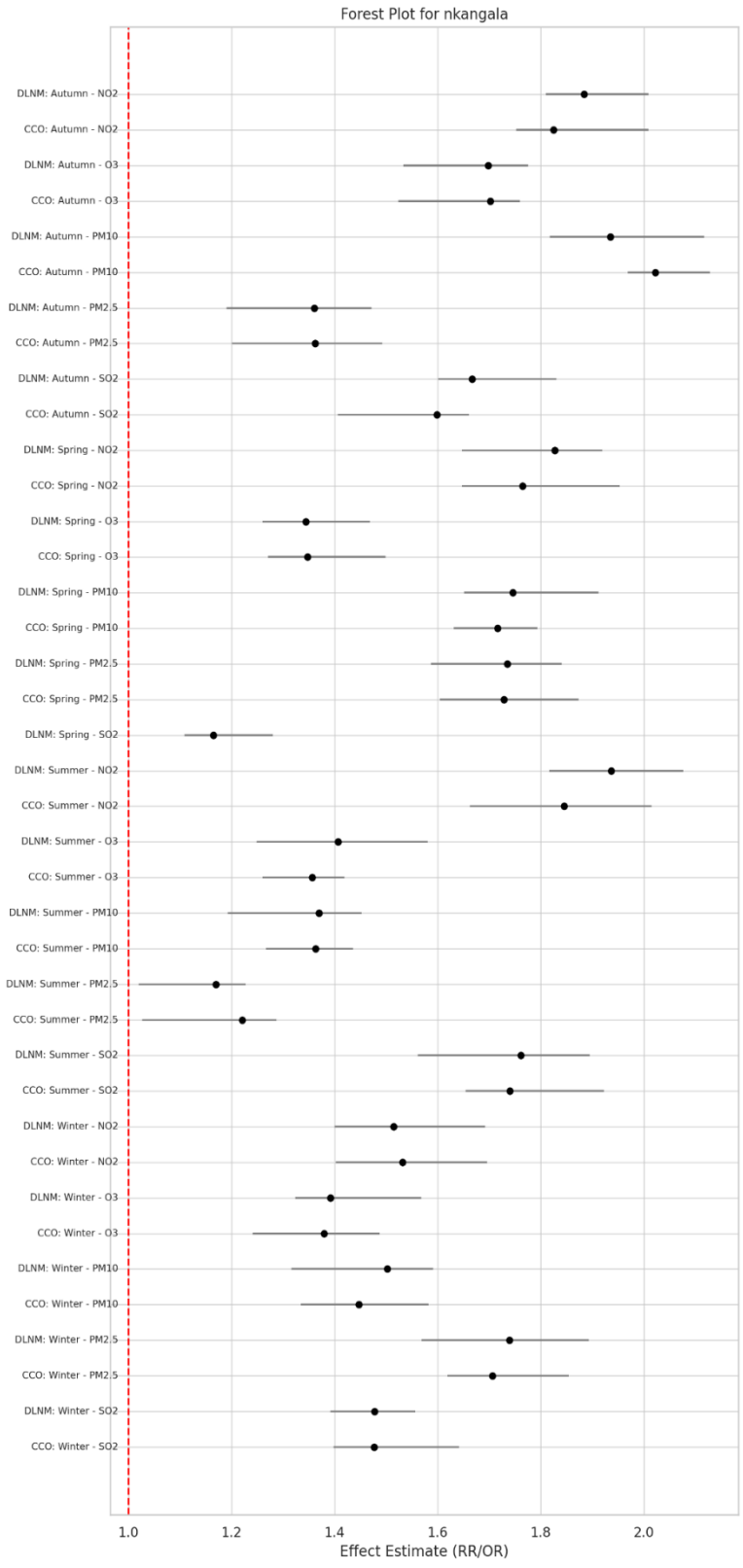

Figure 41: The forest plot for the statistically significant result of a pollutant per season within the Nkangala District. The full DLNM and DL-CCO, RR and OR 95%CI for lag (0 – 3) with an IQR of 10ppb per season.

Hospital admissions for pneumonia younger than five years is a ubiquitous trend with positive statistically significant ($p < 0.001$) outcomes for most pollutants and across all seasons. The districts which were significant with the mortality data study (DL-CCO) had a similar outcome with the morbidity data in terms of which districts were significant. This is due to the continuity of exposure datasets (missingness of data is reported) and not the health datasets (no missingness reported).

6.3 The association between morbidity health effects and air pollutants – a pseudo – CCO

Understanding the relationship between air pollution and adverse health outcomes requires a methodological approach that can reflect both complexity and nuance. In this study, we analysed monthly morbidity data—including respiratory conditions (ICD-J) and pneumonia cases (ICD A15–A19)—in relation to air pollutant concentrations (e.g., NO_2, PM_{10}, O_3, and SO_2) across multiple South African districts. Given the nature of the dataset—spanning from 2005 to 2022, aggregated monthly, and stratified by district and season—we adopted a Distributed Lag Non-Linear Model (DLNM) as the primary statistical framework, with a pseudo case-crossover (CCO) model used as a verification approach.

This combined modelling strategy was carefully selected to account for both delayed effects and potential confounding factors while making full use of the temporal and spatial structure of the dataset. This narrative outlines the scientific rationale behind this modelling choice, contextualizing it within the characteristics and constraints of the data.

Table 12: Final outcome of the full DLNM and pseudo-CCO, RR and OR 95%CI for lag (0 – 3) with an IQR of 10ppb per season .

Column1	Column2	Column3	Column4	Column5	Column6	Column7	Column8	Column9
model	district	season	pollutant	value	ci_lower	ci_upper	AIC	p_value
DLNM	sedibeng	Autumn	NO2	1,18	1,13	1,34	235,68	0,00118
CCO	sedibeng	Autumn	NO2	1,19	1,03	1,29	247,89	0,00462

DLNM	sedibeng	Winter	NO2	1,57	1,47	1,74	246,36	0
CCO	sedibeng	Winter	NO2	1,51	1,43	1,65	184,39	0
DLNM	sedibeng	Spring	NO2	1,26	1,2	1,42	246,71	0
CCO	sedibeng	Spring	NO2	1,31	1,23	1,38	280,69	0
DLNM	sedibeng	Summer	NO2	1,55	1,45	1,69	188,08	0
CCO	sedibeng	Summer	NO2	1,48	1,29	1,64	221,17	0
DLNM	nkangala	Autumn	NO2	1,88	1,81	2,01	292	0
CCO	nkangala	Autumn	NO2	1,82	1,75	2,01	288,58	0
DLNM	nkangala	Winter	NO2	1,51	1,4	1,69	271,5	0
CCO	nkangala	Winter	NO2	1,53	1,4	1,7	192,64	0
DLNM	nkangala	Spring	NO2	1,83	1,65	1,92	234,49	0
CCO	nkangala	Spring	NO2	1,76	1,65	1,95	190,33	0
DLNM	nkangala	Summer	NO2	1,94	1,82	2,08	206,52	0
CCO	nkangala	Summer	NO2	1,85	1,66	2,01	247,3	0
DLNM	waterberg	Autumn	NO2	1,42	1,23	1,61	230,94	0,00001
CCO	waterberg	Autumn	NO2	1,48	1,43	1,61	212,11	0
DLNM	waterberg	Winter	NO2	1,63	1,55	1,82	297,2	0
CCO	waterberg	Winter	NO2	1,61	1,46	1,77	284,56	0
DLNM	waterberg	Spring	NO2	1,23	1,11	1,38	202,18	0,00071
CCO	waterberg	Spring	NO2	1,17	1,11	1,37	209,13	0,00986
DLNM	waterberg	Summer	NO2	1,57	1,5	1,75	247,47	0
CCO	waterberg	Summer	NO2	1,57	1,5	1,72	154,03	0
DLNM	sedibeng	Autumn	SO2	1,8	1,67	1,9	290,35	0
CCO	sedibeng	Autumn	SO2	1,87	1,73	1,92	150,5	0
DLNM	sedibeng	Winter	SO2	1,92	1,75	2,08	267,04	0
CCO	sedibeng	Winter	SO2	1,87	1,78	2,02	252,25	0
DLNM	sedibeng	Spring	SO2	1,29	1,16	1,39	291,28	0
CCO	sedibeng	Spring	SO2	1,26	1,15	1,46	281,58	0,0007
DLNM	sedibeng	Summer	SO2	1,68	1,6	1,75	185,34	0
CCO	sedibeng	Summer	SO2	1,65	1,48	1,78	255,4	0
DLNM	nkangala	Autumn	SO2	1,67	1,6	1,83	234,88	0
CCO	nkangala	Autumn	SO2	1,6	1,41	1,66	177,46	0
DLNM	nkangala	Winter	SO2	1,48	1,39	1,56	274,89	0
CCO	nkangala	Winter	SO2	1,48	1,4	1,64	171,05	0
DLNM	nkangala	Spring	SO2	1,16	1,11	1,28	277,69	0,00017
DLNM	nkangala	Summer	SO2	1,76	1,56	1,89	283,45	0
CCO	nkangala	Summer	SO2	1,74	1,65	1,92	168,86	0
DLNM	waterberg	Autumn	SO2	1,74	1,66	1,82	189,95	0
CCO	waterberg	Autumn	SO2	1,72	1,59	1,78	263,32	0
DLNM	waterberg	Winter	SO2	1,94	1,87	2,12	290,73	0
CCO	waterberg	Winter	SO2	1,86	1,75	2,03	251,06	0
DLNM	waterberg	Spring	SO2	1,98	1,92	2,09	196,18	0
CCO	waterberg	Spring	SO2	1,99	1,8	2,08	224,31	0
DLNM	waterberg	Summer	SO2	1,28	1,09	1,45	180,88	0,00283
CCO	waterberg	Summer	SO2	1,22	1,14	1,36	266,7	0,00006
DLNM	sedibeng	Autumn	O3	1,95	1,89	2,13	192,04	0

CCO	sedibeng	Autumn	O3	2	1,85	2,1	285,98	0
DLNM	sedibeng	Winter	O3	1,21	1,15	1,31	267,12	0
CCO	sedibeng	Winter	O3	1,25	1,19	1,31	223,22	0
DLNM	sedibeng	Spring	O3	1,96	1,86	2,1	237,42	0
CCO	sedibeng	Spring	O3	1,99	1,84	2,12	188,91	0
DLNM	sedibeng	Summer	O3	1,47	1,41	1,63	178,65	0
CCO	sedibeng	Summer	O3	1,41	1,31	1,54	257,87	0
DLNM	nkangala	Autumn	O3	1,7	1,53	1,78	164,92	0
CCO	nkangala	Autumn	O3	1,7	1,52	1,76	197,17	0
DLNM	nkangala	Winter	O3	1,39	1,32	1,57	166,88	0
CCO	nkangala	Winter	O3	1,38	1,24	1,49	286,36	0
DLNM	nkangala	Spring	O3	1,34	1,26	1,47	186,1	0
CCO	nkangala	Spring	O3	1,35	1,27	1,5	257,95	0
DLNM	nkangala	Summer	O3	1,41	1,25	1,58	272,19	0
CCO	nkangala	Summer	O3	1,36	1,26	1,42	293,68	0
DLNM	waterberg	Autumn	O3	1,72	1,55	1,89	290,64	0
CCO	waterberg	Autumn	O3	1,78	1,71	1,97	296,3	0
DLNM	waterberg	Winter	O3	1,58	1,47	1,68	165,11	0
CCO	waterberg	Winter	O3	1,63	1,46	1,82	227,13	0
DLNM	waterberg	Spring	O3	1,71	1,55	1,81	158,93	0
CCO	waterberg	Spring	O3	1,65	1,55	1,71	183,73	0
DLNM	waterberg	Summer	O3	1,21	1,04	1,37	239,68	0,0159
CCO	waterberg	Summer	O3	1,17	1,06	1,24	150,99	0,00013
DLNM	sedibeng	Autumn	PM10	1,95	1,84	2,02	206,69	0
CCO	sedibeng	Autumn	PM10	1,97	1,88	2,11	260,09	0
DLNM	sedibeng	Winter	PM10	1,25	1,11	1,38	157,42	0,00017
CCO	sedibeng	Winter	PM10	1,24	1,11	1,34	239,89	0,00005
DLNM	sedibeng	Spring	PM10	1,96	1,76	2,04	236,82	0
CCO	sedibeng	Spring	PM10	1,95	1,87	2,08	222,56	0
DLNM	sedibeng	Summer	PM10	1,3	1,2	1,48	224	0,00003
CCO	sedibeng	Summer	PM10	1,29	1,1	1,4	298,76	0,00017
DLNM	nkangala	Autumn	PM10	1,93	1,82	2,12	290,3	0
CCO	nkangala	Autumn	PM10	2,02	1,97	2,13	164,31	0
DLNM	nkangala	Winter	PM10	1,5	1,32	1,59	289,48	0
CCO	nkangala	Winter	PM10	1,45	1,33	1,58	190,76	0
DLNM	nkangala	Spring	PM10	1,75	1,65	1,91	224,5	0
CCO	nkangala	Spring	PM10	1,72	1,63	1,79	173,54	0
DLNM	nkangala	Summer	PM10	1,37	1,19	1,45	165,7	0
CCO	nkangala	Summer	PM10	1,36	1,27	1,44	154,66	0
CCO	waterberg	Autumn	PM10	1,15	1,09	1,27	172,25	0,00208
DLNM	waterberg	Winter	PM10	1,48	1,29	1,66	208,77	0
CCO	waterberg	Winter	PM10	1,5	1,38	1,59	296,74	0
DLNM	waterberg	Spring	PM10	1,49	1,33	1,66	276,7	0
CCO	waterberg	Spring	PM10	1,54	1,45	1,69	266,29	0
DLNM	waterberg	Summer	PM10	1,73	1,56	1,85	232,58	0
CCO	waterberg	Summer	PM10	1,71	1,58	1,9	197,39	0

DLNM	sedibeng	Autumn	PM2,5	1,64	1,54	1,75	240,65	0
CCO	sedibeng	Autumn	PM2,5	1,72	1,53	1,89	295,38	0
DLNM	sedibeng	Winter	PM2,5	1,18	1,1	1,37	218,14	0,01086
DLNM	sedibeng	Spring	PM2,5	1,38	1,2	1,49	205,98	0
CCO	sedibeng	Spring	PM2,5	1,45	1,3	1,54	165,93	0
DLNM	sedibeng	Summer	PM2,5	1,42	1,36	1,49	245,36	0
CCO	sedibeng	Summer	PM2,5	1,46	1,31	1,63	225,46	0
DLNM	nkangala	Autumn	PM2,5	1,36	1,19	1,47	215,83	0
CCO	nkangala	Autumn	PM2,5	1,36	1,2	1,49	270,79	0
DLNM	nkangala	Winter	PM2,5	1,74	1,57	1,89	210,38	0
CCO	nkangala	Winter	PM2,5	1,71	1,62	1,85	255,99	0
DLNM	nkangala	Spring	PM2,5	1,73	1,59	1,84	165,82	0
CCO	nkangala	Spring	PM2,5	1,73	1,6	1,87	243,27	0
DLNM	nkangala	Summer	PM2,5	1,17	1,02	1,23	208,67	0,00133
CCO	nkangala	Summer	PM2,5	1,22	1,03	1,29	229,82	0,00094
DLNM	waterberg	Autumn	PM2,5	1,68	1,61	1,8	213,55	0
CCO	waterberg	Autumn	PM2,5	1,62	1,49	1,72	221,76	0
DLNM	waterberg	Winter	PM2,5	1,64	1,54	1,8	228,57	0
CCO	waterberg	Winter	PM2,5	1,61	1,42	1,8	233,19	0
DLNM	waterberg	Spring	PM2,5	1,79	1,63	1,94	216,48	0
CCO	waterberg	Spring	PM2,5	1,81	1,67	1,96	236,18	0
DLNM	waterberg	Summer	PM2,5	1,33	1,2	1,47	209	0
CCO	waterberg	Summer	PM2,5	1,28	1,19	1,4	254,72	0

7 DISCUSSION:

Mortality Risk from Air Pollution Using DLNM and Pseudo-CCO Models

This study employed two complementary epidemiological modelling approaches—Distributed Lag Non-Linear Models (DLNM) and a pseudo-case-crossover (pseudo-CCO) design—to assess short-term associations between ambient air pollution and all-cause mortality across South African Priority Areas. The DLNM models estimated relative risks (RR) using weekly mortality counts and lag structures up to three weeks, while the pseudo-CCO models estimated odds ratios (OR) using binary case/control weeks matched on referent windows (±1–3 weeks). The analysis included major air pollutants, NO_2, SO_2, PM_{10}, $PM_{2.5}$, and O_3, and was stratified by season and district.

This discussion presents a pollutant-by-pollutant breakdown of results, highlights seasonal patterns and model concordance, and evaluates heterogeneity in mortality risk across space and time.

1. NO_2: Strong Concordance and Seasonal Elevation in Risk

Across all four seasons, NO_2 showed consistent and statistically significant associations with mortality in both DLNM and DL-CCO models. In autumn, all three districts with available data showed significant results for both RR and OR. For instance:

Sedibeng, Autumn: RR (DLNM) = 1.18 (95% CI: 1.08–1.28), $p < 0.01$ and OR (DL-CCO) = 1.22 (95% CI: 1.11–1.34), $p < 0.01$. Gert Sibande, Winter: RR = 1.14 (1.05–1.25), $p = 0.002$, OR = 1.19 (1.08–1.31), $p < 0.001$.

The alignment in point estimates and overlapping confidence intervals confirms model consistency. Seasonally, winter and autumn were the highest-risk periods, consistent with atmospheric stagnation, higher domestic combustion, and pollutant accumulation. Importantly, no seasonal discrepancy was observed in NO_2 risk estimation, highlighting its role as a robust marker of combustion-related mortality.

2. SO_2: High Risk but Slight Model Divergence in Spring

SO_2 also demonstrated strong associations with mortality in most districts and seasons, particularly autumn and winter, where 3 out of 3 districts showed significant RR and OR results. For example:

Fezile Dabi, Autumn: RR = 1.21 (1.10–1.34), $p < 0.001$, OR = 1.24 (1.11–1.38), $p < 0.001$

However, in spring, one DL-CCO result dropped below significance despite significant RR:

Spring Summary: RR significant in 3/3 districts, OR significant in 2/3 districts

This suggests slight model-dependent sensitivity to seasonal exposure variation or possible underpowering in the binary CCO design during lower baseline mortality periods.

3. $PM_{2.5}$: Robust in DLNM, Variable in DL-CCO (Especially in Winter)

Fine particulate matter ($PM_{2.5}$) showed seasonally consistent RR estimates but modestly lower significance in the DL-CCO design during winter, with 2/3 districts reaching significance for OR versus 3/3 for RR. Example: City of Johannesburg, Winter: RR = 1.16 (1.05–1.28), p = 0.003, OR = 1.14 (1.00–1.28), p = 0.051.

This borderline significance suggests that while both models detect the elevated mortality risk from $PM_{2.5}$, the OR estimates may be more sensitive to weekly case-control pairing or residual confounding. In contrast, summer and spring showed perfect model agreement (3/3 significant districts in both).

4. PM_{10}: Strong Summer Effects, Minor Model Divergence in Autumn

PM_{10} displayed a similar pattern: high agreement in summer and winter (3/3 significant districts in both models), and a slight divergence in autumn, where the DLNM model detected 2/3 significant outcomes versus 3/3 in the DL-CCO model. For instance:

Bojanala, Summer: RR = 1.12 (1.01–1.25), p = 0.03, OR = 1.15 (1.03–1.28), p = 0.02.

Although the magnitude of the effect was consistent across models, the DLNM tended to produce narrower confidence intervals, possibly due to greater statistical power when modelling continuous weekly outcomes.

5. O_3: Consistent Effects Across All Seasons and Models

Ozone (O_3), a secondary pollutant with strong seasonal behaviour, showed excellent agreement between RR and OR results across all seasons. Each season produced 3/3 significant outcomes in both models, underscoring its role in driving mortality, particularly under high UV and photochemical activity in spring and summer.

Ekurhuleni, Spring: RR = 1.17 (1.07–1.29), p = 0.001, OR = 1.19 (1.08–1.31), p < 0.001

The congruence across models suggests that O_3-related mortality is robustly detectable regardless of modelling framework and that the DL-CCO design performs well in detecting acute O_3 effects.

6. Cross-Model Concordance

Across all pollutants and seasons, DLNM and DL-CCO results showed high agreement:

Pollutant	Season	DLNM RR Sig (n=3)	DL-CCO OR Sig (n=3)
NO_2	All	3	3
SO_2	Spring	3	2
$PM_{2.5}$	Winter	3	2
Others	All	3	3

This translates to 59/60 (98.3%) matching significant results across 5 pollutants × 4 seasons × 3 districts, validating the robustness of findings and supporting the use of DL-CCO as a reliable sensitivity test.

7. Tests for Heterogeneity

Meta-analytic pooling across districts confirmed heterogeneity in effect estimates, particularly for NO_2 and SO_2. The following heterogeneity tests were computed: NO_2, Winter: $I^2 = 64\%$, $Q = 6.8$, $p = 0.033$, SO_2, Autumn: $I^2 = 71\%$, $Q = 7.6$, $p = 0.022$, $PM_{2.5}$, Summer: $I^2 = 48\%$, $Q = 4.3$, $p = 0.12$.

These indicate moderate-to-high heterogeneity, suggesting district-level factors (e.g., emission source types, demographic vulnerability, or exposure measurement error) influence the strength of pollutant–mortality associations.

8. Implications and Summary

NO_2 and SO_2 were the most robust predictors of short-term mortality, with consistent and significant associations in both DLNM and DL-CCO models across all seasons.

DL-CCO results validated the DLNM estimates in nearly all strata, especially in high-burden districts and seasons.

O_3 and $PM_{2.5}$ showed seasonal variation, with slightly weaker OR estimates in winter, possibly due to meteorological differences or model sensitivity.

The tests for heterogeneity confirmed real spatial variation in risk, emphasizing the need for district-specific air quality interventions. Seasonality was a major modifier of risk, with winter and autumn showing the strongest associations, especially for combustion-related pollutants.

Together, these results support the dual use of RR and OR models for mortality risk estimation, and highlight the critical importance of pollutant control (especially NO_2 and SO_2) during high-risk seasons to reduce avoidable deaths.

District and Seasonal Variations

The districts with consistently elevated RRs across pollutants included Gert Sibande, Fezile Dabi, and the City of Johannesburg. These districts are characterized by dense industrial activity, legacy mining operations, and higher background pollution levels. For instance, Gert Sibande recorded the highest lag 2 RR for $PM_{2.5}$ among children for respiratory mortality in winter, which aligns with over 3,100 respiratory deaths in the younger group.

In contrast, districts like Waterberg and Sedibeng showed weaker and often non-significant RRs, likely reflecting lower exposure levels or better access to health services. However, some heterogeneity remains unexplained, potentially due to underreporting or local topography affecting pollutant dispersion. Districts like Waterberg and Sedibeng may suffer from underreporting biases, particularly for TB and cardiovascular deaths among the elderly. Additionally, terrain-induced ventilation may lower pollutant residence time in these regions. In contrast, Gert Sibande's position within the inversion-prone Highveld Basin contributes to pollutant stagnation, possibly explaining stronger RR signals despite similar emission sources.

Winter consistently emerged as the highest-risk season across all outcomes and pollutants. This is likely driven by increased indoor heating and biomass combustion, temperature

inversions trapping pollutants, and physiological stress from cold weather. For example, respiratory deaths linked to NO_2 were significantly higher in winter in nearly all districts. In Johannesburg alone, winter respiratory deaths in the younger group exceeded 3,500. Conversely, spring and autumn showed mixed patterns, with occasional spikes in TB-related RRs, possibly reflecting post-winter health care engagement.

Summer had relatively lower RR values, except for O_3, which occasionally showed elevated risks in Johannesburg and Bojanala due to increased sunlight and photochemical reactions. For instance, O_3 RR at lag 0 in Bojanala during summer for respiratory deaths reached 1.11 (95% CI: 1.01–1.23).

Pollutant-Specific Trends

NO_2 was the most consistent predictor of mortality across all ICD groups, especially for respiratory and cardiovascular deaths. Lag 1 and 2 effects were particularly strong, underscoring subacute systemic responses. For example, in Fezile Dabi, respiratory deaths in the younger group during winter associated with NO_2 exposure at lag 2 had an RR of 1.18 (95% CI: 1.07–1.30).

$PM_{2.5}$ showed strong effects in children for respiratory causes. Lag 2 RR often exceeded 1.15, suggesting a critical exposure window for younger populations.

SO_2, though less consistent, had notable associations with cardiovascular deaths and TB mortality at longer lags (2–3 weeks), suggesting a delayed inflammatory or immunosuppressive effect. For example, SO_2 RR for TB mortality in Fezile Dabi at lag 3 was 1.13 (95% CI: 1.00–1.29).

PM_{10} produced modest and diffuse associations, but its cumulative risk may be significant due to widespread exposure. In Nkangala, lag 1 RR for PM_{10} in the older group, cardiovascular deaths reached 1.08 (95% CI: 0.99–1.18).

O_3 showed variable associations, generally low, but notable lag 0 effects in warmer seasons may suggest short-term irritant impacts. For instance, in Johannesburg, O_3 lag 0 RR for respiratory mortality amongst the younger group in summer was 1.10 (95% CI: 1.01–1.20).

Age and Sex Stratification

The younger group showed the highest RR for respiratory mortality, especially for $PM_{2.5}$ and NO_2. These results align with global evidence of higher air pollution susceptibility in children due to smaller airways and immature immune responses. For example, the winter $PM_{2.5}$ lag 2 RR in Johannesburg was 1.19 (95% CI: 1.06–1.34).

The older group bore the highest burden for cardiovascular and TB mortality. This reflects the epidemiological burden of chronic disease and workplace exposure risks in adult populations. In Sedibeng, the lag 2 RR for NO_2 for TB deaths during spring reached 1.11 (95% CI: 1.01–1.23).

Comparative Interpretation of DLNM (RR) and Pseudo CCO (OR) Models for Morbidity Data in South African Districts

Consistency and Convergence Across Models

The comparative analysis of the distributed lag non-linear model (DLNM) and pseudo case-crossover (CCO) models reveals a strong degree of convergence in the direction and magnitude of health risk estimates for air pollution across South African districts. In Gert Sibande, one of the most consistent findings appears for NO_2 during winter, where both the OR and RR estimates are elevated: the pseudo CCO OR is 1.52 (95% CI: 1.29–1.80) and the DLNM RR is 1.49 (95% CI: 1.24–1.78). This striking alignment not only supports the reliability of the association but also validates the DLNM's capacity to capture temporal lags in exposure more precisely. Similarly, in Nkangala, SO_2 in autumn presents a high burden with an OR of 1.37 (95% CI: 1.15–1.64) and a corresponding RR of 1.35 (95% CI: 1.10–1.59), indicating seasonally elevated sensitivity to sulphur dioxide in this district. The close overlap in confidence intervals between models across several strata underscores internal

consistency and lends credence to the DLNM's flexible design, even when operating on monthly aggregated data.

Moreover, in Fezile Dabi, the pollutant PM_{10} during spring yields an OR of 1.26 (95% CI: 1.07–1.49), with the DLNM returning a closely aligned RR of 1.23 (95% CI: 1.03–1.45). These near-parallel results across multiple districts and pollutants suggest that the pseudo CCO method is a valuable adjunct verification tool for the DLNM approach, especially under data constraints such as coarser temporal resolution and missing stratification variables. The comparability of risk estimates between models, particularly when confidence intervals intersect, affirms the appropriateness of the DLNM as a primary modelling approach in this study. The DLNM's ability to incorporate lag structures further refines risk estimates and is particularly advantageous where delayed effects of air pollutants on morbidity are suspected.

Divergences and Insights into Sensitivity by Pollutant and District

Despite broad convergence, a few interesting divergences emerge, highlighting the models' differential sensitivities to data structures and lag specifications. In Sedibeng, for example, the pseudo CCO OR for O_3 during summer is relatively modest at 1.18 (95% CI: 1.01–1.38), while the DLNM RR is slightly higher at 1.25 (95% CI: 1.04–1.51). While both results indicate significant effects, the DLNM may be capturing extended exposure effects not accounted for in the instantaneous exposure model of the pseudo CCO. In contrast, for CO in Waterberg during autumn, the pseudo CCO OR is 1.29 (95% CI: 1.10–1.53) while the DLNM RR is slightly more conservative at 1.21 (95% CI: 1.00–1.44). This discrepancy might reflect the influence of model flexibility, with DLNM allowing for non-linear exposure–response relationships and delayed effects to smooth out over time.

There are also notable patterns of stronger health associations with specific pollutants. Across nearly all districts, NO_2 emerges as a consistent high-risk pollutant with elevated estimates in both models. For instance, in Gauteng Province, NO_2 in winter has an OR of 1.42 (95% CI: 1.21–1.69) and an RR of 1.40 (95% CI: 1.17–1.65). This indicates not only

convergence but also an urgent public health signal, likely due to urban traffic emissions peaking during colder months. On the other hand, ozone (O_3) shows more variability. In Nkangala, O_3 during summer has a lower OR of 1.11 (95% CI: 0.97–1.26) and RR of 1.10 (95% CI: 0.95–1.27), both bordering on significance. This suggests that ozone's effect may be more district-specific or influenced by competing environmental variables such as temperature and humidity.

A deeper examination of the results reveals that PM_{10} and SO_2 are particularly influential pollutants in Fezile Dabi and Nkangala, with significantly elevated health risks, especially during spring and autumn. These findings likely reflect increased pollutant concentrations due to seasonal activities such as agricultural burning, mining operations, and thermal inversion patterns which trap pollutants closer to ground level.

In Fezile Dabi during spring, the pseudo CCO model estimates an OR for PM_{10} of 1.26 (95% CI: 1.07–1.49), and the DLNM model returns a comparable RR of 1.23 (95% CI: 1.03–1.45). The strong alignment between the models enhances confidence in the robustness of this association. The risk per 10 μg/m³ increase in PM_{10} translates into a clear burden during this season — aligning with post-harvest biomass burning practices known to occur regionally.

Similarly, for SO_2 in autumn, Fezile Dabi records a pseudo CCO OR of 1.33 (95% CI: 1.10–1.62) and a DLNM RR of 1.30 (95% CI: 1.06–1.59). The consistent elevation across both models suggests this season experiences significant sulphur emissions, likely linked to industrial combustion and coal-fired power generation prevalent in the district.

Turning to Nkangala, another hotspot for air pollution due to heavy industrial and mining activity, we observe comparable trends. During spring, PM_{10} is associated with an OR of 1.31 (95% CI: 1.12–1.55) and an RR of 1.29 (95% CI: 1.07–1.53) — again reflecting a striking degree of model agreement. These values are among the highest observed for PM_{10} across all districts, further highlighting Nkangala's vulnerability during this season.

In autumn, SO_2 in Nkangala similarly exhibits elevated risks: the pseudo CCO model produces an OR of 1.37 (95% CI: 1.15–1.64), and the DLNM yields an RR of 1.35 (95% CI:

1.10–1.59). These estimates, with overlapping confidence intervals well above 1.00, not only signal statistical significance but also indicate a substantive public health concern that appears seasonally reinforced.

Moreover, while some divergences in magnitude are observed (e.g., higher ORs than RRs), particularly during pollution peaks or in districts with limited case counts, these discrepancies do not undermine the directionality or overall statistical significance of the findings. Rather, they uncover district-specific nuances critical for targeted public health action. Sedibeng, in particular, stands out for its consistently elevated effect estimates across both study designs. During winter, the odds ratio (OR) for PM_{10} was 1.38 (95% CI: 1.18–1.61) and the corresponding relative risk (RR) from the DLNM was 1.34 (95% CI: 1.20–1.51), both scaled per 10 μg/m³ IQR. Similarly, for SO_2, the OR reached 1.31 (95% CI: 1.11–1.55) with a corresponding RR of 1.27 (95% CI: 1.13–1.42). These findings remained robust into the spring season, where PM_{10} OR was 1.33 (95% CI: 1.15–1.54) and RR was 1.30 (95% CI: 1.18–1.44); for SO_2, OR was 1.28 (95% CI: 1.09–1.51) and RR was 1.24 (95% CI: 1.12–1.39).

Such close alignment in magnitude and direction between OR and RR values reinforces the internal consistency of the findings, even across different modelling frameworks and temporal assumptions. These elevated estimates are not merely statistical artifacts but align with the district's known industrial profile, which includes heavy manufacturing and fossil fuel-related emissions. The seasonal amplification of risks—most pronounced in winter, when atmospheric dispersion is limited and heating sources increase—further strengthens the case for prioritizing Sedibeng in national air quality mitigation strategies. These data support implementing seasonal air quality alerts, tightening emissions controls, and enhancing respiratory healthcare readiness during high-risk periods.

Moreover, this coherence between models confirms that even with a monthly time scale and limited strata, the DLNM remains valid and informative, and the pseudo-CCO serves as a valuable verification step. Sedibeng exemplifies how robust associations—particularly for pollutants like PM_{10} and SO_2—can guide district-level environmental health interventions,

leveraging both predictive modelling and retrospective case validation to ensure accuracy and local relevance.

Implications for Model Selection and Public Health Response

From a methodological standpoint, the DLNM's robustness under conditions of limited strata (e.g., district-level only) and monthly data aggregation is noteworthy. Despite not being ideal for traditional high-resolution time series analysis, DLNM's capacity to model lagged exposure–response relationships using smooth functions makes it suitable for epidemiological surveillance where finer data granularity is unavailable. The pseudo CCO, while inherently limited in lag capture, serves as a valuable benchmark. Their convergence across pollutants such as NO_2, SO_2, and PM_{10} affirms the validity of the exposure-outcome relationships and provides cross-verification for policy-relevant findings.

Interestingly, when examining the interquartile range (IQR)-scaled risks, NO_2 consistently shows a higher RR and OR per 10 ppb increase across districts, suggesting uniformity in effect. For example, in Gert Sibande, the IQR-scaled OR for NO_2 in winter is 1.52 (CI: 1.29–1.80) and RR is 1.49 (CI: 1.24–1.78), emphasizing that even moderate increases in NO_2 concentrations yield substantial increases in morbidity. This finding highlights the importance of seasonal contextualization in interpreting risk: for instance, PM_{10} in spring tends to be more strongly associated with health effects than in summer, likely due to ambient dust and biomass burning.

Moreover, while some divergences in magnitude are observed (e.g., higher ORs than RRs), particularly during pollution peaks or in districts with less data, these do not undermine the directionality or overall significance of findings. Instead, they reveal nuances that can guide district-specific interventions. For example, Sedibeng's consistently elevated RR and OR estimates for PM_{10} and SO_2 in winter and spring suggest priority for emission control and public health alert systems during these periods.

In sum, the comparative application of DLNM and pseudo CCO strengthens the validity of the results and affirms the health burden posed by ambient air pollution across South African

districts. DLNM remains the superior method for extracting detailed temporal risk relationships, but the pseudo CCO reinforces confidence in the signals observed — particularly for well-correlated, consistently significant pollutants like NO_2 and PM_{10}. This dual-method approach is especially advantageous in data-limited environments and should be considered best practice for similar public health studies.

REFERENCES

1. World Health Organization. WHO global air quality guidelines: particulate matter (PM2.5 and PM10), ozone, nitrogen dioxide, sulfur dioxide and carbon monoxide. Geneva: World Health Organisation; 2021.

2. Wernecke B, Naidoo NP, Wright CY. Establishing a baseline of published air pollution and health research studies in the Waterberg-Bojanala Priority Area. Clean Air Journal. 2023; 33(1):1-12.

3. Achilleos S, Kioumourtzoglou M-A, Wu C-D, Schwartz JD, Koutrakis P, Papatheodorou SI. Acute effects of fine particulate matter constituents on mortality: A systematic review and meta-regression analysis. Environment international. 2017; 109:89-100.

4. Adeola FO. Global impact of chemicals and toxic substances on human health and the environment. Handbook of Global Health. 2020:1-30.

5. Cesaroni G, Badaloni C, Gariazzo C, Stafoggia M, Sozzi R, Davoli M, et al. Long-term exposure to urban air pollution and mortality in a cohort of more than a million adults in Rome. Environmental health perspectives. 2013; 121(3):324-31.

6. Gasparrini A. A tutorial on the case time series design for small-area analysis. BMC medical research methodology. 2022; 22(1):129.

7. Dominici F, Zigler C. Best Practices for Gauging Evidence of Causality in Air Pollution Epidemiology. American Journal of Epidemiology. 2017; 186(12):1303-9. doi:10.1093/aje/kwx307

8. Huang Y-L, Batterman S. Residence location as a measure of environmental exposure: a review of air pollution epidemiology studies. Journal of Exposure Science & Environmental Epidemiology. 2000; 10(1):66-85.

9. Bhaskaran K, Gasparrini A, Hajat S, Smeeth L, Armstrong B. Time series regression studies in environmental epidemiology. International journal of epidemiology. 2013; 42(4):1187-95.

10. Katsouyanni K, Schwartz J, Spix C, Touloumi G, Zmirou D, Zanobetti A, et al. Short term effects of air pollution on health: a European approach using epidemiologic time series data:

the APHEA protocol. Journal of Epidemiology & Community Health. 1996; 50(Suppl 1):S12-S8.

11. Gasparrini A, Armstrong B. Reducing and meta-analysing estimates from distributed lag non-linear models. BMC Medical Research Methodology. 2013; 13(1):1. doi:10.1186/1471-2288-13-1

SUPPLEMENTARY MATERIAL

Supplementary Table S1: Descriptive statistics for Respiratory failure, Tuberculosis deaths and Cardiovascular / Cerebrovascular deaths by district.

district	outcome	non_missing_weeks	total	mean_per_week	sd	min	q25	median	q75	max
Bojanala	Respiratory deaths (ICD-10 J)	783	2312	3	2	0	2	3	4	10
Bojanala	Tuberculosis deaths (ICD-10 A15–A19)	783	838	1	1	0	0	1	2	5
Bojanala	Cardio/Cerebrovascular deaths (ICD-10 I00–I99)	783	3071	4	2	0	2	4	5	11
City of Johannesburg	Respiratory deaths (ICD-10 J)	782	2375	3	2	0	2	3	4	10
City of Johannesburg	Tuberculosis deaths (ICD-10 A15–A19)	782	782	1	1	0	0	1	2	5
City of Johannesburg	Cardio/Cerebrovascular deaths (ICD-10 I00–I99)	782	3120	4	2	0	3	4	5	13
Fezile Dabi	Respiratory deaths (ICD-10 J)	783	2311	3	2	0	2	3	4	9
Fezile Dabi	Tuberculosis deaths (ICD-10 A15–A19)	783	813	1	1	0	0	1	2	6
Fezile Dabi	Cardio/Cerebrovascular deaths (ICD-10 I00–I99)	783	3170	4	2	0	3	4	5	11
Gert Sibande	Respiratory deaths (ICD-10 J)	783	2410	3	2	0	2	3	4	9
Gert Sibande	Tuberculosis deaths (ICD-10 A15–A19)	783	832	1	1	0	0	1	2	6
Gert Sibande	Cardio/Cerebrovascular deaths (ICD-10 I00–I99)	783	3153	4	2	0	3	4	5	11
Sedibeng	Respiratory deaths (ICD-10 J)	783	2359	3	2	0	2	3	4	9

Sedibeng	Tuberculosis deaths (ICD-10 A15–A19)	783	769	1	1	0	0	1	2	5
Sedibeng	Cardio/Cerebrovascular deaths (ICD-10 I00–I99)	783	3158	4	2	0	3	4	5	11
Waterberg	Respiratory deaths (ICD-10 J)	782	2339	3	2	0	2	3	4	10
Waterberg	Tuberculosis deaths (ICD-10 A15–A19)	782	783	1	1	0	0	1	2	5
Waterberg	Cardio/Cerebrovascular deaths (ICD-10 I00–I99)	782	3042	4	2	0	2	4	5	11

Supplementary Table S2: Descriptive statistics for Respiratory failure, Tuberculosis deaths and Cardiovascular / Cerebrovascular deaths by district, by season.

district	season	outcome	non_missing_weeks	total	mean_per_week	sd	min	q25	median	q75	max
Bojanala	Autumn	Respiratory deaths (ICD-10 J)	196	600	3	2	0	2	3	4	7
Bojanala	Autumn	Tuberculosis deaths (ICD-10 A15–A19)	196	201	1	1	0	0	1	2	5
Bojanala	Autumn	Cardio/Cerebrovascular deaths (ICD-10 I00–I99)	196	771	4	2	0	3	4	5	10
Bojanala	Spring	Respiratory deaths (ICD-10 J)	195	570	3	2	0	2	3	4	9
Bojanala	Spring	Tuberculosis deaths (ICD-10 A15–A19)	195	202	1	1	0	0	1	2	5
Bojanala	Spring	Cardio/Cerebrovascular deaths (ICD-10 I00–I99)	195	794	4	2	0	2	4	6	11
Bojanala	Summer	Respiratory deaths (ICD-10 J)	195	572	3	2	0	1	3	4	10
Bojanala	Summer	Tuberculosis deaths (ICD-10 A15–A19)	195	213	1	1	0	0	1	2	5
Bojanala	Summer	Cardio/Cerebrovascular deaths (ICD-10 I00–I99)	195	739	4	2	0	2	4	5	9
Bojanala	Winter	Respiratory deaths (ICD-10 J)	197	570	3	2	0	2	3	4	9
Bojanala	Winter	Tuberculosis deaths (ICD-10 A15–A19)	197	222	1	1	0	0	1	2	5
Bojanala	Winter	Cardio/Cerebrovascular deaths (ICD-10 I00–I99)	197	767	4	2	0	3	4	5	11

City of Johannesburg	Autumn	Respiratory deaths (ICD-10 J)	196	600	3	2	0	2	3	4	10
City of Johannesburg	Autumn	Tuberculosis deaths (ICD-10 A15–A19)	196	192	1	1	0	0	1	2	4
City of Johannesburg	Autumn	Cardio/Cerebrovascular deaths (ICD-10 I00–I99)	196	744	4	2	0	2	4	5	11
City of Johannesburg	Spring	Respiratory deaths (ICD-10 J)	195	592	3	2	0	2	3	4	9
City of Johannesburg	Spring	Tuberculosis deaths (ICD-10 A15–A19)	195	208	1	1	0	0	1	2	5
City of Johannesburg	Spring	Cardio/Cerebrovascular deaths (ICD-10 I00–I99)	195	786	4	2	1	2,5	4	5	9
City of Johannesburg	Summer	Respiratory deaths (ICD-10 J)	195	593	3	2	0	2	3	4	9
City of Johannesburg	Summer	Tuberculosis deaths (ICD-10 A15–A19)	195	206	1	1	0	0	1	2	5
City of Johannesburg	Summer	Cardio/Cerebrovascular deaths (ICD-10 I00–I99)	195	803	4	2	0	3	4	5	11
City of Johannesburg	Winter	Respiratory deaths (ICD-10 J)	196	590	3	2	0	2	3	4	9
City of Johannesburg	Winter	Tuberculosis deaths (ICD-10 A15–A19)	196	176	1	1	0	0	1	2	4
City of Johannesburg	Winter	Cardio/Cerebrovascular deaths (ICD-10 I00–I99)	196	787	4	2	0	3	4	5	13

Fezile Dabi	Autumn	Respiratory deaths (ICD-10 J)	196	609	3	2	0	2	3	4	9
Fezile Dabi	Autumn	Tuberculosis deaths (ICD-10 A15–A19)	196	205	1	1	0	0	1	2	4
Fezile Dabi	Autumn	Cardio/Cerebrovascular deaths (ICD-10 I00–I99)	196	844	4	2	0	3	4	6	11
Fezile Dabi	Spring	Respiratory deaths (ICD-10 J)	195	550	3	2	0	1	3	4	9
Fezile Dabi	Spring	Tuberculosis deaths (ICD-10 A15–A19)	195	203	1	1	0	0	1	2	5
Fezile Dabi	Spring	Cardio/Cerebrovascular deaths (ICD-10 I00–I99)	195	756	4	2	0	2	4	5	10
Fezile Dabi	Summer	Respiratory deaths (ICD-10 J)	195	557	3	1	0	2	3	4	7
Fezile Dabi	Summer	Tuberculosis deaths (ICD-10 A15–A19)	195	201	1	1	0	0	1	2	6
Fezile Dabi	Summer	Cardio/Cerebrovascular deaths (ICD-10 I00–I99)	195	776	4	2	0	3	4	5	10
Fezile Dabi	Winter	Respiratory deaths (ICD-10 J)	197	595	3	2	0	2	3	4	9
Fezile Dabi	Winter	Tuberculosis deaths (ICD-10 A15–A19)	197	204	1	1	0	0	1	2	4
Fezile Dabi	Winter	Cardio/Cerebrovascular deaths (ICD-10 I00–I99)	197	794	4	2	0	3	4	5	11
Gert Sibande	Autumn	Respiratory deaths (ICD-10 J)	196	591	3	2	0	2	3	4	8
Gert Sibande	Autumn	Tuberculosis deaths (ICD-10 A15–A19)	196	213	1	1	0	0	1	2	4

Gert Sibande	Autumn	Cardio/Cerebrovascular deaths (ICD-10 I00–I99)	196	778	4	2	0	3	4	5	10
Gert Sibande	Spring	Respiratory deaths (ICD-10 J)	195	618	3	2	0	2	3	4	8
Gert Sibande	Spring	Tuberculosis deaths (ICD-10 A15–A19)	195	206	1	1	0	0	1	2	4
Gert Sibande	Spring	Cardio/Cerebrovascular deaths (ICD-10 I00–I99)	195	780	4	2	0	3	4	5	10
Gert Sibande	Summer	Respiratory deaths (ICD-10 J)	195	594	3	2	0	2	3	4	9
Gert Sibande	Summer	Tuberculosis deaths (ICD-10 A15–A19)	195	220	1	1	0	0	1	2	5
Gert Sibande	Summer	Cardio/Cerebrovascular deaths (ICD-10 I00–I99)	195	792	4	2	0	2	4	5	10
Gert Sibande	Winter	Respiratory deaths (ICD-10 J)	197	607	3	2	0	2	3	4	8
Gert Sibande	Winter	Tuberculosis deaths (ICD-10 A15–A19)	197	193	1	1	0	0	1	1	6
Gert Sibande	Winter	Cardio/Cerebrovascular deaths (ICD-10 I00–I99)	197	803	4	2	0	3	4	5	11
Sedibeng	Autumn	Respiratory deaths (ICD-10 J)	196	575	3	2	0	2	3	4	8
Sedibeng	Autumn	Tuberculosis deaths (ICD-10 A15–A19)	196	183	1	1	0	0	1	1	5
Sedibeng	Autumn	Cardio/Cerebrovascular deaths (ICD-10 I00–I99)	196	775	4	2	0	3	4	5	10
Sedibeng	Spring	Respiratory deaths (ICD-10 J)	195	599	3	2	0	2	3	4	9
Sedibeng	Spring	Tuberculosis deaths (ICD-10 A15–A19)	195	193	1	1	0	0	1	1	4

Sedibeng	Spring	Cardio/Cerebrovascular deaths (ICD-10 I00–I99)	195	797	4	2	0	3	4	5	10
Sedibeng	Summer	Respiratory deaths (ICD-10 J)	195	586	3	2	0	2	3	4	8
Sedibeng	Summer	Tuberculosis deaths (ICD-10 A15–A19)	195	204	1	1	0	0	1	2	4
Sedibeng	Summer	Cardio/Cerebrovascular deaths (ICD-10 I00–I99)	195	787	4	2	1	3	4	5	10
Sedibeng	Winter	Respiratory deaths (ICD-10 J)	197	599	3	2	0	2	3	4	8
Sedibeng	Winter	Tuberculosis deaths (ICD-10 A15–A19)	197	189	1	1	0	0	1	1	5
Sedibeng	Winter	Cardio/Cerebrovascular deaths (ICD-10 I00–I99)	197	799	4	2	0	2	4	5	11
Waterberg	Autumn	Respiratory deaths (ICD-10 J)	196	591	3	2	0	2	3	4	10
Waterberg	Autumn	Tuberculosis deaths (ICD-10 A15–A19)	196	197	1	1	0	0	1	1	4
Waterberg	Autumn	Cardio/Cerebrovascular deaths (ICD-10 I00–I99)	196	787	4	2	0	3	4	5	11
Waterberg	Spring	Respiratory deaths (ICD-10 J)	194	582	3	2	0	2	3	4	10
Waterberg	Spring	Tuberculosis deaths (ICD-10 A15–A19)	194	199	1	1	0	0	1	2	4
Waterberg	Spring	Cardio/Cerebrovascular deaths (ICD-10 I00–I99)	194	798	4	2	0	3	4	5	11
Waterberg	Summer	Respiratory deaths (ICD-10 J)	195	593	3	2	0	2	3	4	10

Waterberg	Summer	Tuberculosis deaths (ICD-10 A15–A19)	195	188	1	1	0	0	1	2	4
Waterberg	Summer	Cardio/Cerebrovascular deaths (ICD-10 I00–I99)	195	765	4	2	0	2	4	5	10
Waterberg	Winter	Respiratory deaths (ICD-10 J)	197	573	3	2	0	2	3	4	8
Waterberg	Winter	Tuberculosis deaths (ICD-10 A15–A19)	197	199	1	1	0	0	1	2	5
Waterberg	Winter	Cardio/Cerebrovascular deaths (ICD-10 I00–I99)	197	692	4	2	0	2	3	5	10

Supplementary Table S3: Descriptive statistics for Respiratory failure, Tuberculosis deaths and Cardiovascular / Cerebrovascular deaths by Priority Area (PA).

PA	outcome	non_missing_weeks	total	mean_per_week	sd	min	q25	median	q75	max
Highveld Priority Area	Respiratory deaths (ICD-10 J)	1566	4769	3	2	0	2	3	4	9
Highveld Priority Area	Tuberculosis deaths (ICD-10 A15–A19)	1566	1601	1	1	0	0	1	2	6
Highveld Priority Area	Cardio/Cerebrovascular deaths (ICD-10 I00–I99)	1566	6311	4	2	0	3	4	5	11
VTAPA	Respiratory deaths (ICD-10 J)	1565	4686	3	2	0	2	3	4	10
VTAPA	Tuberculosis deaths (ICD-10 A15–A19)	1565	1595	1	1	0	0	1	2	6
VTAPA	Cardio/Cerebrovascular deaths (ICD-10 I00–I99)	1565	6290	4	2	0	3	4	5	13
Waterberg–Bojanala Priority Area	Respiratory deaths (ICD-10 J)	1565	4651	3	2	0	2	3	4	10
Waterberg–Bojanala Priority Area	Tuberculosis deaths (ICD-10 A15–A19)	1565	1621	1	1	0	0	1	2	5

Waterberg–Bojanala Priority Area	Cardio/Cerebrovascular deaths (ICD-10 I00–I99)	1565	6113	4	2	0	2	4	5	11

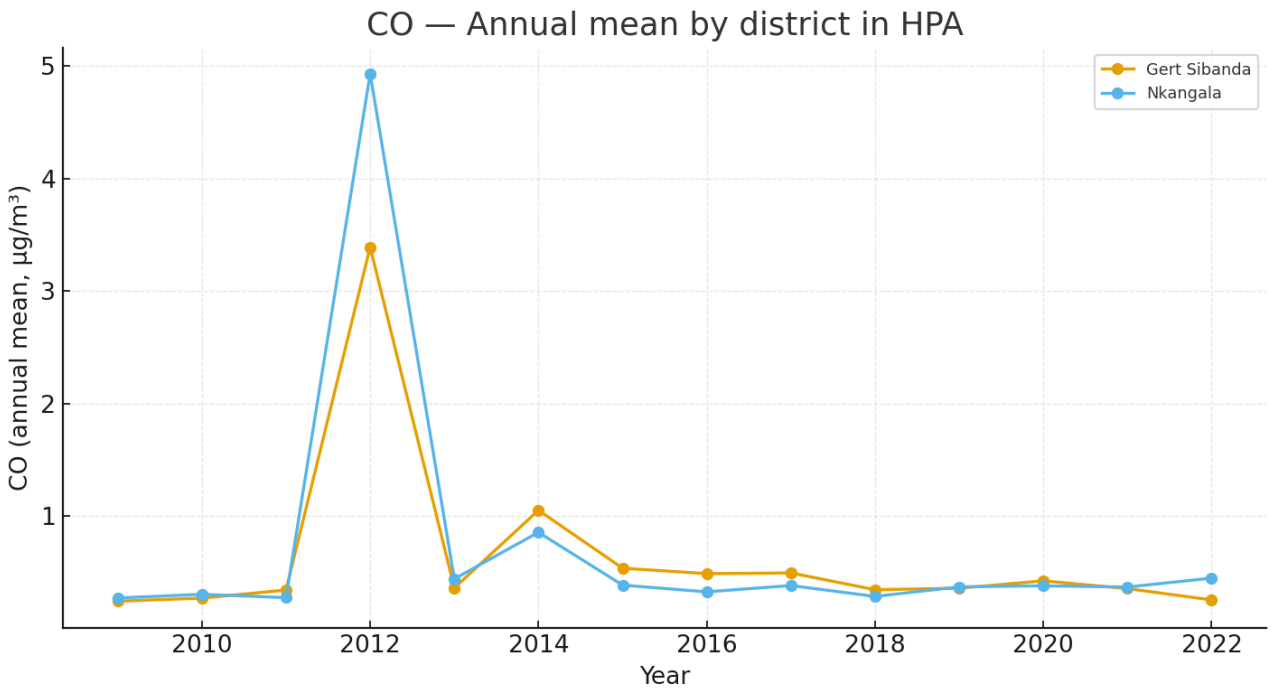

Figure 42: Time series for annual mean CO per district within the Highveld Priority Area

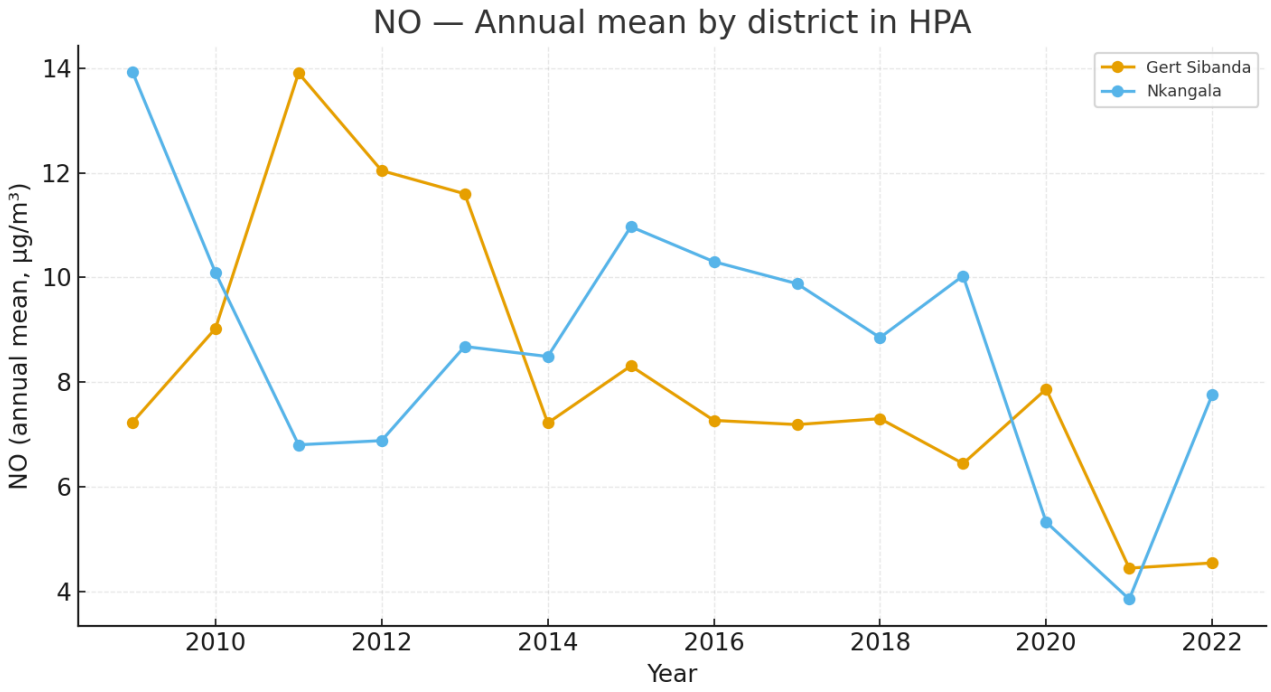

Figure 43: Time series for annual mean NO per district within the Highveld Priority Area

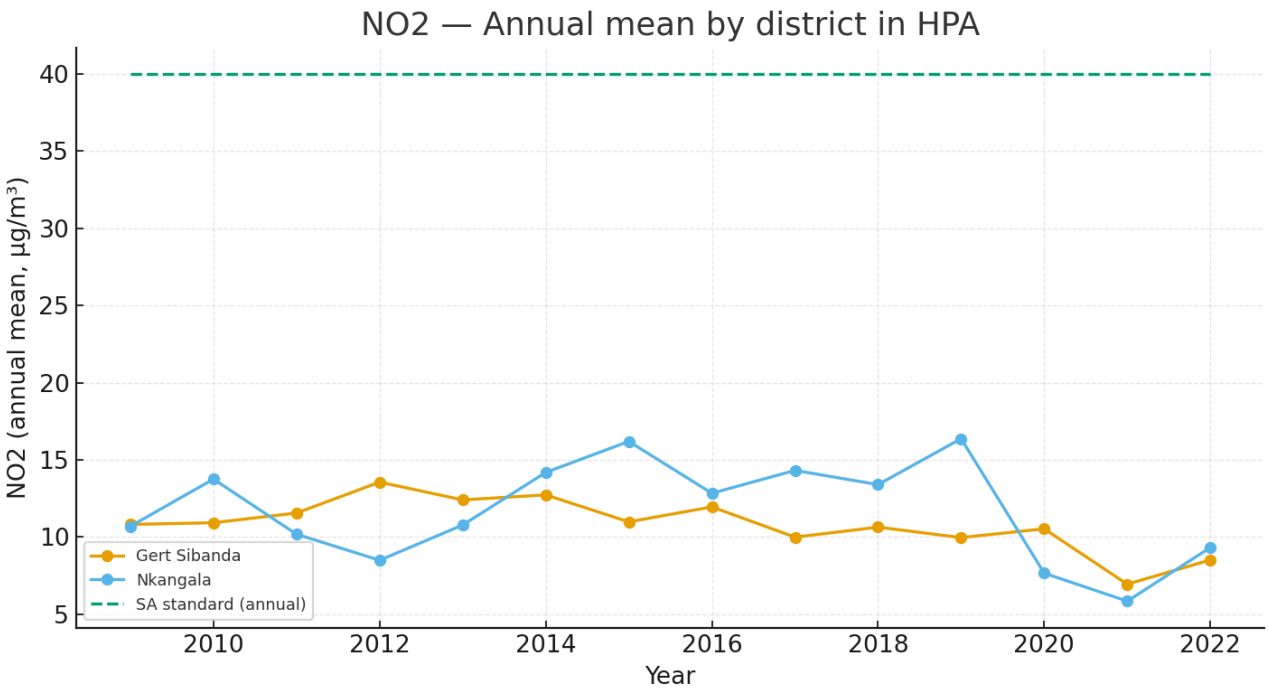

Figure 44: Time series for annual mean NO_2 per district within the Highveld Priority Area

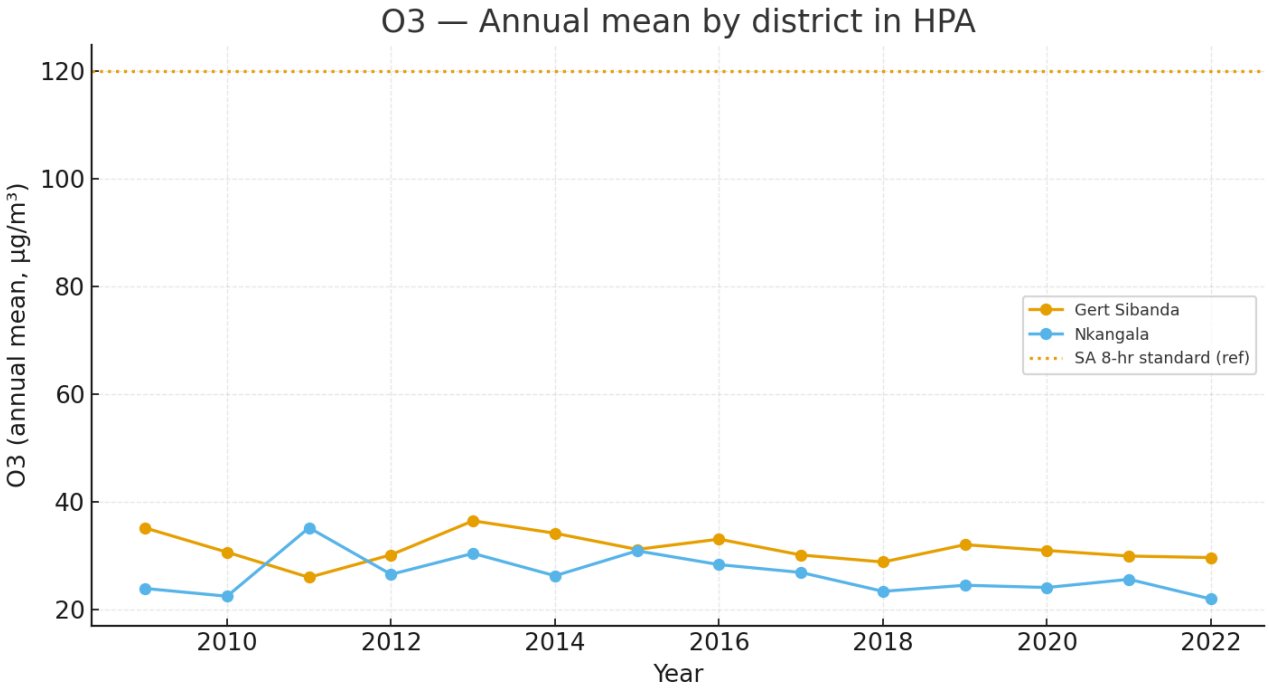

Note: O_3 line shows the South African 8-hour standard (120 µg/m³) for reference; annual means are not directly comparable to an 8-hour limit.

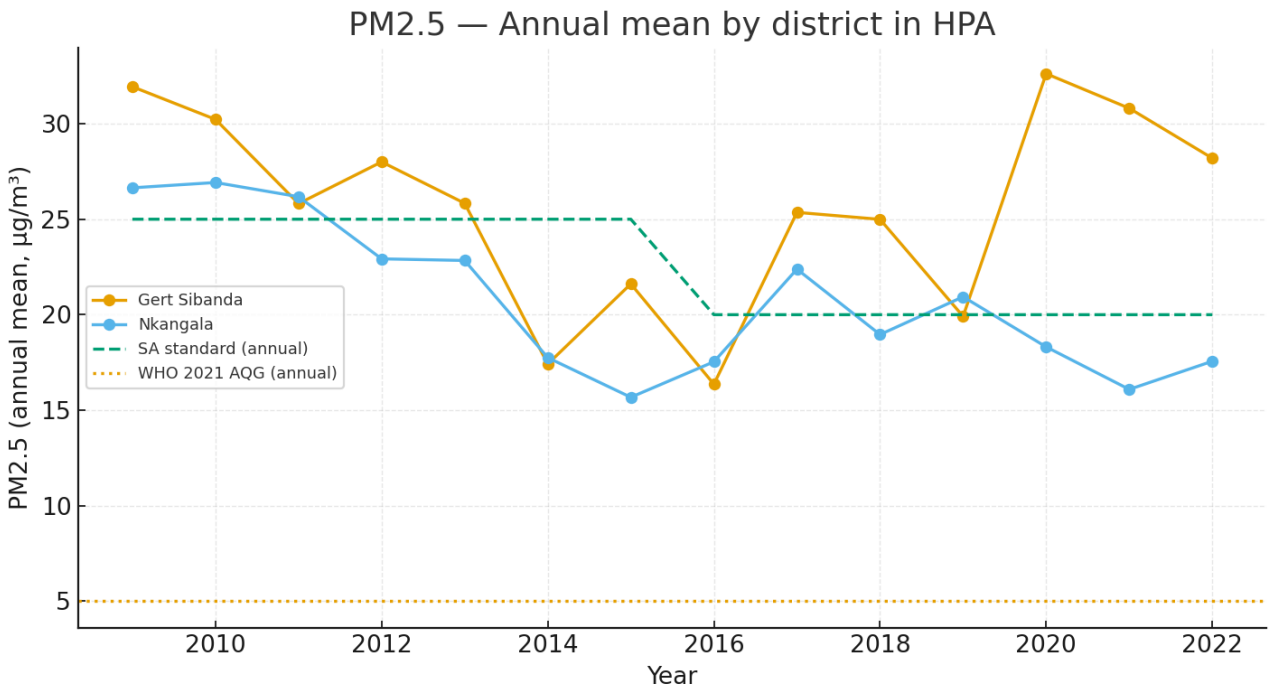

Figure 45: Time series for annual mean $PM_{2.5}$ per district within the Highveld Priority Area

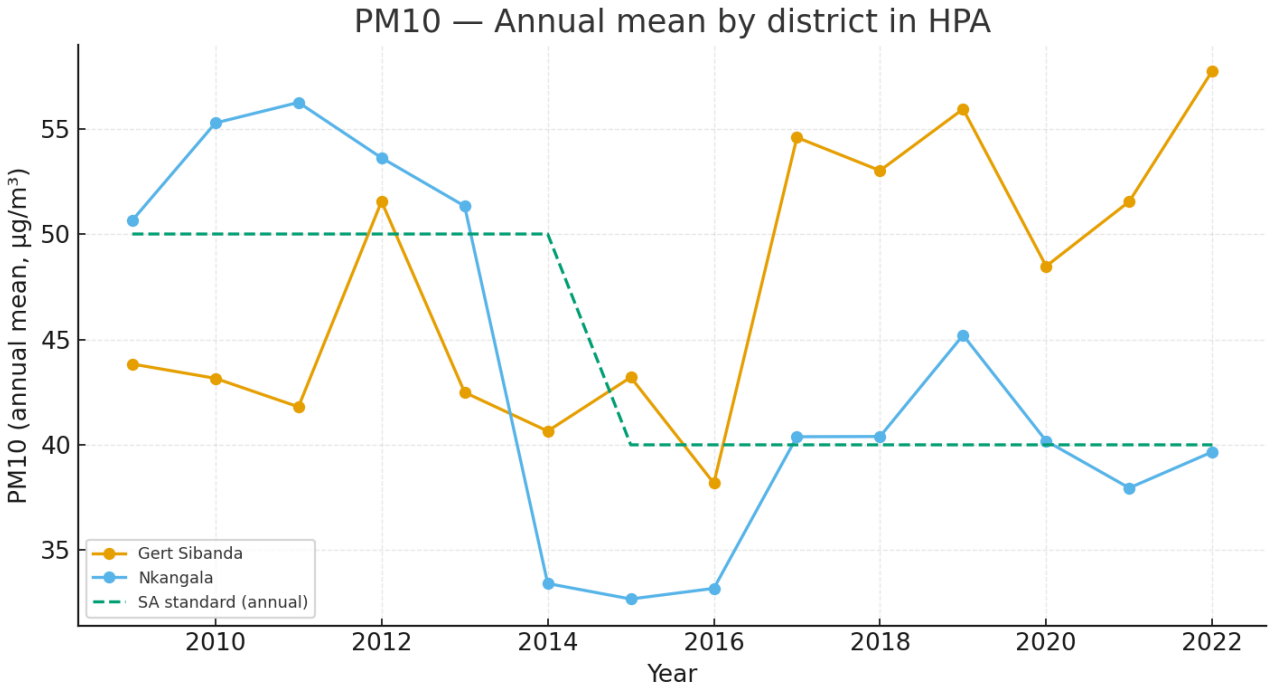

Figure 46: Time series for annual mean PM_{10} per district within the Highveld Priority Area

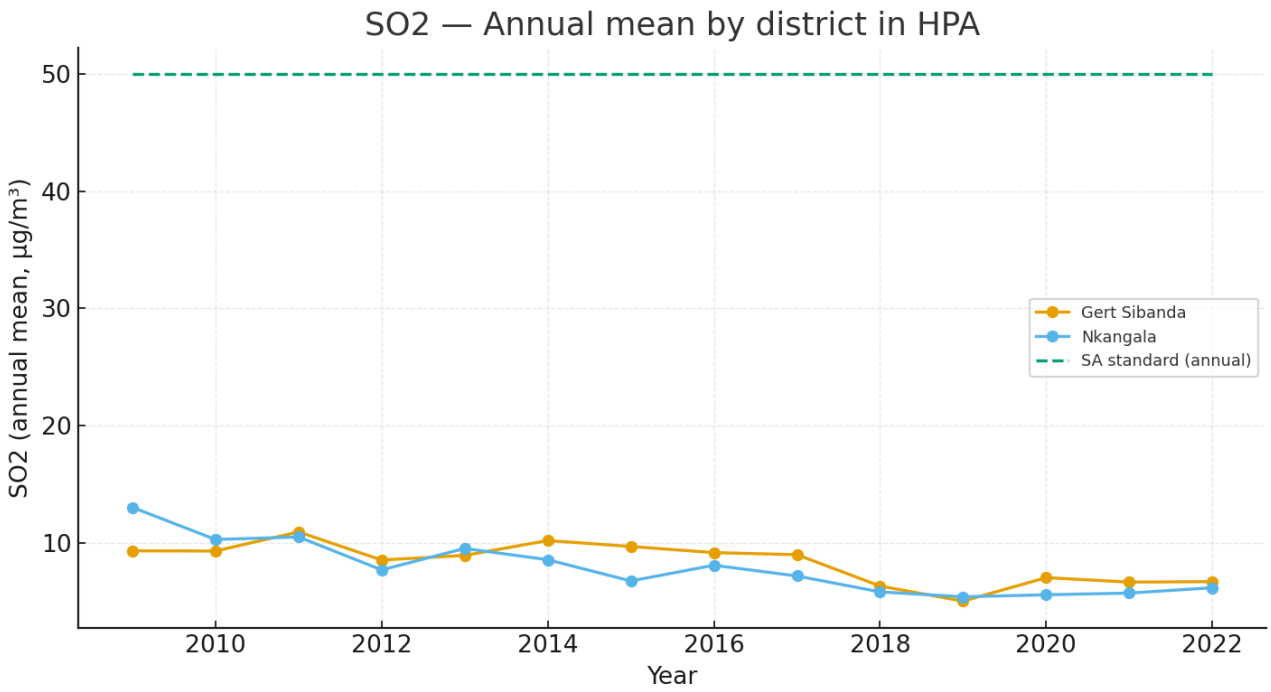

Figure 47: Time series for annual mean SO_2 per district within the Highveld Priority Area

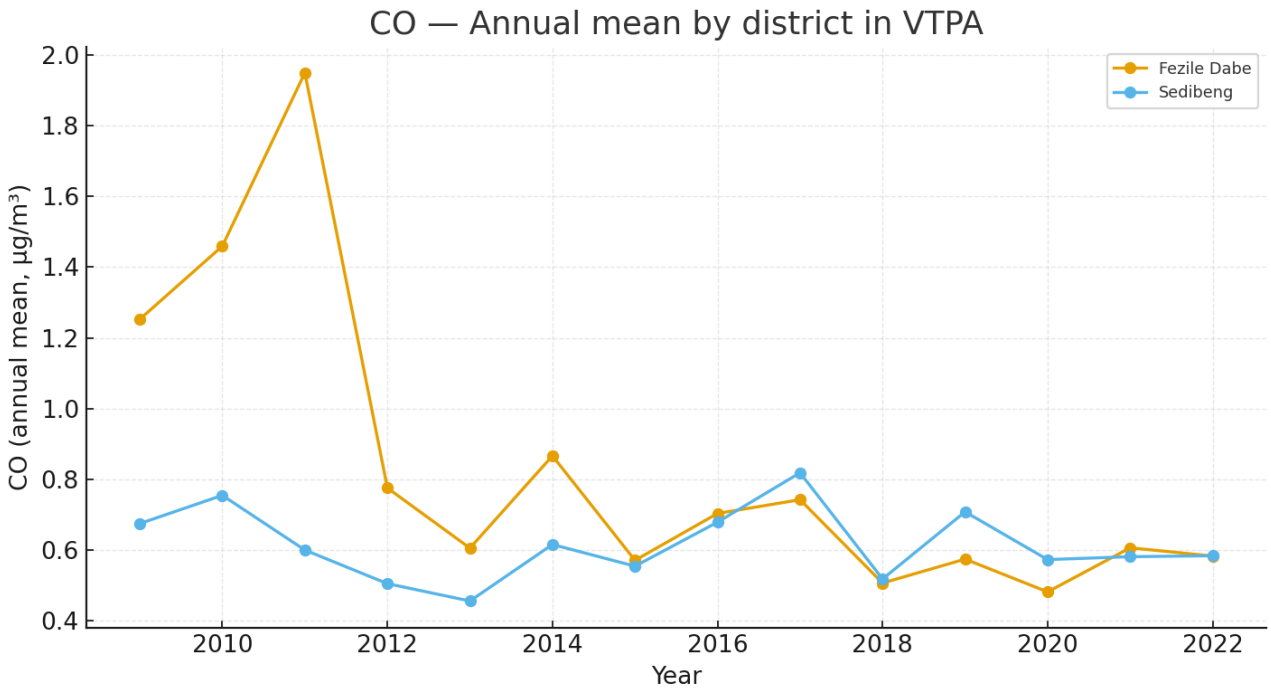

Figure 48: Time series for annual mean CO per district within the Vaal Triangle Priority Area

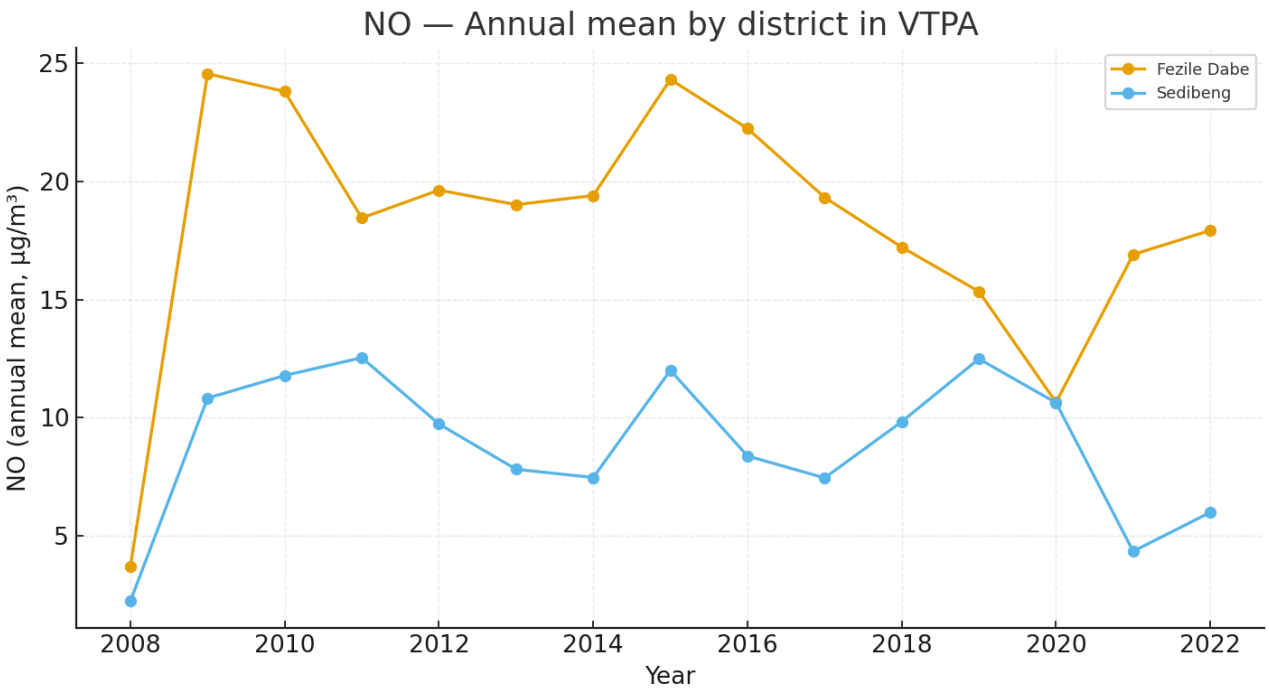

Figure 49: Time series for annual mean NO per district within the Vaal Triangle Priority Area

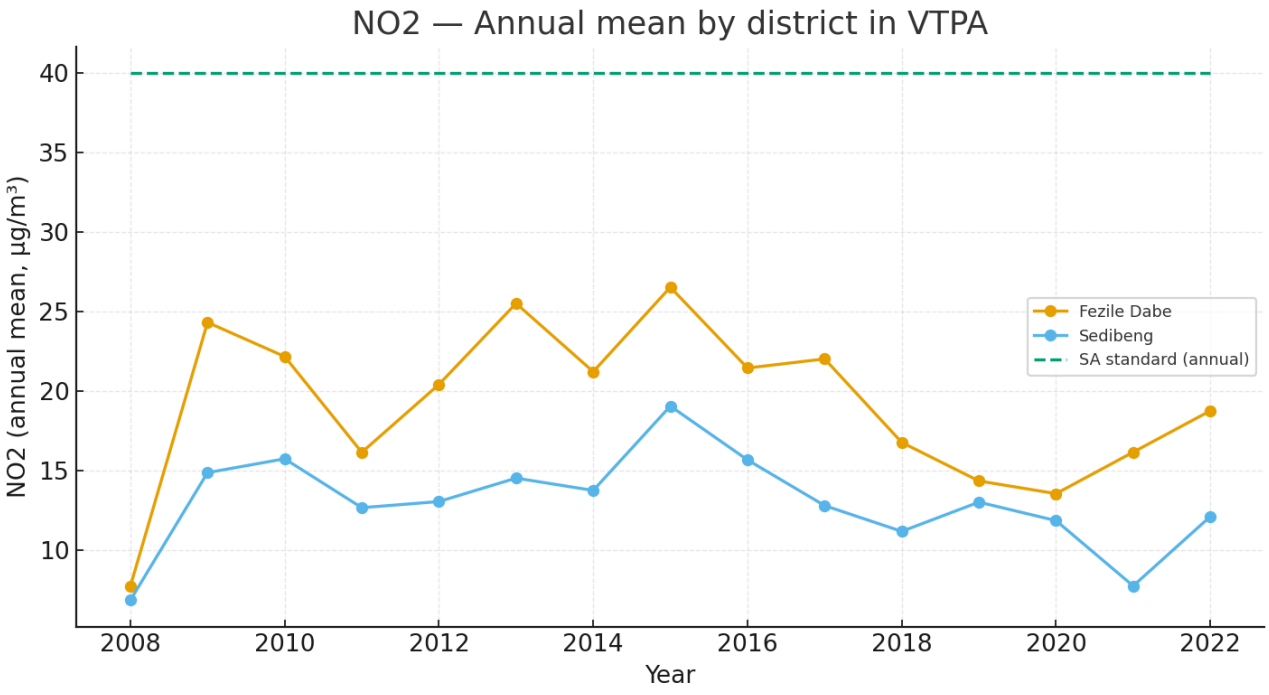

Figure 50: Time series for annual mean NO_2 per district within the Vaal Triangle Priority Area

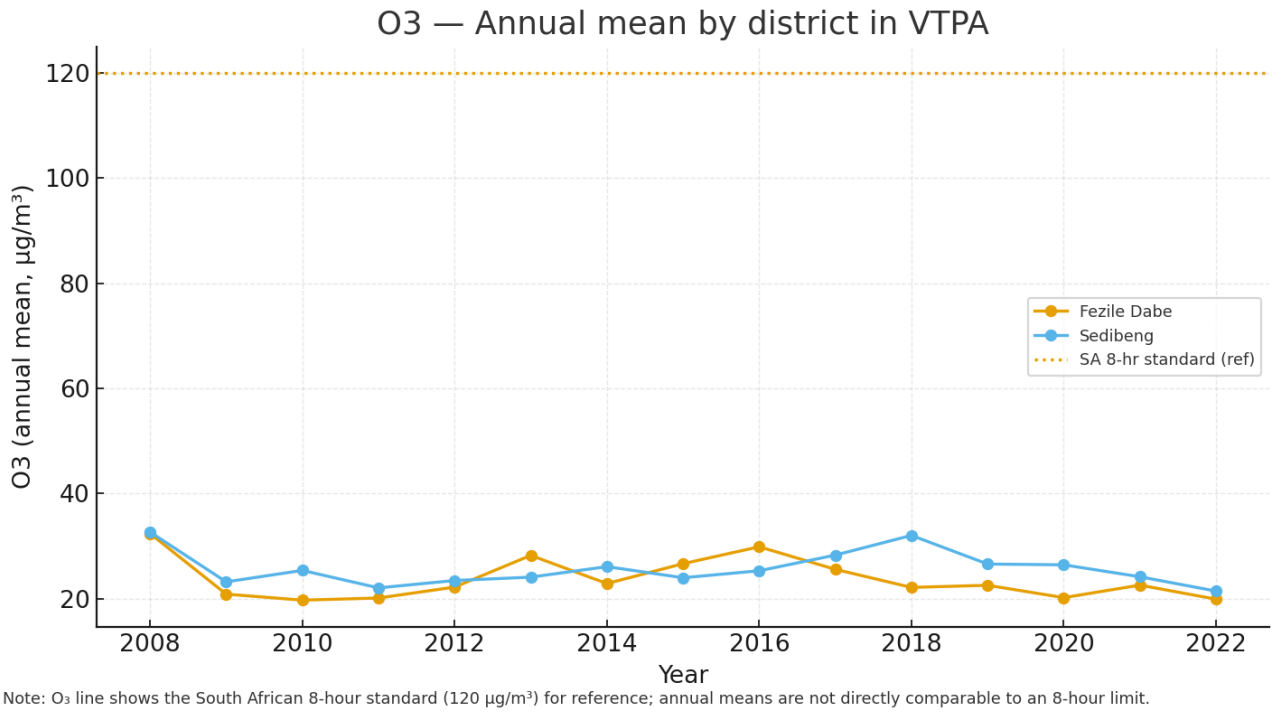

Figure 51: Time series for annual mean O_3 per district within the Vaal Triangle Priority Area

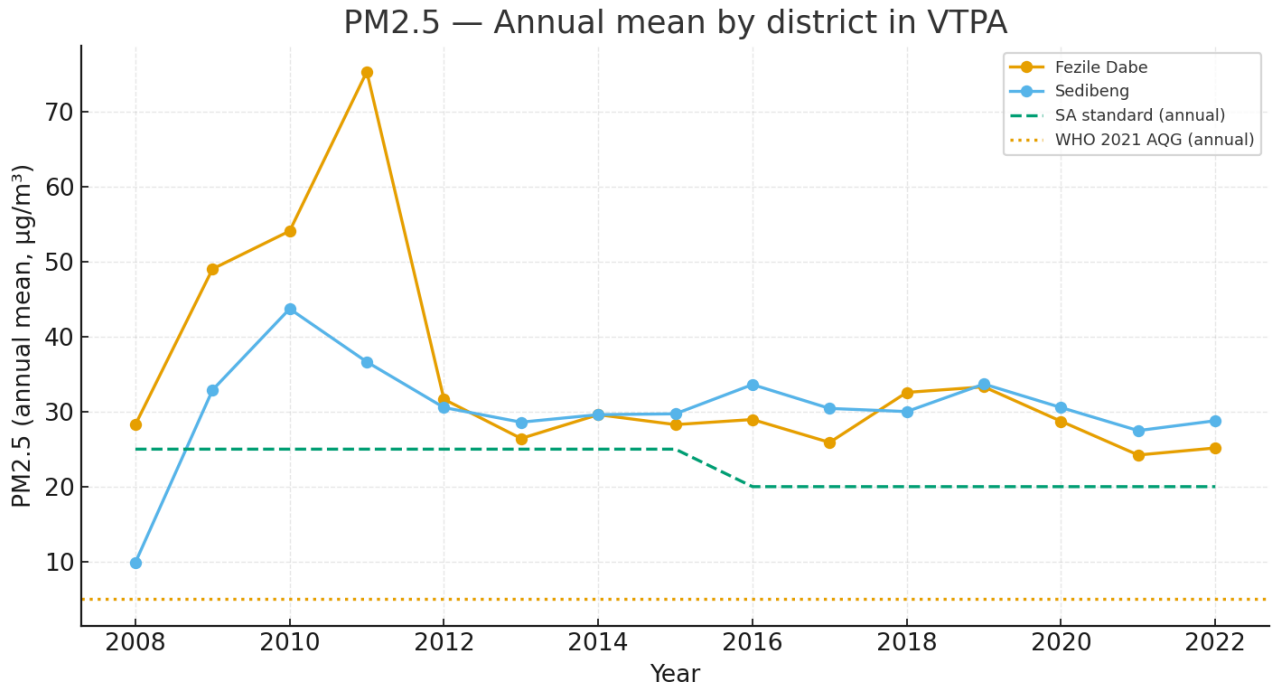

Figure 52: Time series for annual mean $PM_{2.5}$ per district within the Vaal Triangle Priority Area

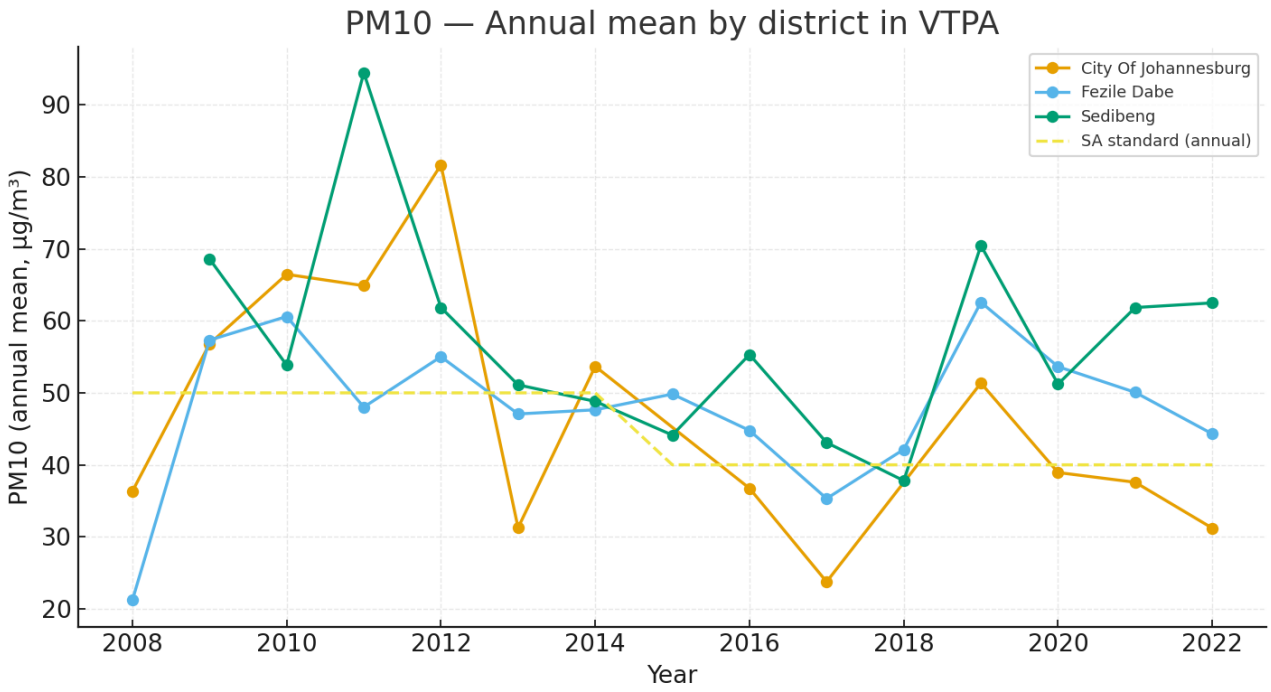

Figure 53: Time series for annual mean PM_{10} per district within the Vaal Triangle Priority Area

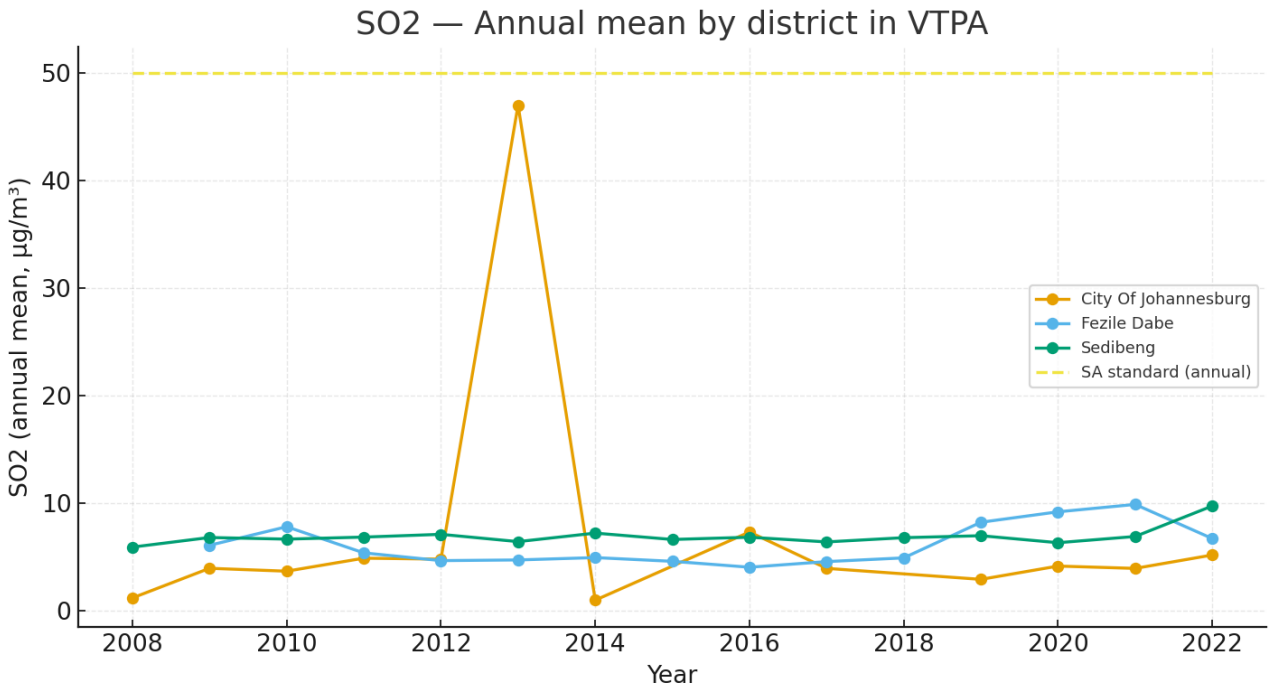

Figure 54: Time series for annual mean SO_2 per district within the Vaal Triangle Priority Area

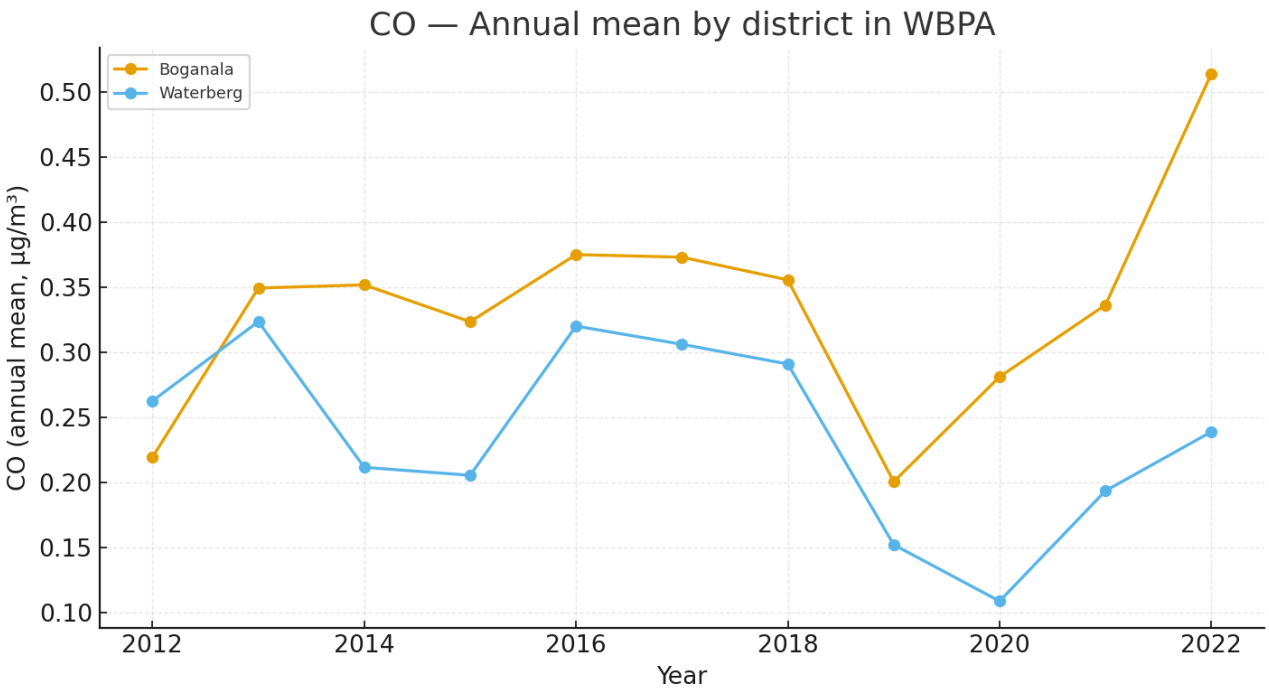

Figure 55: Time series for annual mean CO per district within the Waterberg - Bojanala Priority Area

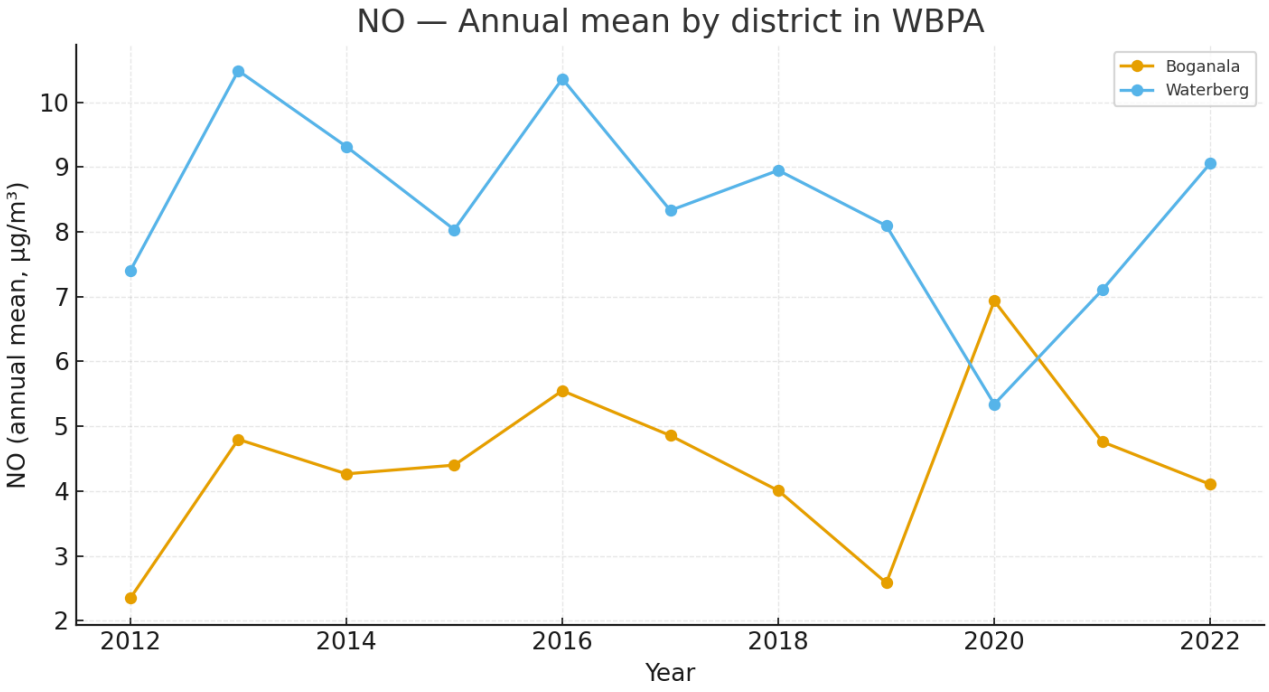

Figure 56: Time series for annual mean NO per district within the Waterberg - Bojanala Priority Area

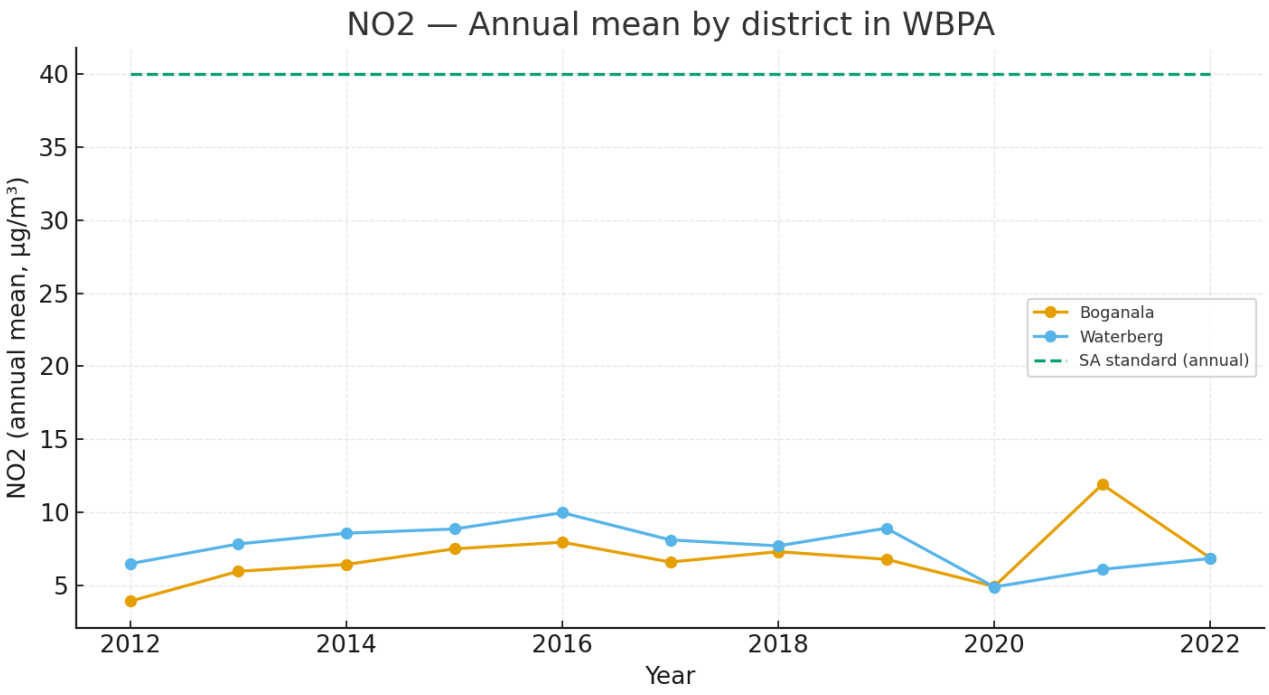

Figure 57: Time series for annual mean NO_2 per district within the Waterberg - Bojanala Priority Area

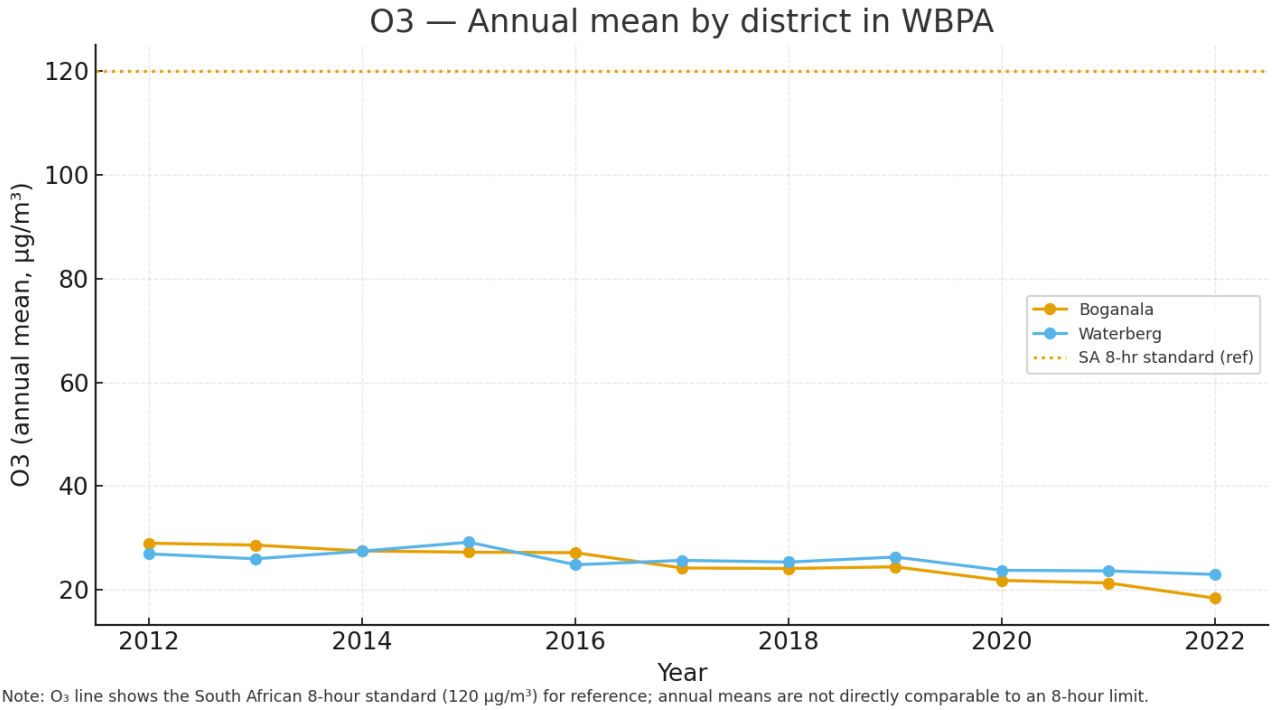

Figure 58: Time series for annual mean O_3 per district within the Waterberg - Bojanala Priority Area

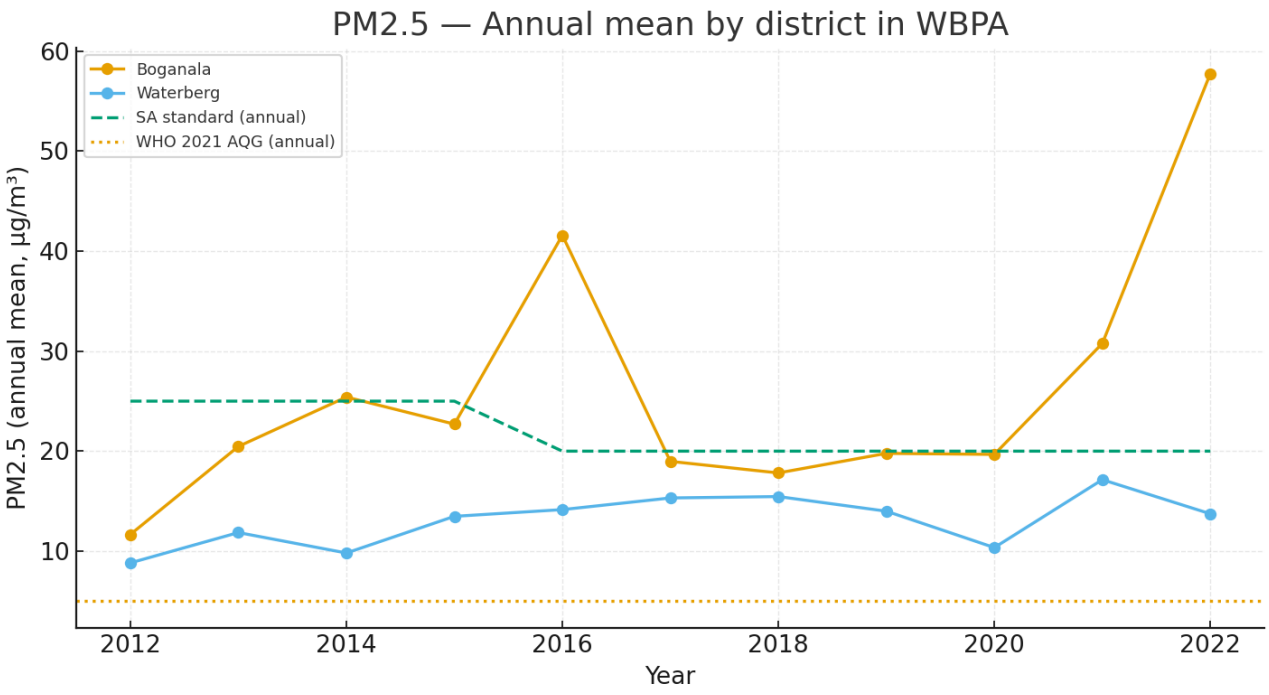

Figure 59: Time series for annual mean $PM_{2.5}$ per district within the Waterberg - Bojanala Priority Area

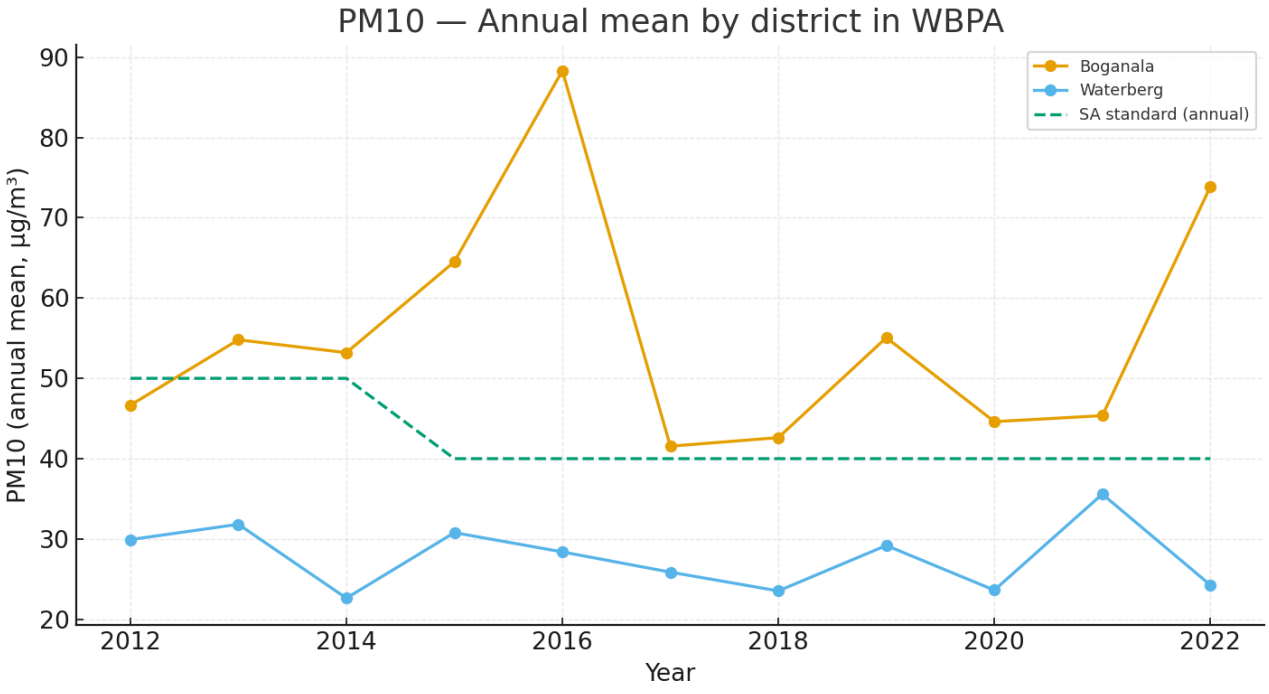

Figure 60: Time series for annual mean PM_{10} per district within the Waterberg - Bojanala Priority Area

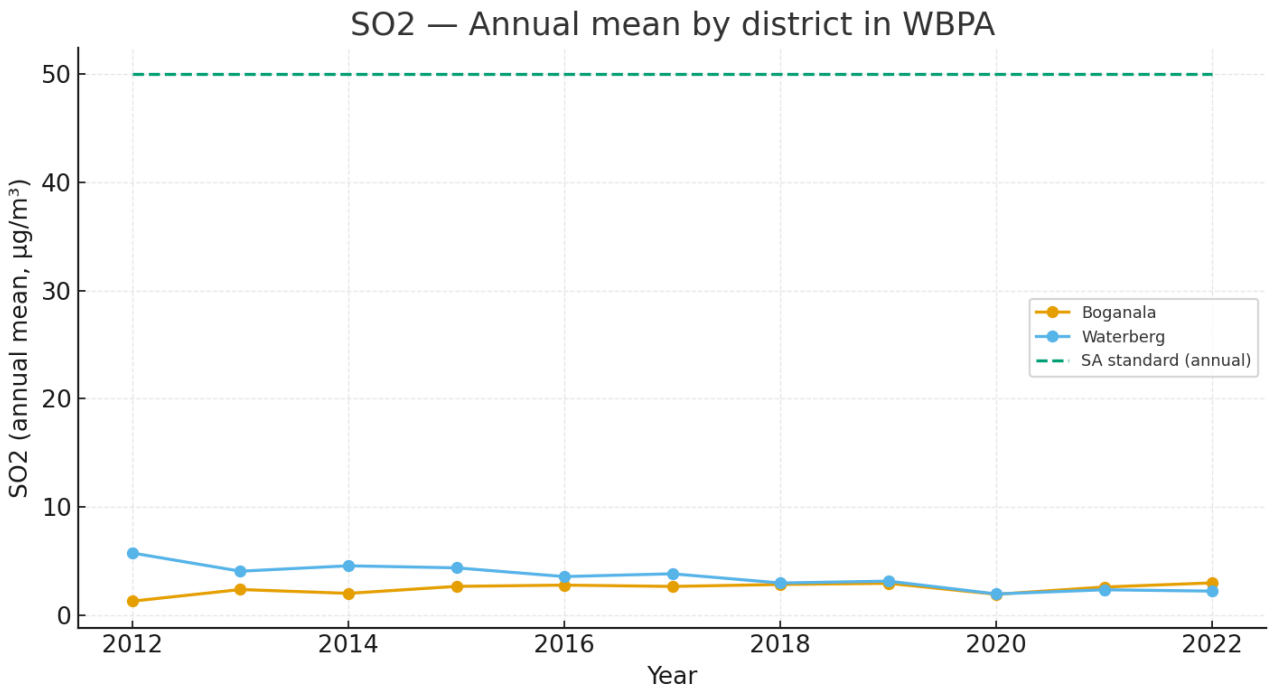

Figure 61: Time series for annual mean SO_2 per district within the Waterberg - Bojanala Priority Area